Some Features of High-Energy Scattering Theory

by

ARJUNA SACHCHIDANANDA SITTAMPALAM

A thesis presented for the Degree of Doctor of Philosophy of the University of London and the Diploma of Membership of Imperial College.

Department of Theoretical Physics,
Imperial College of Science and Technology,
London.

Abstract

This thesis is in four parts, the first part consisting of a general survey on multiperipheralism. The remaining three chapters involve the study of 3 modified multi-Regge models.

In the second chapter, the single trajectory version of the Multi-Regge model in a factorisable approximation is modified by including a cut in the input and a new set of bootstrap equations is obtained. The relative contributions of the pole and the elastic $2 \to 2$ amplitude cut are also examined.

In the third chapter, a multi-Regge model with nucleon loops inserted between the high sub-energy rungs is analysed.

In the final chapter, it is shown how the addition of amplitudes with correlations can have the effect of pushing upwards the position of the Regge trajectory in the multi-Regge bootstrap.

Preface

The work described in this thesis was carried out under the supervision of Professor P.T. Matthews in the department of Physics, Imperial College, London between July 1969 and September 1971. The material presented is the original work of the author and has not been submitted for a degree in this or any other University.

The author wishes to thank Dr. I.G. Halliday who suggested the problems the study of which led to this thesis for his constant advice and encouragement. The author also wishes to thank Professor T.W.B. Kibble for a critical reading of the thesis. Finally, thanks are also due to Ashley Wickremaratne for most of the diagrams in this work;

CONTENTS

		Page
	Abstract	2
	Preface	3
	Chapter I	
1.	The A.B.F.S.T. Model	6
2.	The multi-Regge Model	11
	Chapter II	
1.	Introduction	18
2.	The Sudakov Variables and Kinematics	24
3.	The Unitarity Equation and the M.R.M.	31
4.	The Total Cut Discontinuity	55
5.	Pole and Cut in the input	58
6.	Comparison of Pole and Elastic Cut Contributions	65
7.	Conclusion	68
	Chapter III	
1.	Introduction	70
2.	Notation and Kinematics	72
3.	Factorisation of Phase Space and Kinematics	75
4.	The $2 \to N$ contribution	82
5.	The Propagator and Coupling Functions	86
6.	Leading Order terms and Asymptotic Approximations	96
7.	Impact of Nucleon Loops on the M.R.M.	110
8.	Incorporation of Off-mass-shell terms	119
9.	Conclusion	121
	Chapter IV	
1.	Introduction	123
2.	The corrected multi-Regge model	123

		Page
3.	The mechanism of a negative correction	135
4.	The correlating amplitude	136
5.	Conclusion	142
	References -	143

CHAPTER I

INTRODUCTION

1. The ABFST Model

It was proposed by Amati, Fubini and Stanghellani (Ref. 1) that a multiperipheral model of high-energy scattering would provide a dynamical description of Regge poles and hence a dynamical model of the low-mass particles that lie on these trajectories. Their paper featured both inelastic and elastic scattering, the latter being a summary of the work already done by Bertocchi, Fubini and Tonin (Ref. 2). The multiperipheral mechanism was first studied by Berestetsky and Pomeranchuk (Ref. 3) before the general Regge pole concept was developed. They described it in terms of pion-exchange and repeated diffraction scattering which, in the multi-Regge model to be described below, corresponds to alternating pions $\left(\alpha_\pi \approx 0\right)$ and Pomeranchuk $\left(\alpha_\pi \approx 1\right)$ trajectories.

Multiperipheralism is the generalisation at very high energies of the peripheral model which is useful in interpreting the main features of inelastic scattering in the energy range 1-2 Gev. For instance, in the process

$$\pi + N \longrightarrow S_1 + S_2$$

the peripheral model represents the reaction in terms of Fig. 1

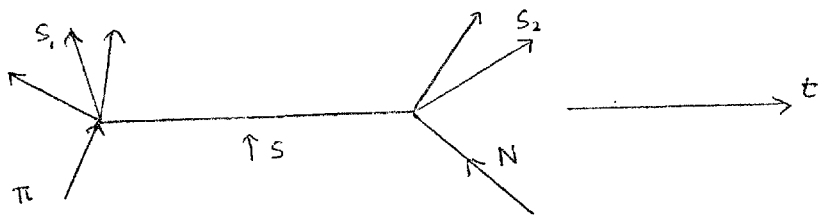

fig 1

where the s and t channels are given as in the figure. The reaction products are identified by the sub-energies s_1 and s_2 carried by them. The experimentally observed fact is that this description of the process is valid only when t_1 is small. Then the peripheral idea states that the amplitude for the process is approximately given by the product of the amplitudes corresponding to

$$\pi\pi \longrightarrow s_1$$

and

$$\pi N \longrightarrow s_2$$

where one of the incoming pions in both reactions is virtual and off mass-shell. Thus the full amplitude is effectively factorised. If s_1 in turn is sufficiently large, the reaction $\pi\pi \longrightarrow s_1$ will itself permit a peripheral description of its own, splitting the products s_1 into 2 groups. Extending this process to the $2 \to N$ production amplitude, we arrive at the multiperipheral graph at sufficiently high energy which is given by Fig. 2.

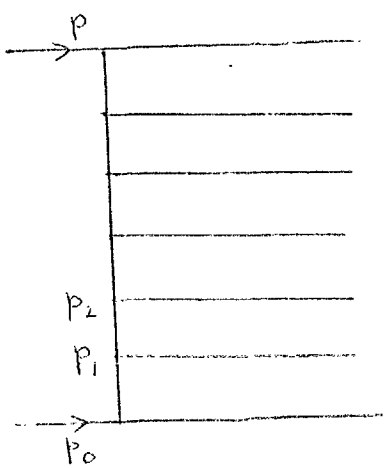

Fig 2

When this amplitude is combined with its complex conjugate to obtain the cross-section, we obtain the ladder structure which enables us to evaluate the multiparticle production contribution to the total cross-section by the iteration of an elastic cross-section. In the ADFST model, the multiperipheral chain for the production amplitude was comprised of elementary pion exchanges leading to a Regge behaviour of the imaginary part of the forward amplitude which is related to the total cross-section through the optical theorem. However, many of the conclusions arrived at in the AFS paper do not depend on the specific form of the $\pi - \pi$ amplitude or the low-energy input, but only on the topological form of the multiperipheral graphs. That is, their conclusions are model independent in the sense they are true for all multiperipheral models.

The AFS paper analysed both the high-energy total cross-sections and the elastic scattering amplitude, the graphs for both of which are analogous except that the latter is more complicated kinematically since the momenta flowing through the two sides of the unitarity cut are different. The main technique used was to reduce the sum over all individual multiperipheral effects for a particular $2 \to N$ production reaction to the solution of a linear integral equation. In the high-energy limit, the equations become rather simple. The kernel of their integral equation, have the property, in fact shared by all multiperipheral kernels in general, of being invariant under the group of multiplicative transformations

$$s \to cs \quad , \qquad s' \to cs'$$

where s' is any sub-energy. This result can be derived from the fact that when the number of emitted secondaries is large, the

main features of the process should be the same independently of whether one considers as target, the particle $p_0, p_1, p_2 \ldots\ldots\ldots$ (see Fig. 2). The change in the description of the process from a fixed target p_0 to a moving target p_1 entails a Lorentz transformation which in the extreme relativistic limit (Ref.4) is given by the above mentioned group of transformations. This property of inveriance suggests that the solution of the multiperipheral integral equation could be expressible in terms of the irreducible representations of the above group, given by s^{α}. In fact, the solution is found to be of this form. The same result is also achieved by summing the leading behaviour of each multiperipheral graph, which for the $2 \to N$ case is proportional to

$$\frac{1}{s} \frac{(\alpha \log s)^{n-1}}{(n-1)!}$$

Thus the multiperipheral model gives a Regge behaviour in the asymptotic limit. The trajectory α in the AFS case was determined as a functional of the low-energy resonance input $A^R(s_0)$ which they used for the kernel.

i.e.

$$\alpha = \alpha\left[A^R(s_0)\right]$$

This holds for all multiperipheral models, that is, the position and residue of the Regge pole which describes the high-energy behaviour is determined by the kernel.

The other "model independent" predictions of the AFS paper are

summarised as follows :

(1) The high-energy behaviour of the elastic scattering amplitude is

$$T_j(s,t) = s^{\alpha_j(t)} C_j(t) \left| -\cot\frac{\pi\alpha_j(t)}{2} + i \right| \qquad (1\text{-}1\text{-}1)$$

or

$$T_j(s,t) = s^{\alpha_j(t)} C_j(t) \left| \tan\frac{\pi\alpha_j(t)}{2} + i \right| \qquad (1\text{-}1\text{-}2)$$

according as whether the amplitudes are symmetric or antisymmetric under crossing. Also the slope of the trajectory is positive and $\alpha(t) > -1$ The quantity $C(t)$ admits of factorisation such that the relation between different amplitudes, dominated by the same pole is

$$\frac{T_{xy}(s,t)}{T_{2y}(s,t)} = \frac{T_{x\omega}(s,t)}{T_{2\omega}(s,t)}$$

where $x, y, 2$ and ω represent any kind of particle.

(2) The inelastic amplitude also has average properties which are simple and depend only on the multiperipheral mechanism. The multiplicity grows with the logarithm of the energy. The inelasticity and the branching ratio between different secondaries are energy independent. Also, the spectra of the secondary particles are given, for k_L considerably smaller than the initial energy, by

$$N(k)\, d^4k = F(k_1^2 k_2^2)\, dk_1^2\, dk_2^2 \frac{dk_L}{k_L} \qquad (1\text{-}1\text{-}3)$$

where k_T and k_L are the transverse and longitudinal momenta and $F(k^2, k_T^2)$ is a universal function independent both of s and k_L and strongly peaked for small k_T^2.

Another feature of the AFS paper was their pointing out the presence of cuts through s-channel unitarity. They also suggested that these should be included in the multiperipheral kernel, with resultant renormalisation effects of the output Regge pole trajectory, though they did not attempt to solve this problem. Our next chapter describes a model, modifying the multi-Regge model along these lines. The AFS paper explicitly calculated the cut in the 2 - particle discontinuity which was assumed to be reproduced in the elastic amplitude. Mandelstam (Ref. 5) showed that this was not so. In the complete contribution obtained by cutting by unitarity in all possible ways the diagram calculated by AFS, this cut is shown to disappear, though it reappears on computing other classes of diagrams. This conflict is resolved in the multi-Regge model, when one uses a Regge pole in the input and assumes all sub-energies to be high.

2. The Multi-Regge Model

An extension of the ABFST model, the multi-Regge model, first proposed by Kibble (Ref. 6.) and Ter Martirosyan (Ref. 7) had the feature that the exchanged pions along the multiperipheral chain were replaced by Regge Poles. The attraction of this model was enhanced both by the phenomenological model of Chan, Loskievsky and Allison (Ref. 8) which was extensively used in successfully fitting individual reactions and the duality hypothesis proposed by Dolen - Horn - Schmid (Ref. 9). The theoretical justification of multi-Regge models relies heavily on the latter which is used to assume

that Regge pole asymptotic representations are valid even in the low resonance region. Experimentally, it is established that the mean sub-energy of neighbouring final particles fall into this region (Ref. 10).

Owing to the presence of input and out put Regge poles, the multi-Regge model has provided a suitable framework for a bootstrap theory embracing multiperipheralism. This model, in conjunction with the unitarity equation can be used to obtain self-consistency conditions imposing constraints on the Regge parameters. A crude bootstrap of this nature was analysed by Chew and Pignotti (Ref. 11) A more exact treatment with the derivation and analysis of the multi-Regge integral equation was developed by several authors (Refs. 12, 13, 14, 15, 16). This integral equation, whose kernel consisted of the elastic $2 \to 2$ amplitude described by a Regge representation, arises from the unitarity conditions imposed on the multi-Regge model. Its solution leads to selfconsistency conditions relating to the imput and out put Regge poles, which impose constraints on the trajectory slopes and intercepts and the coupling constants.

The solution is possible only with the use of asymptotic approximations to the phase space which enables a diagonalisation of the integral equation. The main problem in achieving this through an asymptotically exact description of phase-space was the definition of a suitable set of Kinematic variables. Bali, Chew and Pignotti (Ref. 17) used Toller $[O(2,1)]$ variables for this purpose. Their variables provide a means by which the Toller-angle dependence of the two-Reggeon particle coupling is easily understood. These variables also provide a group-theoretical basis for the multi-Regge model.

Chew and de Tar (Ref. 18) made use of variables similar to these to achieve an almost complete diagonalisation of the kernel of the multi-Regge integral equation at zero momentum transfer by invoking Lorentz symmetry. This formed the basis for the subsequent work of Chew and Frazer (Ref. 19) which established the relation between the Pomeranchuk pole and the cut. The group theoretical analysis was extended to include general momentum transfers by Ciafaloni, de Tar and Mishelloff (Ref. 20) who used a set of variables analogous to the foregoing to obtain a partial diagonalisation of the equation. Their technique was applicable to both the multi-Regge model and the AFS model.

Another set of variables that is especially suited to the asymptotic requirements of Multi-Regge phase space is that first used by Sudakov (Ref. 21). The derivation of Halliday and Saunders's multi-Regge integral equation was carried out using these variables, of which they performed a detailed analysis (Ref. 22). In this equation, they assumed the existence of only one type of particle of mass m, and zero spin, isospin and electric charge and only one type of trajectory. This assumption was only for convenience and did not entail an unrealistic description of nature. As pointed out in the AFS paper, only the external particles at the end of the multiperipheral chain are replaced to account for different reactions, the chain itself being uniform, and the properties of the model do not depend on the external particles.

Halliday's (Ref. 14) output trajectory in the $2 \to 2$ unitarity equation is produced by repeated exchanges of the same trajectory in inelastic amplitudes, enabling one to obtain a closed

set of equations for the parameters and couplings associated with this trajectory. This model differs from that of the others (Refs. 11, 15, 16) who suggest that multiple exchange of lower meson trajectories in the $\pi \rightarrow N$ amplitude is responsible for the Pomeranchuk trajectory output in the elastic amplitude, the Pomeron in the input producing only perturbation effects.

Earlier, it was stated that the multi-Regge model is heavily dependent on the duality idea to justify its employing Regge representation for sub-energies which are indicated by experiment to be low. Halliday (Ref. 23) and Chew, Rogers and Snider (Ref. 10) questioned the validity of this assumption. The latter confined their arguments to the ABFST model, which they indirectly related to the multi-Regge model. The former cast doubt on the assumption in the context of multi-Reggeism. The question of low sub-energies was connected to the problem of crossed rungs and shown to be the same for Kinematic reasons. Without these crossed rungs, the multi-Regge formalism contains only planar diagrams, the calculation of which is similar to the AFS cut calculation. Thus it is preferable to include diagrams with the crossed rungs, as in Fig. 3

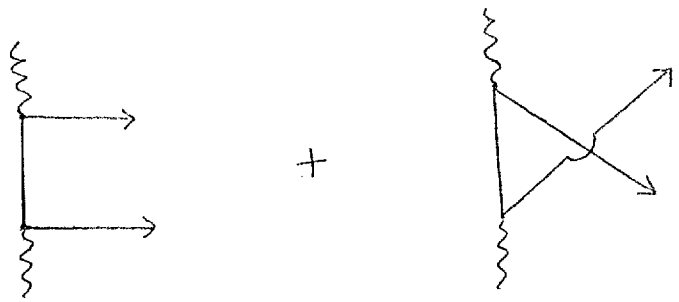

Fig. 3.

Having thus reduced the study of low sub-energies to the study of crossed rungs, it was shown that the use of duality expressed in terms of Cauchy's theorem, to get round this problem was not possible owing to two effects. One was that the appropriate analytic amplitude has singularities at $s=0$ as well as the threshold at $s=4m^2$ leading to the application of Cauchy's theorem needing not only the imaginary part but also the real part. The second is that the phase space integral contains extra terms due to the dissection of phase-space to fit the multi-Regge region.

Chew, Rogers and Snider used the duality concept based on the Veneziano model to cast doubt on its validity in the context of multi-peripheralism. The asymptotic form of the Veneziano model was used in the low-energy region to determine the kernel. This led to a qualitatively wrong isospin dependence of the ABFST kernel. For this reason, they re-examined the original ABFST model with a low-sub-energy kernel, forswearing the high-subenergy assumptions of multi-Reggeism and compared this with the multi-Regge model, to throw further light on it. A crucial defect in their model was that, using experimental values for the kernel, i.e. the low-energy amplitude, they fell far short of producing the output pole at $j=1$.

This failure of the Chew, Rogers and Snider version of the ABFST model is shared by the various multi-Regge models studied hitherto. All their models fail to account for total cross-sections tending to a constant as required by experimental evidence. At the beginning of the next chapter, we shall describe the work done in the multi-Regge framework in relation to this point.

Another feature in respect of which multiperipheral models

disagree with experimental evidence is the sign of the elastic cut correction. The latter obtained through the application of two particle unitarity gives a sign opposite to that of the absorption model (Ref. 24). This question is examined in our model introduced in the next chapter.

In this thesis, we study three modified versions of the multi-Regge model analysed by Halliday and Saunders (Ref. 22) and Frazer and Mehta (Refs. 14,16). Throughout our work, we confine ourselves to the use of Sudakov variables in the derivation of the integral equation. Our models are also based on the single trajectory input version of the M.R.M. mentioned earlier. Our entire study assumes the momentum transfer either to be zero or close to it, together with large s, both of which are essential for the validity of multiperipheral models.

In the next chapter, we consider the effects of adding a cut correction to the single pole input in order to attempt to push up the output trajectory closer to one than the single pole input model, where Frazer and Mehta (Ref. 16) established the position to be 0.8. The cut correction used is that which is dynamically produced by the single-pole input and as such, should have been present in the input in a complete bootstrap. We also investigate numerically the value of the elastic cut correction in both our modified model and that of Frazer and Mehta's for comparisons with the absorption model. The results which we obtain are dissappointing on both counts. Self-consistency constraints on the parameters involved actually force the position of our trajectory lower than Frazer and Mehta's trajectory, our value being 0.7 instead of producing an enhanced trajectory as we had hoped. Also the sign of the elastic cut correction in our

model also is opposite to that of the absorption model.

In chapter 3, we study a multi-Regge model which is modified by the exchange of low-energy nucleons alternating with the high sub-energy Reggeons in the multi-Regge chain. The type of diagram calculated by us is very similar to that calculated by Cheng and Wu (Ref.25) in their analysis of high energy quantrum electrodynamics. In their case, insertion of Fermion loops into diagrams containing Vector Meson exchanges gave an enhanced s-behaviour for the amplitudes which led us to surmise that a similar result might occur with the insertion of nucleon loops in the multi-Regge model, possibly producing constant cross-sections. For the nucleon-Reggeon couplings that figure in this multi-Regge chain, we use the Reggeised form of the Fermion-Boson couplings and propagators as prescribed by Scadron (Ref. 26) and Jones and Scadron (Ref. 27). We find that the nucleon loops have the effect of multiplying each multi-Regge diagram by a constant factor leading to the result that the trajectory position in the multi-Regge bootstrap remains unaltered while the Reggeon-Reggeon-particle coupling constant is "renormalised".

In the final chapter, we indicate how the addition of correction terms representing amplitudes in which non-adjacent particles in the chain correlate, to the standard multi-Regge model amplitude of Frazer and Mehta in which only neighbouring links correlate, can produce the effect of enhancing the leading behaviour by pushing up the position of the output trajectory.

CHAPTER II

CUT EFFECTS IN THE MULTI-REGGE BOOTSTRAP

I. Introduction

Various papers have been published on the possibility of a closed bootstrap in the multi-Regge model (Refs. 11, 12, 13, 14, 15, 16). The simplest of these consists of a single Regge pole input in the multi-Regge ladder emerging self-consistently in the output. The identification of the residue and position of the output pole with those of the input pole leads to a set of equations that determine the parameters of the common trajectory for the input and output. Assuming that the Regge trajectory is linear, of the form

$$\alpha(t) = a + bt \qquad 2.1.1$$

Frazer and Mehta (Refs. 15, 16) obtained a relation between the trajectory intercept $\alpha(0)$ and the Reggeon-Reggeon-particle coupling constants g occuring at each internal vertex of the multi-Regge ladder, which was given by

$$a = 1 - g^2 \qquad 2.1.2$$

The actual number obtained by Frazer and Mehta for $\alpha(0)$ was 0.8, consistent with a high-ranking meson trajectory. In fact, relation 2.1.2 implies (Ref. 15) that $\alpha(0)$ cannot approach unity without an inadmissibly low value for g leading to the physically unrealistic result that the elastic cross-section is large compared to the production cross-section. Chew and Pignotti (Ref. 11) arrived at a similar result by establishing that $g^2 \leq 1-a$.

Finkelstein and Kajantie (Ref. 28), by assuming a physically realistic g, also proved that multiply Pomeranchuk exchange violates the Froissart bound by leading to cross-sections that increase faster than any power of logs and suggested the inclusion of cuts as a possible remedy. Thus it is well established that the self-consistent singularity in the one-pole version of the multi-Regge model which determines the leading behaviour of the amplitude cannot be identified with the Pomeron pole alone. Yet, if cross-sections tend to a constant at high energy as experimental evidence suggests, this identification is necessary (Ref. 29). A solution is to include additional lower lying singularities either cuts or poles in the input.

Chew and Pignotti (Ref. 11) used two input poles, one of them the Pomeron at $j=1$ and the other a lower ranking meson trajectory which represents the effects of all meson trajectories. They suggested that it was the multiple exchange of the lower ranking meson trajectory that leads to the output Pomeron while the effects of multiple Pomeron exchange were negligible. Frazer and Mehta (Ref. 15, 16) using Chew, Goldberger and Low's multi-Regge integral equation (Ref. 13) also studied a bootstrap with the same input as Chew and Pignotti's. Both Chew and Pignotti and Frazer and Mehta assume that the leading output trajectory as well as one of the input poles is the Pomeron and use the bootstrap conditions to obtain values for the parameters of the other input trajectory. The output Pomeron is thus a hypothesis in these models rather than the inevitable outcome of a set of input singularities including itself. In this sense, the bootstrap is not contained within those 2 pole models. In contrast, the bootstrap of a single pole, which unfortunately cannot be the Pomeron as stated above is inherent in

the one-pole model (Refs. 14, 15, 16). The schizophrenic Pomeron model of Chew and Snider (Ref. 30), with a more sophisticated version of the 2-pole input similarly imposes the assumption that the leading output pole is at $j=1$ and obtains numerical estimates for the other parameters. The two output poles are very close to each other, with comparable residues for sufficiently small spacing and can be regarded as a single pole.

All these two pole input models have either neglected or represented by a pole in the input, the output cuts arising from the input pole through unitarity. The input of a single pole, through s-channel unitarity, leads to an output cut with its branch-point at the maximum of the expression

$$\alpha(t_1) + \alpha(t_2) - 1$$

where t_1 and t_2 are the momentum transfers flowing through two sides of the unitarity diagram (Refs. 1, 31). On the assumption that $\alpha(t)$ depends linearly on t, then the maximum value of $\alpha(t_1) + \alpha(t_2) - 1$ is given by

$$t_1 = t_2 = \frac{t}{4}$$

on the boundary of the curve

$$t_1^2 + t_2^2 + t^2 - 2t_1t - 2t_2t - 2t_1t_2 = 0 \qquad 2.13$$

where t is the momentum transfer.

This cut at $2\alpha\left(\frac{t}{4}\right)-1$ together with the pole at $\alpha(t)$ in turn produces a cut at $3\alpha\left(t/9\right)-2$ In this manner the continued iteration in the s-channel of the unitarity equation leads to the set of Regge cut trajectories

$$\alpha_n(t) = n\alpha\left(t/n^2\right) - n + 1 \qquad (n = 2,3, \cdots) \qquad 2.1.4$$

A complete bootstrap scheme therefore requires the inclusion of all these cuts in the input.

Hwa (Ref. 32) was able to achieve this complete bootstrap in the s-channel of the Pomeranchuk singularity, the latter turning out to be a branch-point in this scheme. Of course, this bootstrap is not within the multiperipheral model.

Within the framework of multi-Reggeism this motif of the leading singularity being wholly or p artly a cut was discussed by Branson (Ref. 33). He assumes an input corresponding to the asymptotic behaviour

$$s^{\alpha(t)} / (\log s)^{\beta}$$

His output singularity consists of a branch-point and a pole. The branch-point has the nature

$$(j - \alpha_c)^{1/3}$$

or

$$(j - \alpha_c)^{\frac{2}{3}}$$

according as whether a flat input trajectory or a linearly rising one is employed. For positive t, the pole is to the right of the branch-point. For negative t, it is on an unphysical sheet and at $t = 0$ it coincides with the branch-point, its residue vanishing. Thus he achieves self-consistency only in the forward direction since the input pole and branch-point coincide for all t. Also the output singularity corresponds to an asymptotic behaviour of

$$s/(\log s)^{\frac{2}{3}}$$

or

$$s/(\log s)^{\frac{1}{3}}$$

according as whether the input trajectory is flat or linearly rising. This behaviour implies vanishing total cross-sections at asymptotic energies in the single pole input model.

It is possible that a single Pomeron pole, given by a trajectory $\alpha(t)$ together with its associated cuts at branch-points $\alpha_n(t)$ as given by equation 2.1.4 can be bootstrapped obviating the need for either lower-ranking input poles or the assignment of a complex value tothe Pomeranchuk trajectory. In this case, we will have the result that cross-sections tend to a constant.

Such a bootstrap program is as yet technically too difficult. Nevertheless, since for sufficiently small t, the threshold behaviour of cut discontinuities of scattering amplitudes weakens as n

increases (Refs. 1, 34), the inclusion of only the first cut for $n=2$ might be a satisfactory approximation. At any rate, such a partial bootstrap will be a closer approximation to the total bootstrap of pole plus cuts then the partial bootstrap involving a single input pole only. We may then hope, given the hypothesis of the Pomeron pole and its associated cuts bootstrapping themselves, that the inclusion of this cut will push the output trajectory closer to one than in the pole only model. More accurate schemes, involving the input of the iterated cuts for $n=3,4\ldots\ldots$ by the same argument, will result in trajectories closer and closer to one. The pole only model will correspond to the zeroth order and the pole plus $n=2$ cut will correspond to the first order approximations in a series of approximate bootstraps. If in such a bootstrap, we include the pole plus cut up to $n=k$ (say), then there would emerge self-consistently in the output. Also, there will be output cuts for $n>k$ which are neglected in this approximation. From the foregoing, we then have $\alpha(0)$ increasing as k increases.

In this paper, we study the effects of including the cut for $n=2$ in the input in the hope it will lead us to an output trajectory close to one and cross-sections tending to a constant with increasing s. We use Frazer and Mehta's (Ref. 15, 16) multi-Regge integral equation in a factorisable approximation but deriving it by a different method involving the use of Sudakov variables (Refs. 21, 22) following Halliday and Saunders. The parametrisation is the same as that of Frazer and Mehta in order that we may compare the results. We use for the formulae for the discontinuity and

location of the cut, those emerging in the output of the pole only model.

Finally, we also compare the relative contributions of the pole and the elastic $2 \to 2$ amplitude cut in both Frazer and Mehta's model and our model in order to investigate whether the sign agrees with that of the absorption model in view of the well-known disagreement of the latter will multiperipheral models in this respect (Ref. 35).

2. The Sudakov Variables and Kinematics

In this section we shall discuss and outline the characteristics of the Sudakov variables (as in Ref. 22) and their relation to the invariants of the multi-Regge production amplitude in order to facilitate the subsequent derivation of the multi-Regge integral equation

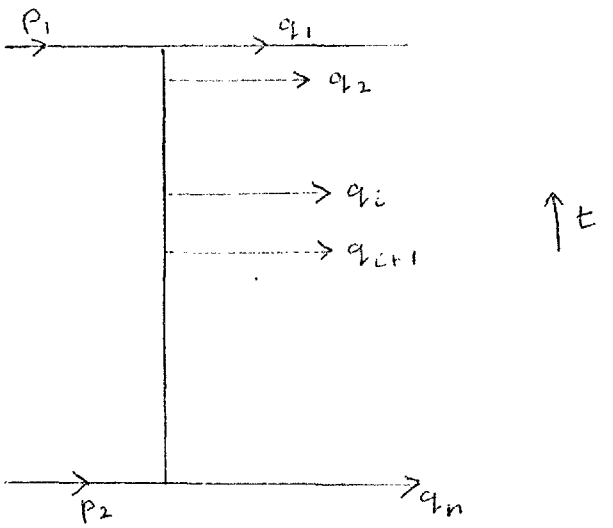

Fig. 4.

The $2 \to N$ amplitude, the Kinematics of which we analyse is

represented by Fig. 4, the variables being as in the Figure. For convenience all particles are taken to be identical and of unit mass.

We define the invariants

$$S = (p_1 + p_2)^2 \qquad 2.2.1$$

$$s_i = (q_i + q_{i+1})^2 \qquad 2.2.2$$

$$t_i = (p_i - \sum_{r=1}^{i} q_r)^2 \qquad 2.2.3$$

Further, we define

$$p_1' = p_1 - \frac{p_2}{S} \qquad 2.2.4$$

$$p_2' = p_2 - \frac{p_1}{S} \qquad 2.2.5$$

and

$$q_i = \alpha_i p_1' + \beta_i p_2' + K_i \qquad 2.2.6$$
$$i = 1, \ldots n$$

the variables α_i, β_i and K_i which is a two vector, are the Sudakov variables.

In the centre of mass frame of p_1 and p_2 it is obvious from 2.2.4 - 2.2.6 that K_i is the transverse part of q_i

$$K_i \cdot p_i = K_i \cdot p_2 = 0$$

and

$$K_i^2 \leq 0$$

Also, since s is large, we have

$$p_1'^2 = p_2'^2 \sim \frac{2}{s} \qquad 2.2.7$$

and

$$2\, p_1' \cdot p_2' \sim s \qquad 2.2.8$$

This in addition implies that

$$p_1^0 = p_2^0 = \frac{\sqrt{s}}{2}$$

Equations 2.2.4 and 2.2.5 also lead to

$$K_i \cdot p_1' = K_i \cdot p_2' = 0$$

Since the q_i are on the mass-shell, we have from 2.2.7 and 2.2.8

$$\alpha_i \beta_i s + K_i^2 = 1 + O\left(\frac{1}{s}\right) \qquad 2.2.9$$

Also, conservation of 4-momentum leads to

$$\sum_{i=1}^{n} \alpha_i = 1 + O\left(\frac{1}{s}\right) \qquad 2.2.10$$

$$\sum_{i=1}^{n} \beta_i = 1 + O\left(\frac{1}{s}\right) \qquad 2.2.11$$

and

$$\sum_{i=1}^{n} K_i = 0 \qquad 2.2.12$$

since

$$q_i^0 \sim (\alpha_i + \beta_i)\sqrt{s}/2 > 0$$

and $\alpha_i \beta_i > 0$ from equation 2.2.9, we have

$$\alpha_i, \beta_i > 0$$

From the above equations, we also obtain

$$s_i = s(\alpha_i + \alpha_{i+1})(\beta_i + \beta_{i+1}) + (K_i + K_{i+1})^2 \qquad 2.2.13$$

and

$$t_i = -s(1 - \alpha_1 - \cdots - \alpha_i)(\beta_1 + \cdots \beta_i) + \left(\sum_{r=1}^{i} K_r\right)^2 \qquad 2.2.14$$

We now introduce the assumptions that

$$s_i \to \infty \quad \text{as} \quad s \to \infty$$

and that the t_i remain small. Equation 2.2.14 then makes it clear that the K_i^2 must be finite. Also from equation 2.2.13, we have

$$s(\alpha_i + \alpha_{i+1})(\beta_i + \beta_{i+1}) \longrightarrow \infty$$

because the term $(K_i + K_{i+1})^2$ gives a negligible contribution

Let

$$a_k = 1 - \sum_{j=1}^{k} a_j \qquad k=1, \ldots n$$

$$a_0 = 1 \qquad 2.2.15$$

and

$$b_k = \sum_{j=1}^{k} \beta_j \qquad k=1, \ldots n$$

$$b_0 = 1 \qquad 2.2.16$$

Clearly, the set a_k is monotonic decreasing and the set b_k is monotonic increasing. Also we have

$$S_i \sim s(a_{i-1} - a_{i+1})(b_{i+1} - b_i) \qquad 2.2.17$$

$$\tau_i = -t_i + \left(\sum_{j=1}^{i} K_j\right)^2$$

$$= s a_i b_i \qquad 2.2.18$$

and

$$s(a_{i-1} - a_i)(b_i - b_{i-1})$$

$$= (1 - K_i^2) = \mu_i^2 \qquad 2.2.19$$

The qualities μ_i^2 are defined by 2.2.19 and are clearly Finite and positive. The conditions, $S_i \to \infty$, τ_i remain finite as $s \to \infty$ and the monotonicity properties of the a_k and b_k lead to

$$s\, a_{i-1}\, b_{i+1} \to \infty \qquad 2.2.20$$

Equations 2.2.19 implies that $S a_{i-1} b_i$ and $S a_i b_{i+1}$ remain finite

Hence

$$\frac{b_{i+1}}{b_i} \longrightarrow \infty$$

and

$$\frac{a_{i-1}}{a_i} \longrightarrow \infty \qquad 2.2.21$$

Therefore equation 2.2.15 leads to

$$\frac{\alpha_i - \alpha_{i+1}}{a_i} = \left[\frac{a_{i-1}}{a_i} - 1\right] - \left[1 - \frac{a_{i+1}}{a_i}\right]$$

$$\longrightarrow \infty \qquad 2.2.22$$

Thus the sequence $\{\alpha_i\}$ is monotonic decreasing and $\{\beta_j\}$ is monotonic increasing. It also follows that

$$\tau_i = S a_{i-1} b_i \frac{a_i}{a_{i-1}}$$

$$\longrightarrow 0 \qquad 2.2.23$$

The above equation states that all momentum transfers arise from the transverse components

$$\left(\sum_i^i K_j\right)^2$$

Applying this equation to τ_i leads to

$$\alpha_i \rightarrow 1$$

and

$$\beta_i \longrightarrow 0\left(\frac{1}{s}\right) \qquad 2.2.24$$

By symmetry, we then have

$$\alpha_n \sim O\left(\frac{1}{s}\right) \qquad 2.2.25$$

and

$$\beta_n \longrightarrow 1$$

We also obtain relations between s and the S_i From equations 2.2.9, 2.2.13 and 2.2.21

$$S_i \sim \frac{\alpha_i}{\alpha_{i+1}} \mu_{i+1}^2 \qquad 2.2.26$$

This leads to

$$\prod_{i=1}^{n-1} S_i = \frac{\alpha_1}{\alpha_2} \cdot \cdots \cdot \frac{\alpha_{n-1}}{\alpha_n} \prod \mu_{i+1}^2$$

$$\sim s \prod \mu_{i+1}^2 \qquad 2.2.27$$

2.2.27 follows from $\beta_n \longrightarrow 1$ and 2.2.9

We now define a further set of subenergies used in the next chapter

Let

$$S_{ij} = \left[\sum_{r=1}^{j} q_r\right]^2 \qquad 2.2.28$$

where

$$i = 1, 2, \ldots n-1 \quad \text{and} \quad i < j$$
$$j = 2, 3, \ldots n$$

then

$$S_i = S_{i\,i+1}$$

Clearly, similar to equation 2.2.13, we have

$$S_{ij} = s\left(\sum_{r=i}^{j} \alpha_r\right)\left(\sum_{r=i}^{j} \beta_r\right) + \left(\sum_{r=i}^{j} K_r\right)^2 \qquad 2.2.29$$

Also, obviously the $s_{ij} \to \infty$

It is then a simple matter to go through similar arguments to those preceding 2.2.27 and arrive at the corresponding equation for the s_{ij}. Evidently s could be expressed as proportional to a product of the such that none of the sub-energies overlap. It will have to be of the form

$$s \propto s_{1i_1} s_{i_1 i_2} s_{i_2 i_3} \cdots s_{i_r n}$$

where

$$1 < i < i_2 < \cdots < i_r < n$$

There are a number of such possible equations between the s and the s_{ij} Consider one of them

$$s_1 s_2 s_3 \cdots s_{i-1} s_{ij} s_j \cdots s_{n-1}$$

$$= s \left[\prod_{r=1}^{i-1} \mu_{r+1}^2 \right] \mu_j^2 \left[\prod_{j}^{n-2} \mu_{r+1}^2 \right] \qquad 2.2.30$$

Equation 2.2.30 together with 2.2.27 then leads to

$$s_{ij} = \frac{\prod_{r=i}^{j-1} s_r}{\prod_{r=1}^{j-2} \mu_{r+1}^2} \qquad 2.2.31$$

3. <u>The Unitarity Equation and the M.R.M.</u>

In this section, we use the Sudakov formalism just described to derive very easily the bootstrap equations of the pole-only model. These were arrived at by a different method by Frazer and Mehta (Ref. 16). The latter derived their equations using the formalism of

Chew, Goldberger and Low (Ref. 13).

The $2 \to 2$ unitarity equation reads

$$\mathrm{Im}\, A_{22}(s,t) = \sum_{N=2}^{\infty} \left\{ \int \prod_{i=1}^{N} \left[d^4 q_i\, \delta(q_i^2 - M^2) \right] \delta_4 \left(\Sigma q_i - p_1 - p_2 \right) A_{2N}\, A_{2N}^{*} \right\} \qquad 2\cdot3\cdot1$$

where Fig. 5 represents a typical term on the right-hand side, M is the particle mass and the blobs represent the $2 \to N$ amplitudes A_{2N}. We have eliminated the factors $(2\pi)^{-3}$ by normalising suitably the amplitudes A_{2N} in order to facilitate comparison of our work with that of Frazer and Mehta. We have also cancelled an $n!$ and agreed to integrate over only one of the $n!$ possible M.R.M. configurations of the n particles.

In the multi-Regge model (Refs. 13, 14) A_{2N} is represented by Fig. 6, the wavy lines standing for Reggeons and the straight lines for particles. As mentioned earlier, all particles are assumed to be identical and of zero spin, isospin and electric charge.

A_{2N} is given by

$$A_{2N} = G(t_1)\, G(t_{n-1}) \left\{ \prod_{i=1}^{N-2} g(t_i, t_{i+1}, \omega_i) \prod_{i=1}^{N-1} \left[s_i^{\alpha(t_i)}\, e^{\frac{1}{2} i\pi\alpha(t_i)} \right] \right\}$$

where $e^{\frac{1}{2} i\pi\alpha(t_i)}$ is the signature factor $G(t_1)$

and $G(t_{n-1})$ are the Reggeon-particle-particle coupling functions at the end of the multi-Regge chain. $g(t_i, t_{i+1}, \omega)$ is the Reggeon-Reggeon-particle coupling function occuring at each internal vertex and $\alpha(t)$ is the input Regge trajectory which we shall assume to be linearly rising and parametrised in the form $a+bt$. Though the slope of the Pomeranchuk trajectory seems small experimentally (Ref. 35) we do not assume a flat trajectory for the Pomeron as it isolates the Froissart bound when used in conjunction with the M.R.M. (Ref. 22).

Also

$$s_i = (q_i + q_{i+1})^2$$

$$t_i = \left[p_i - \sum_{r=1}^{i} q_r\right]^2$$

and the ω_i are the Toller angles between different frames in the multi-Regge amplitude

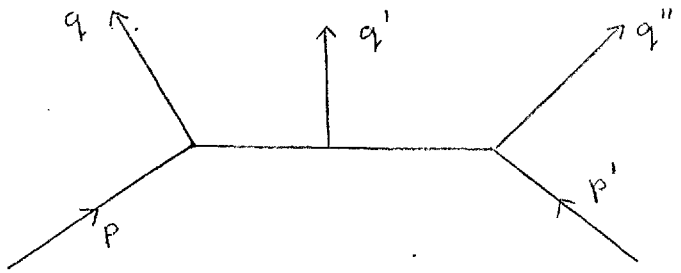

Fig. 7.

The Toller angle is defined with reference to Fig. 7 as the spatial angle between the plane formed by the three vectors p' and q'' and the plane formed by p and q in the rest frame of q'

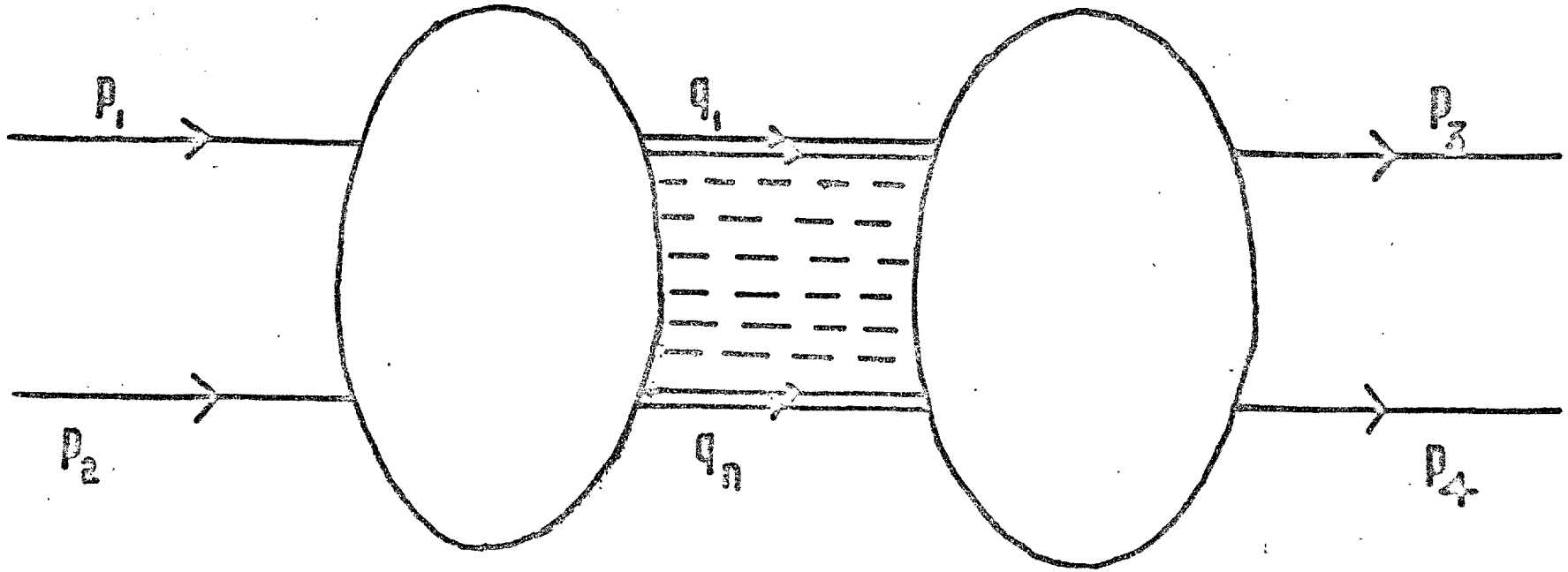

Fig. 5

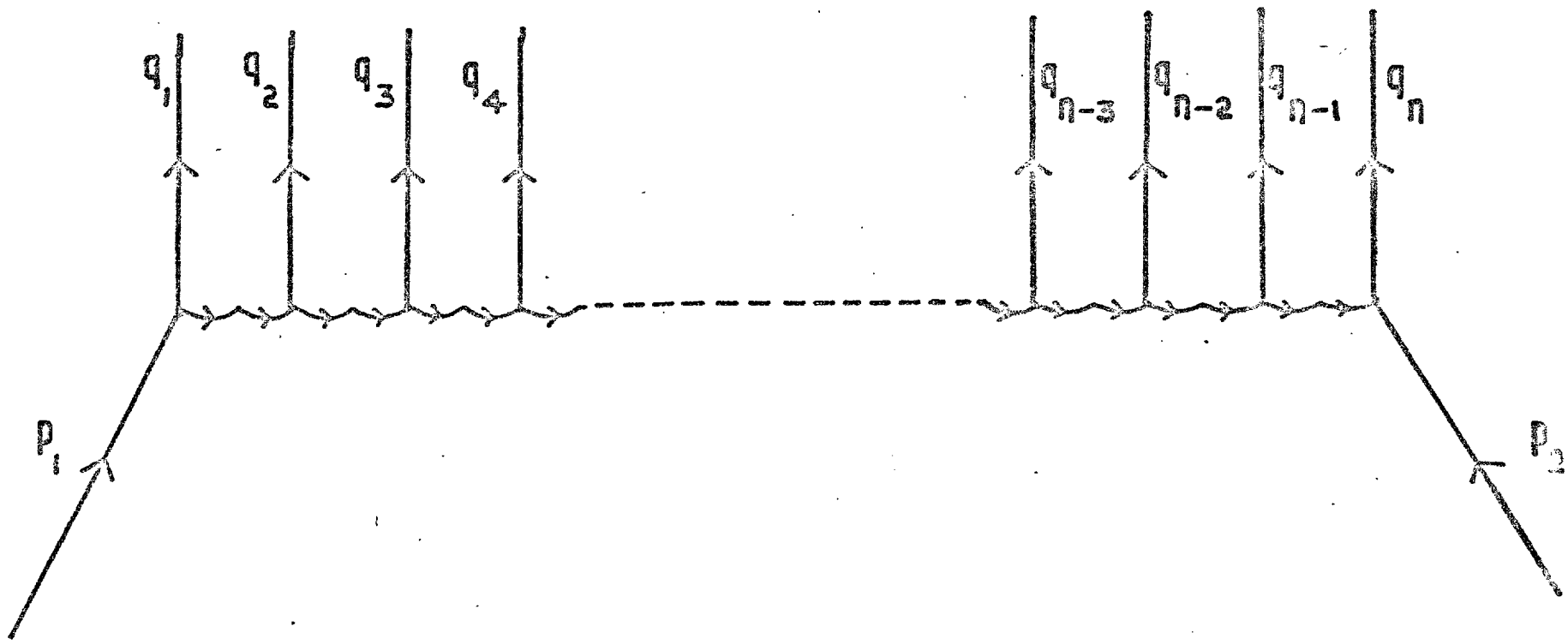

Fig. 6

Thus the N intermediate particles state contribution to the amplitude B_N (corresponding to Fig. 8) is given by

$$B_N(s,t) = \frac{1}{2^n s}\left\{\prod^{N}\left[\int d^4q_i\,\delta(q_i^2-M^2)\right]\delta\left(\Sigma q_i - P_1 - P_2\right)\right.$$

$$G(t_1)G(t_1')\,G(t_{n-1})\,G(t'_{n-1})\prod_{1}^{N-2}\left[g(t_i,t_{i+1},\omega)\right.$$

$$g^{*}(t_i',t_{i+1}',\omega)\Big]\prod_{1}^{N-1}\left[s_i^{\,\alpha(t_i)+\alpha(t_i')}\right.$$

$$\left.\left.e^{\frac{1}{2}i\pi\left[\alpha(t_i)-\alpha(t_i')\right]}\right]\right\} \qquad 2.3.3$$

where the variables not defined in Fig. 5 are given by

$$t_i = \left[p_3 - \sum^{c} q_r\right]^2$$

$$t = (p_3 - p_1)^2$$

and

$$s = (p_1 + p_2)^2$$

We now change to the Sudakov variables defined in the previous section. The Jacobian of the transformation from d^4q_i to $d\alpha_i\,d\beta_i\,d^2K_i$ is clearly $s/2$ and thus

$$\delta(q_i^2 - M^2)\,d^4q_i = \frac{s}{2}\,d\alpha_i\,d\beta_i\,\delta(\alpha_i\beta_i s - \mu_i^2)\,d^2K_i$$

We then obtain

$$\mathrm{Im}\,A_{22}(s,t) = \sum_{N=2}^{\infty} B_N(s,t) \qquad 2.3.4$$

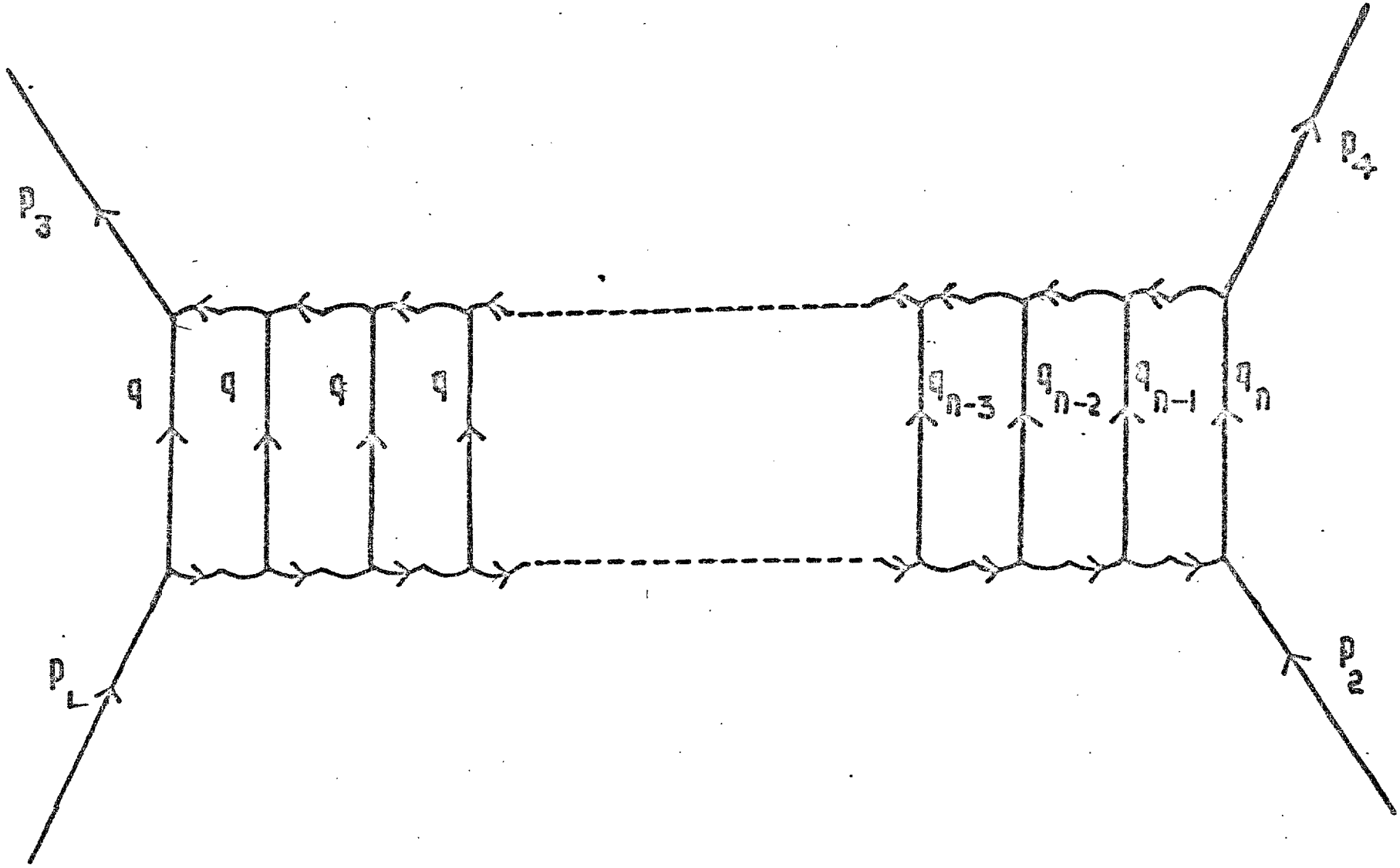

Fig. 8

where

$$B_N(s,t) = \frac{1}{2^n s}\left\{\prod^{N}\left[\int d\alpha_i\, d\beta_i\, \delta\left(\alpha_i\beta_i - \frac{\mu_i^2}{s}\right)\right]\delta(\Sigma\alpha_i - 1)\right.$$

$$\delta(\Sigma\beta_i - 1)\,\delta(\Sigma K_i)\,G(t_1)\,G(t_1')\,G(t_{n-1})\,G(t_{n-1}')$$

$$\prod_1^{N-2}\left[q(t_i,t_{i+1},\omega)\,q^*(t_i',t_{i+1}',\omega)\right]\prod_1^{N-1}\left[s_i^{\alpha(t_i)+\alpha(t_i')}\right.$$

$$\left.\left.e^{\frac{1}{2}i\pi[\alpha(t_i)-\alpha(t_i')]}\right]\right\} \qquad 2.3.5$$

The factor s^{-1} on the right-hand side arises from the transformation of the δ– functions which satisfy the relations

$$\delta(ax) = \frac{1}{a}\,\delta(x)$$

We now make the substitution

$$u_i = \frac{\log s_i}{\log s}$$

From 2.2.26, we have

$$s_i = \frac{\alpha_i}{\alpha_{i+1}}\,\mu_{i+1}^2$$

We use the n factors $\delta\left(\alpha_i\beta_i - \frac{\mu_i^2}{s}\right)$ to dispose of the β_i integrals. Next we effect the transformation from the α_i integration to the u_i integration. The Jacobian J of the transformation is, after taking into account the 2 δ–functions already present and the fact that α_1 and β_N can be assumed to be unity, given by

$$J = (\log s)^{n-2}\,\delta\left(\Sigma u_i - 1 - \frac{\Sigma \log \mu_i^2}{\log s}\right) \qquad 2.3.6$$

We also make the additional transformations from the set of n two-vectors to the set of $n-1$ two vectors $\bar{K}_i$ which are given by

$$\bar{K}_i = \sum_{r=1}^{i} K_r \quad , i = 1, \ldots, n-1 \qquad 2.3.7$$

The extra K_i is absorbed by the factor $\delta(\Sigma K_i)$ in 2.3.5. Hence, we have

$$B_N(s,t) = \frac{(\log s)^{n-2}}{2^n s} \left\{ \prod_{i=1}^{n-1} \left[\int_{\varepsilon}^{1} du_i \right] \delta\left(\Sigma u_i - 1 - \frac{\Sigma \log \mu_i^2}{\log s} \right) \right.$$

$$\prod_{i=1}^{N-2} \left[g(t_i, t_{i+1}, \omega) \right] g^*(t_i', t_{i+1}', \omega) \Big]$$

$$\left. \prod_{i=1}^{N-1} \exp\{ u_i \log s \left[\alpha(t_i) + \alpha(t_i') \right] \} \right\} \qquad 2.3.8$$

To improve the convergence properties of the above equation, we multiply the right-hand side by a factor

$$\exp\left[-2\alpha(0) \log s \left(\Sigma u_i - 1 - \frac{\Sigma \log \mu_i^2}{\log s} \right) \right] = 1$$

In equation 2.3.8, the lower limit ε of the u_i integrations is given by

$$\varepsilon = \frac{\log M^2}{\log s}$$

where M^2 is a number such that we believe the multi-Regge model to hold true only when all the $s_i \geq M^2$. Also the upper bound is

not really unity but determined by the factor

$$\delta\left(\sum u_i - 1 - \frac{\sum \log \mu_i^2}{\log s}\right)$$

and hence it wont make a difference if we replace the upper limit unity with infinity. Performing the u_i integrations is facilitated by replacing the δ— function in the right-hand side of equation 2.3.8 with its integral representation

$$\int_{-\infty}^{+\infty} dy\, e^{iy\left(\sum u_i - 1 - \frac{\sum \log \mu_i^2}{\log s}\right)}$$

We now integrate the u_i from ξ to ∞ and obtain

$$B_N(s,t) = \frac{(\log s)^{N-2}}{2^N s} \int_{-\infty}^{+\infty} dy \left\{ e^{-iy} s^{2\alpha(0)} G(t_1) G(t_1') \right.$$

$$G(t_{n-1}) G(t_{n-1}') \prod_{i=1}^{N-2} [g(t_i, t_{i+1}, \omega)]$$

$$\prod_{i=1}^{N-2} [g^*(t_i', t_{i+1}', \omega)] \prod_{i=1}^{N-1} \left\{ \frac{d^2 \bar{K}_i \cdot [-M^{2[\alpha(}}{iy + \log s\,(\alpha(t_i)} \right.$$

$$\left. \frac{(t_i) + \alpha(t_i') - 2\alpha(0) + \frac{iy}{\log s}]}{+\alpha(t_1') - 2\alpha(0)} \right\} \exp\left[-iy \log \mu_{i+1}^2 \right.$$

$$\left. + 2\alpha(0) \log \mu_{i+1}^2 \right] \Bigg\}$$

2.3.9

We now undo one of the end integrations and define

$$\mathcal{D}_N(\bar{K},\gamma,s,t) = \frac{(\log s)^{n-3}}{2^n}\left\{ G(t_{n-1})\, G(t'_{n-1})\, g(t_1,t_2,\omega) \right.$$

$$g^*(t_1,t_2',\omega)\prod_{2}^{N-2} g(t_i,t_{i+1},\omega_i)\, g^*(t_i',t_{i+1}',\omega_i)$$

$$\prod_{i=2}^{N-1}\left\{ d^2\bar{K}_i \frac{-M^2\left[\alpha(t_i)+\alpha(t_i')-2\alpha(0)+\frac{i\gamma}{\log s}\right]}{i\gamma+\log s\left[\alpha(t_1)+\alpha(t_1')-2\alpha(0)\right]} \exp\left(\right.\right.$$

$$\left.\left. -i\gamma\frac{\log\mu_{i+1}^2}{\log s} + 2\alpha(0)\log\mu_{i+1}^2 \right\}\right\}$$

This enables us to write down the multi-Regge integral equation as it is easy to see that $\mathcal{D}_N(\bar{K},\gamma,s,t)$ satisfies the recurrence relation

$$\mathcal{D}_N(\bar{K},\gamma,s,t) = \frac{\log s}{2}\left\{\int d^2K\left[g(k^2,\bar{k}^2,\omega)\, g^*(\bar{k}'^2,k'^2,\omega)\right.\right.$$

$$\left\{\frac{-M^2\left[\alpha(\bar{t})+\alpha(\bar{t}')-2\alpha(0)+\frac{i\gamma}{\log s}\right]}{i\gamma+\log s\left[\alpha(t_1)+\alpha(t_1')-2\alpha(0)\right]}\right\}$$

$$\left.\left.\exp\left\{-i\gamma\frac{\log\mu_i^2}{\log s}+2\alpha(0)\log\mu_i^2\right\}\right]$$

$$\left. B_{N-1}(\bar{K},\gamma,s,t)\right\}$$

2-3-10

where

$$k' = \hat{p} - K, \quad t = \hat{p}^2$$

$$\bar{t} = K^2 \quad \text{and} \quad \bar{t}' = K'^2$$

The kernel of the integral equation is enclosed within the square bracket and the equation itself is obtained by summing

$$\mathcal{D}(\bar{K},\beta,s,t) = \sum D_N(\bar{K},\beta,s,t)$$

Actually as proved by Halliday and Saunders (Ref. 22) the summation should be performed only for $h \lesssim$ logs. The proof is very simple. Referring back to the previous section on Sudakov variables, we define

$$\alpha_i = s^{-x_i}$$

2.3.11

Then clearly $\{x_i\}$ is monotonic increasing

$$x_0 = 0 \qquad \text{and} \qquad x_n = 1$$

Thus

$$s_i = \mu_{i+1}^2 \exp\left[\log s\,(x_{i+1} - x_i)\right]$$

2.3.12

and we have

$$\min_{i=1,n-1} (x_{i+1} - x_i) = \varepsilon$$

where

$$\frac{1}{\varepsilon} = o(\log s)$$

and

$$n\varepsilon \lesssim 1$$

However, we follow Halliday (Ref. 14) in assuming that the correct answer is obtained by summing to ∞ since $s \to \infty$

Frazer and Mehta, to solve their integral equation, used the

weak coupling approximation of Chew, Goldberger and Low (Ref. 13) We shall make a similarly drastic assumption in order to solve our integral equations. It is that we may ignore the terms $\Sigma \log \mu_i^2$ in the factor

$$\delta\left(\Sigma u_i - 1 - \frac{\Sigma \log \mu_i^2}{\log s}\right)$$

which occured above. Then the exponential term in the kernel of the integral equation becomes one.

Hitherto, we have parametrised the two Reggeon-particle coupling function by $g(t_i, t_{i+1}, \omega)$ From this point onwards, we shall assume independence of the Toller angle ω From group theoretical considerations, as analysed by Bali, Chew and Pignotti (Ref. 17), the inclusion of the Toller angle in addition to the adjacent momentum transfers to describe the couplings at the internal Reggeon-Reggeon-particle vertices is very natural. Such a dependence was also established by Drummond, Landshoff and Zakrewski (Ref. 36). We base our assumption on peripheral considerations.

There have been a number of attempts to determine the dependence of the internal couplings on ω (Refs. 37, 38, 39) Tan and Wang (Ref. 40) examined this problem, basing their study on analyticity properties of production amplitudes. They pointed out that the internal Regge couplings associated with the leading asymptotic power term is independent of ω if either one or both of the adjacent momentum transfers associated with this vertex reduce to zero. On the assumption of factorisation of the leading s-behaviour of the multi-Regge model, the internal Regge

vertex appearing in the $2 \to 3$ production amplitude is the same as those in the $2 \to N$ amplitude and hence they confined their discussion to the former represented by Fig. 7. They also gave a brief intuitive explanation as follows.

We consider only the events for which the 3-momenta $\underline{p}$ and $\underline{q}$ are parallel. For these events, it is not possible to distinguish geometrically or physically one value of ω as from another. Therefore, the differential cross-sections for these events must be independent of ω It is easy to prove algebraically, from the Kinematics that

$$s_1 t_1 (3M^2 + t_2 - s_1 - t_1) - M^2 (t_2 - M^2) = 0 \qquad 2.3.13$$

From this equation, it is clear that for fixed t_2, $t_1 \to \infty$ as s_1 and $s_2 \to \infty$ however, the M.R.M. is the description of the scattering amplitude in the phase-space region given by $s_1, s_2 \to \infty$ and fixed t_1, t_2 Therefore, the independence of the differential cross-section for the above mentioned events implies the ω independence of the leading M.R.M. asymptotic term at $t_1 = 0$ (i.e. t_1 is kept fixed at zero). This means that the internal Regge coupling is independent of ω Since a fundamental assumption in multiperipheral models is the smallness of the momentum transfers, the above arguments justify assuming Toller angle independence.

The other assumption we make concerning $g(t_i, t_{i+1})$ following Halliday (Ref. 14) and Frazer and Mehta (Ref. 16) is that it is factorisable in t_i and t_{i+1} Thus we write

$$g(t_i, t_{i+1}) = g f(t_i) f(t_{i+1}) \qquad 2.3.14$$

where g is the Reggeon-Reggeon-particle coupling constant. Up to now, we have assumed that g is a complex number. Halliday and Saunders (Ref. 41) analysing the $2 \to 3$ multi-Regge unitarity equation along the same lines as Halliday's analysis of the $2 \to 2$ equation (Ref. 14) came to the conclusion that g is probably complex. This was due to the fact that unlike in the $2 \to 2$ case, $Im T_{23}$ is not automatically forced to be a real number by the unitarity equation for the s-matrix

$$S S^{+} = 1 \qquad 2.3.15$$

but we also have to impose the conjugate equation

$$S^{+} S = 1 \qquad 2.3.16$$

This follows from the lack of symmetry of the $2 \to 3$ diagram (Fig. 9) which means that the signature factors are not automatically cancelled out.

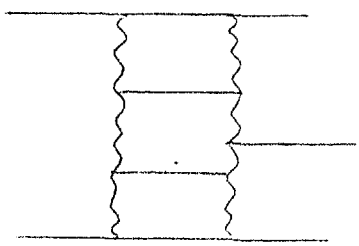

Fig. 9

Drummond, Landshoff and Zakrewski also concluded that g is complex by analytical means.

For our bootstrap equations both in the pole-only model and the pole plus cut model which will be introduced by us, this point is irrelevant as it can be seen from 2.3.9 that the phase factors

in g and g^* cancel. Nevertheless, it is worth noting that what we calculate in this chapter is $|g|$ and not g. To evaluate the phase of g, one needs to study the $2 \to 3$ unitarity equation.

We now incorporate the approximations mentioned above and the separability and Toller angle independence of the coupling constant g in our multi-Regge integral equation 2.3.10. These assumptions enable us to solve 2.3.10 by summing 2.3.9 directly since they cause the right-hand side of the latter to factorise.

Thus we obtain from 2.3.4. and 2.3.9

$$\text{Im } A_{22}(s,t) = \frac{1}{8}\int_{-\infty}^{+\infty} d\gamma\, e^{-i\gamma} s^{2\alpha(0)-1} \left\{ \sum_{n=1}^{\infty} \left[\right.\right.$$

$$\left[\bar{\rho}(s,\gamma,t)\right]^2 \log s \left[\frac{\log s}{2} \bar{\bar{\rho}}(\right.$$

$$\left.\left. s,\gamma,t)\right]^{n-1} \right] \Bigg\}$$

2.3.17

where

$$\bar{\rho}(s,\gamma,t) = g\int \frac{d^2K\; G(\bar{t})\,G(\bar{t}')\,f(\bar{t})\,f(\bar{t}')\, e^{i\pi[\alpha(\bar{t})-\alpha(\bar{t}')]}}{i\gamma + \log s\,[\alpha(\bar{t})+\alpha(\bar{t}')-2\alpha(0)]}$$

and

$$\bar{\bar{\rho}}(s,\gamma,t) = g\int \frac{d^2K\; f^2(\bar{t})\, f^2(\bar{t}')\, e^{i\pi[\alpha(\bar{t})-\alpha(\bar{t}')]}}{i\gamma + \log s\,[\alpha(\bar{t})+\alpha(\bar{t}')-2\alpha(0)]}$$

2.13.18

2.3.17 leads to

$$\text{Im } A_{22}(s,t) = \frac{1}{8}\int_{-\infty}^{+\infty} d\gamma\, e^{-i\gamma} s^{2\alpha(0)-1} \frac{\left[\bar{\rho}[s,\gamma,t]\right]^2 \log s}{1+\left[\frac{\log s}{2}\bar{\bar{\rho}}(s,\gamma,t)\right]}$$

2.3.19

From 2.3.10, it can be seen that the kernel has a cut in γ starting at the maximum value of $\{i\,[\alpha(\bar{t}_i)+\alpha(\bar{t}_1')-2\alpha(0)]$ logs$\}$ which is $i\,[2\alpha(t/4)-2\alpha(0)]$ logs as clear from the reasoning in section one. There are also poles in γ which determine the asymptotic behaviour of the amplitude. These poles occur when the denominator of 2.3.19 is zero. That is when

$$1 = -\frac{\log s}{2}\,\bar{\rho}(\gamma,s,t) \qquad 2.3.20$$

The solution is obviously of the form

$$\gamma = -\,i\gamma(t)\log s \qquad 2.3.21$$

giving rise to the asymptotic behaviour

We now proceed to obtain Frazer and Mehta's bootstrap equations by shifting to the conventional J -plane. We achieve this by using the Mellin transform technique, which is a powerful tool to study high-energy behaviour.

The Mellin transform and its inverse are defined by

$$F(\beta) = \int_0^\infty f(t)\,t^{-\beta-1}\,dt \qquad 2.3.22$$

and

$$f(t) = \frac{1}{2\pi i}\int_{C-i\infty}^{C+i\infty} F(\beta)\,t^{\beta}\,d\beta \qquad 2.3.23$$

where c is chosen, such that the contour parallel to the imaginary axis running from $C-i\infty$ to $C+i\infty$ is to the right of all singularities of $f(t)$ in the t-plane.

In equations 2.3.13 and 2.3.19 by making the substitution

$$j+\bar{c} = 2\alpha(0)-1+\bar{c}-2i\gamma/\log s \qquad 2.3.24$$

where $\bar{c}$ is an arbitrary quantity introduced to ensure that $2\alpha(0)-1+\bar{c}$ is to the right of all j -plane singularities, it is easy to see that the right-hand side of 2.3.19 represents the inverse Mellin transform of $A_{22}(j,t)$ expressed in the form of 2.3.23.

Hence we can write

$$\mathrm{Im}\ A_{22}(j,t) = \frac{[\bar{\rho}(j,t)]^2}{1-\bar{\bar{\rho}}(j,t)} \qquad 2.3.25$$

where

$$\bar{\rho}(j,t) = g\int \frac{d^2K.\ G(\bar{t})\,G(\bar{t}')f(\bar{t})f(\bar{t}')}{j-\alpha(\bar{t})-\alpha(\bar{t}')+1}\exp[\alpha(\bar{t})-\alpha(\bar{t}')] \qquad 2.3.26$$

and $\bar{\bar{\rho}}(j,t)$ is the same except that we replace the $G(\bar{t})\,G(\bar{t}')$ by $f(\bar{t})\,f(\bar{t}')$

We use Frazer and Mehta's parametrisation for the two-particle-Reggeon and two-Reggeon-particle coupling functions and define

$$G(t) = \sqrt{2}\ G e^{\frac{1}{2}kt} \qquad 2.3.27$$

and

$$f(t) = e^{\frac{1}{2}kt}$$

This parametrisation in exponential form is consistent with the multiperipheral requirement that the amplitude is dominated by small values of the momentum transfers along the chain and falls off rapidly for large values. We follow Frazer and Mehta in assuming the same momentum transfer dependence K in both 2.3.26 and 2.3.27.

The s-plane version of equation 2.3.26 (after incorporating the equations 2.3.27 and 2.3.28), is given by

$$\bar{\rho}(s,t) = g G^2 \int d^2K \, e^{k\bar{E}+k\bar{E}'} e^{i\pi[a(\bar{t})-a(\bar{t}')]} s^{a(\bar{E})+a(\bar{E}')-1}$$

2.3.29

it is obvious that $\bar{\rho}(s,t)$ and $\bar{\bar{\rho}}(s,t)$ are proportional to the elastic $2 \to 2$ amplitude given by Fig.10 which is in fact equal to $G^2\bar{\rho}(s,t)$ Also clearly the right-hand side of equation 2.3.25 does not contain this amplitude and is equal to only the production contribution to $Im A_{22}(s,t)$ Since the pole position and the asymptotic behaviour is determined by the latter, it hasn't affected the arguments hitherto, but for an accurate evaluation of the residue, the inclusion of this is necessary.

Thus on adding $G^2\bar{\rho}(s,t)$ to the right-hand side of 2.3.25, we have

$$Im\, A_{22}(s,t) = \frac{G^4 \rho(s,t)}{1 - g^2(s,t)} \qquad 2.3.30$$

where

$$\rho(s,t) = G^{-2} g^{-1} \bar{\rho}(s,t) \qquad 2.3.31$$

$\rho(s,t)$ the s-plane equivalent of $\rho(s,t)$ can be recognised as the expression on the right-hand side of equation 6.4 in (Ref. 22) where n is equal to 2. As suggested in that paper, the easiest method of tackling the integration is by considering the integrand to be a Gaussian converting all the terms accordingly into the appropriate form. However, we are interested in deriving the same bootstrap equations as Frazer and Mehta in order to demonstrate the equivalence of the two methods and the approximations used. Hence

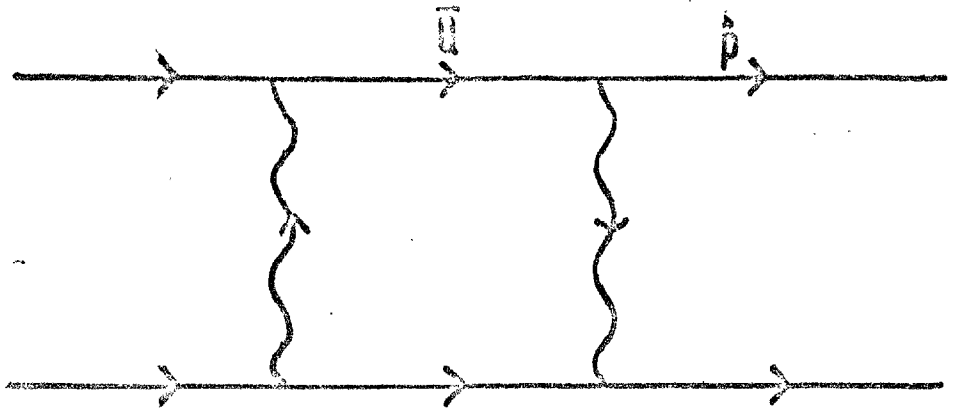

Fig. 40

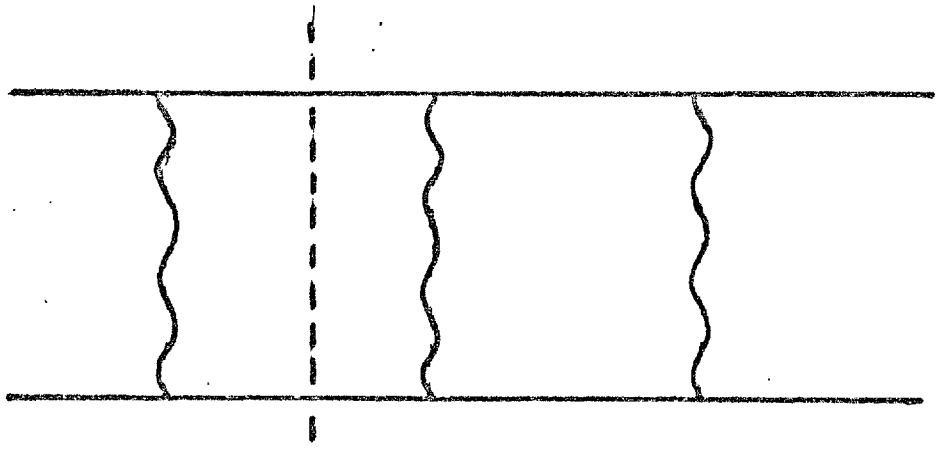

Fig. 41

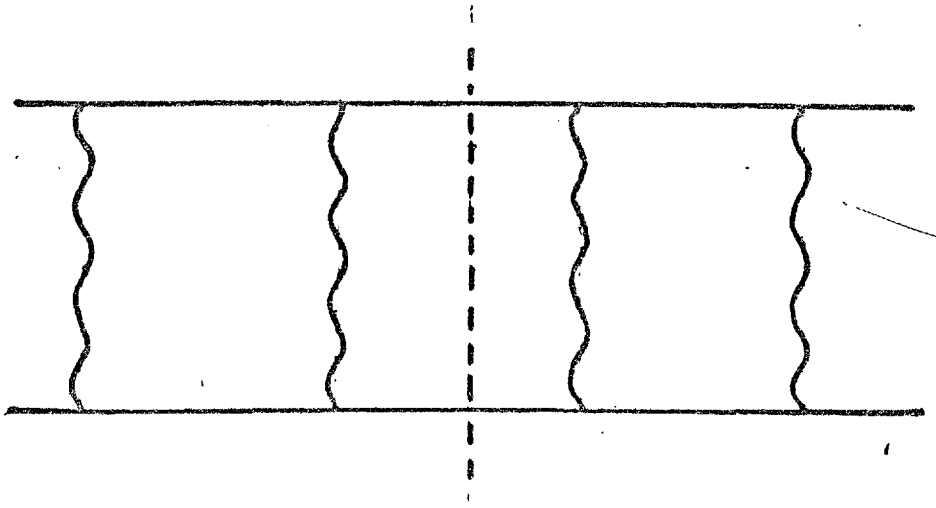

Fig. 42

we transform the integration from the variables $\bar{K}$ to the invariants $\bar{t}$ and $\bar{t}'$ The Jacobian J of the transformation is given by

$$J = \frac{\theta\,[2\bar{t}\bar{t}' + 2\bar{t}t + 2\bar{t}'t - \bar{t}^2 - \bar{t}'^2 - t^2]}{[2\bar{t}\bar{t}' + 2\bar{t}t + 2\bar{t}'t - \bar{t}^2 - \bar{t}'^2 - t^2]^{1/2}}$$

2-3.32

The expression in the denominator is the Kibble function (Ref. 42) which occurs frequently (see Ref. 1) in multiperipheral phase space evaluation when the integration is over invariants rather than the momenta as in 2.3.29. The curve determines the limits of the integration.

Thus we obtain

$$\rho(j,t) = \int d\bar{t}\, d\bar{t}' \left\{ \frac{e^{k(\bar{t}+\bar{t}')}\, e^{\frac{1}{2}i\pi(\alpha(\bar{t})-\alpha(\bar{t}'))}}{j - \alpha(\bar{t}) - \alpha(\bar{t}') + 1} J \right\}$$

2.3.33

The integral is reduced by means of the successive transformations

$$\xi = \bar{t} + \bar{t}' \quad , \quad \eta = \bar{t} - \bar{t}'$$

$$p = \eta \quad , \quad q = -\eta^2 + 2t\xi - t^2$$

and

$$p = -4tr^2\cos\theta \quad , \quad q = -4tr^2\sin\theta$$

We then obtain

$$\rho(j,t) = \pi e^{\frac{1}{2}kt} \int_0^\infty \frac{dr^2\ e^{-2kr^2} J_0[\pi b r\sqrt{-t}]}{j - 2\alpha(-r^2 + \frac{1}{4}t) + 1} \qquad 2\cdot3\cdot34$$

Equation 2.3.39 is the same as equation 3.14 of (Ref.16) except for a normalisation factor. Frazer and Mehta analysed this equation in (Ref. 15) approximately and in (Ref. 16) exactly. It is worthwhile repeating the approximate analysis in order to pinpoint the importance of the signature factor in the multi-Regge bootstrap.

Making the approximation that the value of j is far from the cut beginning at $2\alpha(\frac{t}{4})-1$ in 2·3·34 we obtain

$$\rho(j,t) \approx \frac{1}{j - 2\alpha(\frac{t}{4}+1)} \pi e^{\frac{kt}{2}} \int_0^\infty dr^2 e^{-2kr^2} J_0[\pi b r\sqrt{-t}]$$

$$= \frac{1}{j - 2\alpha(\frac{t}{4})+1} e^{k't} \qquad 2\cdot3\cdot35$$

where

$$k' = \frac{k}{2} + \frac{\pi^2 b^2}{8k} \qquad 2\cdot3\cdot36$$

Thus from 2.3.30 we obtain

$$\mathrm{Im}\, A_{22}(j,t) \propto \frac{e^{k't}}{j - 2\alpha(t/4)+1-g^2 e^{k't}} \qquad 2\cdot3\cdot37$$

In the multi-Regge bootstrap, the pole is given by the zero of the denominator and on equating the t- dependence of the input and output residues, we get

$$k = \frac{k}{2} + \frac{\pi^2 b^2}{8k}$$

Thus if not for the term $\frac{\pi^2 b^2}{8k}$ which originates from the signature factor, self consistency would be impossible.

We now proceed to obtain the bootstrap equation from equation 2.3.34 without making the above approximation. At high energy, the left-hand side of equation 2.3.30 is approximately expressed in terms of the output Regge pole with trajectory $\alpha(t)$ since we assume the output and input trajections are the same in the single pole bootstrap. i.e.

$$\text{Im } A_{22}(j,t) = \frac{G^2 e^{kt}}{j - \alpha(t)} \qquad 2.3.39$$

The right-hand side of 2.3.30 has a pole at the value of j for which

$$g^2 \rho(j,t) = 1 \qquad 2.3.40$$

and the residue $R(t)$ at this pole is given by

$$R(t) = -G^4 \left[g^4 \frac{\partial \rho(j,t)}{\partial j} \right]^{-1} \qquad 2.3.41$$

Equating the trajectory slopes and intercepts of the poles on the right-hand side and left-hand side

$$\rho[\alpha(0),0] = \frac{1}{g^2} \qquad 2.3.42$$

$$\left[\frac{d}{dt}\left\{\rho[\alpha(t),t]\right\}\right]_{t=0} = 0 \qquad 2\cdot3\cdot43$$

Similarly bootstrapping the residue functions

$$R(0) = G^2 \qquad 2\cdot3\cdot44$$

$$k = R'(0)/R(0) \qquad 2\cdot3\cdot45$$

Equations 2.3.42 up to 2.3.45 lead to the bootstrap equations

$$\frac{\pi g^2}{2k\Delta} e^A E_c(A) = 1 \qquad 2\cdot3\cdot46$$

$$e^A E_c(A)\left[1 - \frac{1}{8}\pi^2\Delta^2 A\right] + \frac{1}{8}\pi^2\Delta^2 - \frac{1}{2A} = 0 \qquad 2\cdot3\cdot47$$

$$-e^A E_c(A) + \frac{1}{A} = e^A E_c(A)\left[1 - \frac{1}{8}\pi^2\Delta^2 - \frac{1}{8}\pi^2\Delta^2 A\right] + \frac{1}{8}\pi^2\Delta^2 - \frac{1}{A} - \frac{1}{2A^2} \qquad 2\cdot3\cdot48$$

$$\frac{\pi G^2}{2k} = -\frac{1}{\Delta^2}\left(\frac{\pi g^2}{2k}\right)^2\left[e^A E_c(A) - \frac{1}{A}\right] \qquad 2\cdot3\cdot49$$

where

$$A = \frac{1-a}{\Delta} \quad \text{and} \quad \Delta = \frac{b}{k}$$

Numerical solution of equations 2.3.46 - 2.3.49 yields

$$\alpha(0) \simeq 0.79 \qquad b/k \approx 0.51$$

$$\frac{\pi g^2}{2k} \approx 0.49 \quad \text{and} \quad \frac{\pi G^2}{2k} \approx 1.3$$

The first three of these results are arrived at in (Ref. 16). The different normalisation used by them resulting in the factor $2K$ instead of π in 2.3.34 leads to their having g^2 and G^2 instead of $\frac{\pi g^2}{2K}$ and $\frac{\pi G^2}{2K}$ In the single pole bootstrap, it is not possible to evaluate the actual value of the coupling constants, but only these ratios. The slight discrepancy in the values gives in (Ref. 16) and our values is probably due to computing inaccuracy in their paper. Another point that is worth noting is that G^2 does not figure in three of the four bootstrap equations. Hence one can calculate $\alpha(0)$ without evaluating G^2 and this enabled Frazer and Mehta to omit G^2 from their consideration. It will be shown that G^2 does not decouple itself from any of the bootstrap equations in the pole plus cut model which we shall introduce in the following sections

Section 4. - The Total Cut Discontinuity

From equation 2.3.34, it is obvious that $\rho(j,t)$ has a cut in the j-plane with its branch-point at

$$j = 2\alpha\left(\frac{t}{4}\right) - 1$$

$$= \alpha_c(t) \qquad 2.4.1$$

This cut in the elastic amplitude makes a contribution to the total amplitude given by

$$\pi e^{\frac{1}{2}kt} \int_0^\infty dr^2 e^{-2kr^2} J_0[\pi br\sqrt{-t}]\, s^{2\alpha\left(-r^2+\frac{t}{4}\right)-1}$$

We can express this as

$$\int_{-\infty}^{\alpha_c(t)} dj' \, \mathrm{disc}(j',t)\, s^{j'}$$

where

$$\text{disc}\,[-2br^2,t] = \frac{\pi}{2b}\, e^{\frac{1}{2}kt}\, e^{-2kr^2}\, J_0[\pi br\sqrt{-t}] \qquad 2.4.2$$

In order to evaluate its contribution to the total discontinuity, that is, the discontinuity of the full amplitude, we express

$$\rho(j,t) = \int_{-\infty}^{\alpha_c(t)} dj'\, \frac{\text{disc}\,\rho(j',t)}{j-j'} \qquad 2.4.3$$

where

$$\text{disc}\,\rho(j,t) = \frac{1}{2\pi i}\left[\rho^+(j,t) - \rho^-(j,t)\right] \qquad 2.4.4$$

and

$$\rho^{\pm}(j,t) = \int_{-\infty}^{\alpha_c(t)} dj'\, \frac{\text{disc}\,\rho(j',t)}{j-j' \mp i\varepsilon}$$

$$= P\int_{-\infty}^{\alpha_c(t)} dj'\, \frac{\text{disc}\,\rho(j',t)}{j-j'} \pm i\pi\, \text{disc}\,\rho(j,t) \qquad 2.4.5$$

The cut in $\rho(j,t)$ is reproduced in $\text{Im}\,A_{22}(j,t)$ as can be easily seen on examining 2.3.30. We now evaluate the discontinuity of the full amplitude

Let

$$\text{Im}\,A_{22}(j,t) = G^4\, a(j,t) \qquad 2.4.6$$

Then

$$\text{disc}\,a(j,t) = a^+(j,t) - a^-(j,t) \qquad 2.4.7$$

where

$$a^{\pm}(j,t) = \frac{\rho^{\pm}(j,t)}{1-g^2\rho^{\pm}(j,t)} \qquad 2.4.8$$

Equations 2.4.3, 2.4.5, 2.4.7 and 2.4.8 together lead to the result

$$\text{disc } a(j,t) = \frac{\text{disc. } \rho(j,t)}{\left\{\left[1 - g^2\rho \int_{-\infty}^{\alpha_c(t)} dj' \frac{-\text{disc}\rho(j',t)}{j-j'}\right]^2 + \pi^2 g^4 [\text{disc } \rho(j,t)]^2\right\}} \qquad 2.4.9$$

On substituting equation 2.4.2 in 2.4.9, we obtain

$$\text{disc. } a(j,t) = \frac{\frac{\pi}{2b} e^{\frac{1}{2}kt} e^{-\mu} J_0\left[\pi\sqrt{\frac{b^2}{2k}\mu(-t)}\right]}{(1-g^2R)^2 + \pi^2 g^4 \left\{\frac{\pi}{2b} e^{\frac{1}{2}kt} e^{-\mu} J_0\left[\pi\sqrt{\frac{-b^2}{2k}}\mu t\right]\right\}^2}$$

where

$$R = \pi e^{kt/2} e^{-\mu} \sum_{s=0}^{\infty} \frac{\mu^s}{(s!)^2} \left\{ \sum_{\rho=0}^{s-1} (s-\rho-1)!\, \mu^\rho e^{\mu} + \mu^s \left[-\gamma - \log\mu - \sum_{k=0}^{\infty} \frac{\mu^k}{k.k!}\right]\right\} \qquad 2.4.10$$

$$\mu = \frac{k}{b}[\alpha_c(t) - j] \qquad 2.4.11$$

and γ is the Euler constant here and not the integration variable used earlier. Since t is small, we evaluate 2.4.10 to the first order in t and obtain

$$\text{disc } a(j,t) = \frac{\pi}{2bx} e^{-\mu + k_2 t} \qquad 2.4.12$$

where

$$x = \left[1 + \frac{\pi g^2}{2k\Delta} e^{\mu} Ei^*(\mu)\right]^2 + \frac{\pi^2}{\Delta^2}\left(\frac{g^2\pi}{2k}\right)^2 e^{-2\mu} \qquad 2.4.13$$

$$y = 2\pi^2 \left(\frac{\pi g^2}{2k}\right)^2 \frac{e^{-2\mu}}{\Delta^2} \left(\frac{\pi^2 b^2 \mu}{8k^2} + \frac{1}{2}\right) - \frac{2}{\Delta}\left(\frac{\pi g^2}{2k}\right)\Big\{ \left[\frac{\pi g^2}{2k} e^{\mu} E_i^*(\mu) + 1\right]\left[-\frac{1}{2} E_i^*(\mu) + \frac{1}{8}\pi^2 \Delta^2 e^{\mu} - \frac{1}{8}\pi^2 \Delta^2 \mu E_i^*(\mu)\right] e^{-\mu}\Big\}$$

and 2.4.14

$$Z = \frac{1}{2} + \frac{1}{8}\pi^2 \Delta^2 \mu - \frac{y}{\alpha} \qquad 2.4.15$$

At the branch-point

$$j \to \alpha_c(t)$$

and

$$E_i^*(\mu) \Rightarrow \infty$$

Hence from 2.4.10, we find that the discontinuity of the cut in the full amplitude is singular at the end-points and also vanishes there. This cut in the full amplitude arises from the cut in the two-particle amplitude $\rho(j,t)$ corresponding to the AFS cut, mentioned in chapter one of this thesis, obtained by calculating Feynman diagrams, which itself does not vanish and is non-singular at the end-point. Our result about the end-point properties of the cut in the full amplitude is in agreement with that of Bronson and Jones (Ref. 43).

Section 5 - Pole and Cut In the Input

In section three, we saw that for values of j near the pole $\alpha(t)$ the amplitude is given by the right-hand side of equation 2.3.39. Provided the pole is separated from cut, we obtain from equations 2.4.6, 2.4.9 and the argument at the beginning of the last section, the behaviour of the amplitudes for values of j near the cut. In the s-plane, the pole at $j=\alpha(t)$ makes a contribution to the asymptotic behaviour given by

$$G^2 e^{kt} s^{\alpha(t)} e^{\frac{1}{2} i\pi\alpha(t)}$$

The corresponding asymptotic contribution from the cut which starts at $2\alpha(\frac{t}{4})-1$ is given by

$$G^4 \int_{-\infty}^{\alpha_c(t)} dj \; \text{disc}\,[a(j,t)]\, s^j e^{-i\pi j}$$

This cut contribution dominates over the pole contribution only if $\alpha(0) > 1$ which is precluded by the Froissart bound. If $\alpha(0)$ is much less than unity, then as s tends to infinity, the cut contribution is negligible compared to the pole contribution. However if $\alpha(0)$ equals one, then the pole and cut both coincide at $t=0$ and their asymptotic s-dependence is the same for both. The relative contributions from the pole and the cut are thus determined by the relative strengths of the residue at the pole and the discontinuity across the cut for small values of t. Hence if $\alpha(0)$ is close to unity, the cut contribution is not necessarily negligible.

The two expressions given above reflect the relative strengths of the particle-particle-pole and particle-particle-cut couplings respectively in the elastic amplitude. In the multi-Regge chain for the production amplitude, in a previous section we used the input $s_i^{\alpha(t_i)}$ in each link corresponding to the output Regge pole $\alpha(t)$ If we are to account for the output cut discussed in the previous section, we need to include a cut in the input. On the addition of a cut to the input pole in each link of the chain, we now find that each of the n produced particles except for the two end ones is linked to a pole and a cut in both directions along the chain. This means that we have to introduce two more parameters to describe the strength of the couplings particle-cut-pole and particle-cut-cut. Earlier, in the pole-only model, we assumed

that the particle-pole-pole couplings factorise in the form given by equation 2.3.14. Continuing in the same spirit, we assume that the particle-cut-pole and particle-cut-cut coupling functions also factorise in their dependence on the adjacent momentum transfers. We now make the further assumption that the relative strengths with which the pole and the cut couple to an external particle in the elastic amplitude are preserved in the production amplitude. This is in keeping with the spirit of multiperipheral models where we iterate the production amplitude with the elastic amplitude which provides the kernel of the integral equation. These two assumptions are tantamount to the relationship between the couplings given by

$$\frac{\text{Particle-Particle-Pole}}{\text{Particle-Particle-Cut}} = \frac{\text{Particle-Pole-Pole}}{\text{Particle-Pole-Cut}} = \frac{\text{Particle-Pole-Cut}}{\text{Particle-Cut-Cut}}$$

Thus the need for additional parameters is eliminated. If not for these assumptions (also made in Ref.44), a study of the production amplitude would have been necessary in order to obtain a closed set of bootstrap equations since the number of equations arising from our model alone would be less than the number of parameters.

Therefore, to each factor in the multi-Regge amplitude

$$e^{k t_i} s_i^{\alpha(t_i)} e^{\frac{1}{2} i\pi\alpha(t_i)}$$

the addition of the correction

$$G^2 \int d_j\, s^j e^{\frac{1}{2} i\pi j}\, \mathrm{disc}\, a(j,t)$$

in line with their relative strengths in the elastic amplitude will represent the effects of the cut.

Thus following the procedure of section 3,

$$\mathrm{Im}\, A_{22}(j,t) = \frac{G^4 \rho'(j,t)}{1 - g^2 \rho'(j,t)} \qquad 2.5.1$$

where $\rho'(j,t)$ is the $2 \to 2$ amplitude obtained after adding the cut correction to the propagator and residue functions associated with the input pole. Using the notation of section 3

$$\rho(s,t) = \int d^2K \; \mathrm{Pole}(\bar{t})\, \mathrm{Pole}^*(\bar{t}') \qquad 2.5.2$$

where

$$\mathrm{Pole}(\bar{t}) = e^{k\bar{t}}\, s^{\alpha(\bar{t})}\, e^{\frac{1}{2} i\pi \alpha(\bar{t})}$$

then

$$\rho'(s,t) = \int d^2K \left[\mathrm{Pole}(\bar{t}) + \mathrm{Cut}(\bar{t})\right]\left[\mathrm{Pole}^*(\bar{t}') + \mathrm{Cut}^*(\bar{t}')\right] \qquad 2.5.4$$

where

$$\mathrm{Cut}(t) = G^2 \int_{-\infty}^{a_c(t)} d_j\, s^j\, e^{\frac{1}{2} i\pi j}\, \mathrm{disc}\, a(j,t) \qquad 2.5.5$$

then

$$\rho'(s,t) = \rho(s,t) + f_1(s,t) + f_2(s,t) + f_3(s,t) \qquad 2.5.6$$

where

$$f_1(s,t) = f_2^*(s,t) = \int d^2K\, \mathrm{Pole}(\bar{t})\, \mathrm{Cut}^*(\bar{t}') \qquad 2.5.7$$

and

$$f_3(s,t) = \int d^2K \; \mathrm{Cut}(\bar{t})\, \mathrm{Cut}^*(\bar{t}') \qquad 2.5.8$$

$f_1(s,t)$ is given by Fig. 11 (it is also obtained by putting $n=3$ in Fig. 4 of Ref. 22) where the part of the diagram on the left of

the dotted line represents the pole and that on the right represents the cut. As in section 6 of (Ref. 22), we only integrate over the region of phase space where the momentum transfers flowing along the Reggeons are finite.

$f_3(s,t)$ is represented by Fig. 12 (it is obtained by putting $n=4$ in Fig. 4 of Ref. 22). We ignore $f_3(s,t)$ as it represents a cut starting at $4\alpha(t/16)-3$ whose effects we ignore owing to the reasons we gave in section one.

Thus equation 2.5.1 follows from equation 2.3.30 after replacing $\rho(j,t)$ by $\rho'(j,t)$ where

$$\rho'(j,t) = \rho(j,t) + 2G^2 f(j,t) \qquad 2.5.9$$

and

$$f(j,t) = \mathrm{Re}\int d^2K \int_{-\infty}^{\alpha_c(\bar{t}')} dj' \left\{ \left[\frac{e^{k\bar{t}}\, e^{\frac{1}{2}i\pi[\alpha(\bar{t})-j']}}{j-\alpha(\bar{t})-j'+1} \right] [\mathrm{disc}.\, a(j',\bar{t}')] \right\} \qquad 2.5.10$$

We use the identity

$$\int_0^\infty dh\, e^{-\alpha h} = \frac{1}{\alpha} \qquad 2.5.11$$

to convert the denominator in the integral of equation 2.5.10 into exponential form which becomes

$$f(j,t) = \mathrm{Re}\int d^2K \int_0^\infty dh \int_0^\infty d\mu \frac{\pi}{2\pi k} \exp\psi \qquad 2.5.12$$

where

$$\psi = -\mu + kzt + k\bar{t} + \tfrac{1}{2}i\pi[\alpha(\bar{t}) - \alpha_c(\bar{t}') + \Delta\mu] - h[j-\alpha(\bar{t})-\alpha_c(\bar{t}')+\Delta\mu+1] \qquad 2.5.13$$

The transformation from j' to μ was essential in order that x may be expressed solely in terms of the latter and hence not figure in the integration over the momenta. We now diagonalise ψ a quadratic form in $\underline{k}$ by means of an orthogonal transformation of the variables k, whose Jacobean is unity and express it in the form $A_1 \underline{k}^2 + A_2 t$. The transformation is given by $\underline{k} \Rightarrow \underline{k} + \underline{\chi}$ where χ is a constant vector. We finally transform to angular variables by replacing $\int d^2 k$ with

$$\int_0^{2\pi} \frac{1}{2} d\theta \int_0^{\infty} d|k|^2$$

It is now easy to do the k integrations and we obtain to the first order in t

$$f(j,t) = \frac{\pi}{2k^2} \int_0^{\infty} d\mu \frac{e^{-\mu}}{x} \int_0^{\infty} dh \left\{ \frac{[1+kpt]\,\phi(t)\exp}{[1+z+\frac{3}{2}h\Delta]^2 + \frac{1}{16}\pi^2\Delta^2} \right.$$

$$\left. [-h(j-3q+2+\mu\Delta] \right\} \qquad 2.514$$

where

$$P = [1+h\Delta]\left[z+\frac{1}{2}h\Delta\right]\left[1+z+\frac{3}{2}h\Delta\right] + \frac{1}{16}\pi^2\Delta^2(1+h\Delta)$$

$$+ \frac{1}{4}\pi^2\Delta^2\left(z+\frac{1}{2}h\Delta\right) \qquad 2.5.15$$

$$q = \frac{1}{4}\pi\Delta \left\{ 2\,\frac{\left(z+\frac{1}{2}h\Delta\right)^2 - (1+h\Delta)^2 - \frac{1}{8}\pi^2\Delta^2}{\left(1+z+\frac{3}{2}h\Delta\right)^2 + \frac{1}{16}\pi^2\Delta^2} \right.$$

and $\qquad 2.5.16$

$$\phi(t) = \left[1+z+\frac{3}{2}h\Delta+\frac{1}{4}\pi\Delta kqt\right]\cos\left[\frac{1}{2}\pi\Delta(A+\mu)\right]$$

$$+\left[\frac{1}{4}\pi\Delta - kqt\left(1+z+\frac{3}{2}h\Delta\right)\right]\sin\left[\frac{1}{2}\pi\Delta(A+\mu)\right]$$

$$2.5.17$$

Equations 2.5.14 - 2.5. 17, 2.5.9, 2.5.1 and the equations obtained by replacing $\rho(j,t)$ with $\rho'(j,t)$ in equations 2.3.42 - 2.3.45 leads to the bootstrap equations of our model given by

$$I = \frac{e^{-M}}{\alpha} \frac{e^{-h\Delta(2A+\mu)}\phi(0)}{\left[1+Z+\frac{3}{2}h\Delta\right]^2+\frac{1}{16}\pi^2\Delta^2} \qquad 2.5.18$$

$$I' = \frac{I}{\phi(0)}\left\{(p-h\Delta)\phi(0)+\frac{1}{K}\phi'(0)\right\} \qquad 2.5.19$$

$$\left(\frac{\pi g^2}{2K}\right)\frac{1}{\Delta}e^{A}Ei(A)+\frac{8g^2G^2\pi^2}{4\Delta K^2}\int_0^\infty\int_0^\infty d\mu dh\, I = 1 \qquad 2.5.20$$

$$e^{A}Ei(A)\left[1-\frac{1}{8}\pi^2\Delta^2A\right]+\frac{1}{8}\pi^2A^2-\frac{1}{2A}$$

$$+\frac{8\pi G^2}{2K}\int_0^\infty\int_0^\infty d\mu dh\, I' = 0 \qquad 2.5.21$$

$$e^{A}Ei(A)\left[2-\frac{1}{8}\pi^2\Delta^2-\frac{1}{8}\pi^2\Delta^2A\right]+\frac{1}{8}\pi^2\Delta^2-\frac{2}{A}+\frac{1}{2A^2}$$

$$+\frac{8\pi G^2}{2K}\Delta\int_0^\infty\int_0^\infty d\mu\, dh\left[(-h)(I+I')\right] = 0 \qquad 2.5.22$$

and

$$\frac{\pi G^2}{2K} = \frac{\left(\frac{1}{A} - e^A E_c(A)\right) \frac{1}{\Delta^2} \left(\frac{\pi g^2}{2K}\right)^2}{1 + 8\left(\frac{\pi g^2}{2K}\right)^2 \Delta \int_0^\infty \int_0^\infty d\mu\, dh(-h) I} \qquad 2.5.23$$

It can be observed that the above four equations reduce to equations 2.3.46 - 2.3.49 if we put I and I' equal to zero. Thus the integrals of 2.5.18 and 2.5.19 represent the cut-effects in the above multi-Regge bootstrap in equations. As we remarked at the end of section 3, G occurs in all four equations.

Solving these equations numerically, we obtain

$$\alpha(0) \approx 0.7 \qquad b/K \approx 0.8$$

$$\frac{\pi g^2}{2K} \approx 0.5 \quad \text{and} \quad \frac{\pi G^2}{2K} \approx 0.8$$

Contrasted with the pole-only model results at the end of section 3, it can be seen that while $\alpha(0)$ decreases by 0.1, $\pi g^2/K$ does not change appreciably. There is also a noticeable difference in b/K and $\pi G^2/K$ implying that in our model, the trajectory has a smaller slope and also that the elastic amplitude forms a proportionately smaller part of the cross-section.

Section 6 - Comparison of Pole and Elastic Cut Contributions

As explained in the earlier sections, the generation of Regge cuts in multiperipheral models occurs through the application of s-channel unitarity. A type of approximation

used in such applications is where we consider the output Regge pole to be obtained from the many particle intermediate states and the Regge-cut to arise from considering only the quasi-two body channels as intermediate states where the individual amplitudes are given by Regge pole exchanges. Thus in this approximation, the unitarity equation reads

$$\mathrm{Im}\, A_{22} = P + | P \otimes A | \qquad 2\text{-}6\text{-}1$$

where P represents the Regge-pole contribution and the symbol $\otimes$ represents integration over intermediate states. The second term in 2.6.1 represents the elastic cut correction which as observed by Finkelstein and Jacob (Ref. 24) is opposite in sign t the absorptive correction, which is more in agreement with experiment. In this section, we compare the relative contributions of the pole and the elastic $2 \to 2$ cut corrections to the amplitude in both Frazer and Mehta's model and our model in order to investigate whether the sign in our model is in agreement with the absorption model result in contrast to what the usual application of unitarity and multiperipheralism achieves as in 2.6.1.

Hence we define the following expression in the s-plane which are obtained by taking the inverse Mellin transforms of equations 2.3.39, 2.3.34 and 2.5.14, multiplied by the appropriate constants

$$\text{POLE} = G^2 s^{\alpha} \exp\left[(k + b \log s)\, t\right] \qquad 2\text{-}6\text{-}2$$

$$\text{CUT} = G^2 \left(\frac{\pi G^2}{2k}\right) \frac{s^{2\alpha-1}}{(1+\Delta \log s)} \exp\left[\frac{1}{2}(k + b\log s)\, t + \frac{1}{8}\frac{\pi^2 b^2 t}{k + b\log s}\right] \qquad 2\text{-}6\text{-}3$$

and

$$CUTC = G^2 \left(\frac{\pi G^2}{2K}\right)^2 \frac{2s^{3a-2}}{\Delta} \int_0^\infty d\mu \frac{e^{-\mu}}{x} \left\{ e^{-\mu \Delta \log s} \left[\frac{(1+kpt)\phi(t)}{(1+z+\frac{3}{2}h\Delta)^2 + \frac{1}{16}\pi^2\Delta^2} \right] \right\} \qquad 2.6.4$$

POLE is the s-plane equivalent of $G^2 e^{kt} [j - \alpha(t)]^{-1}$ which is the asymptotic contribution of the pole term to the amplitude. CUT is the elastic $2 \to 2$ contribution to the amplitude, i.e. minus times the absorption model cut in s and t. The expression CUT + CUTC is the corresponding contribution in our imput pole plus cut version.

After fixing the free parameter b = 1 in equations 2.6.2 - 2.6.4 for small t (t = 0.01) and large s, varying from 20 - 1000, we find after numerical computation that the ratio $\frac{CUT}{POLE}$ in the pole-only model is about 3 - 4 times the corresponding ratio $\frac{CUT + CUT\,C}{POLE}$ in our model. Thus the cut correction becomes much smaller when there is an input cut. The more important result is that we do not find the sign of the cut correction in our model agreeing with the absorption model. Both ours and Frazer and Mehta's model produce the opposite sign. This effect does not change appreciably for $b < 1$ (altering b has the same effect as altering t as from equations 2.6.2 - 2.6.4, it can be seen that b always occurs in conjunction with t).

There are markedly different effects for $b \gg 1$ but they are meaningless in view of the small bt approximations made during the course of the calculations.

Section 7 - Conclusion

The presence of the input cut has not had a significant impact on the position of the bootstrapped Regge pole which drops by 0.1 to 0.7. However, assuming the exponential fall off in the momentum transfer dependence to be the same in both models, we find that the slope of the trajectory is less in our model than in Frazer and Mehta's. Also the Reggeon-particle-particle constant having a smaller value in our model than in theirs while the Reggeon-Reggeon-particle coupling constant is the same in both implies that the elastic amplitude makes a proportionately smaller contribution to the total cross-section in the input pole plus cut model than in the pole only model.

The position of the output pole having actually dropped is rather dissappointing from the point of view of the Pomeron and its associated iterated cuts forming a closed bootstrap as discussed in section one, where we had hoped that the output trajectory would emerge closer to one, thus justifying our argument of section one. Self consistency constraints on the parameters decreed otherwise by destroying our expectations that the cut would enhance the kernel strength and produce a higher trajectory. Thus we fail to produce evidence that the inclusion of cuts will lead to the bootstrap of a single pole at $\alpha(0)=1$

We also find that the inclusion of the input cut, conserves the sign, though reducing the size of the elastic cut correction which follows from the application of quasi-two body unitarity. This belies our hope that our model would be in agreement with the absorption model.

In assessing these results, it should be remembered that all the sub-energies have been assumed to be large. This assumption

is implicit in the multi-Regge formalism. Duality is invoked to average over the low sub-energy regions by asymptotic expressions. However, as pointed out in (Ref. 23) and in chapter one of this thesis, the use of duality in this context is dubious.

CHAPTER THREE - Nucleon Loops in the M.R.M.

Section 1 - Introduction

In this chapter we shall be studying a modified multi-Regge model which includes nucleon loops. Instead of the usual multi-Regge $2 \to N$ production amplitude in which the $2N$ produced particles are linked together by Regge exchanges, we shall be considering a model in which the links in the chain consist of Reggeons alternating with nucleons. Conservation laws then require that all the produced particles, except the ones at the ends which are the same as the incoming particles, be nucleons. The sub-energies across the Reggeons are assumed to be in the asymptotic region in line with the usual multi-Regge phase space requirements. The sub-energies across the nucleons is assumed to be non-Regge, that is they belong to a range above the two-particle threshold and less than that energy above which Regge representation is suitable. Since the sub-energies across the nucleons are low, diagrams, in which the rungs containing the nucleons are crossed, also have to be evaluated as the contributions from such diagrams are not negligible. We find that the phase space factorises into a purely multi-Regge part and a separate contribution from the nucleons, greatly facilitating the analysis of the model.

The alternating occurrence of nucleons and Reggeons in the amplitude necessitates the introduction of the complicated nucleon-Reggeon coupling functions. For these, we use the prescription of Scadron (Ref. 26) for the Boson-nucleon couplings which we shall use after Reggeising the Boson contributions.

The type of diagram which we have to calculate is similar

to those calculated by Cheng and Wu (Ref. 25) in their analysis of high-energy quantum electrodynamics using a conbination of perturbation theory and impact parameter formalism. Their diagram had vector mesons at high-energy with Fermion loops and obtained an extra logs factor for each diagram giving an enhanced asymptotic s-behaviour for the amplitude owing to the presence of the Fermion loops.

The analysis of our model is divided into seven sections. In the next section, we define the amplitudes, variables and the kinematical approximations used. In section three we show how the phase space factorises, allowing the integration over the loop momenta and the loop sub-energies to be carried out separately. The contribution from each intermediate state is described next in section four. The propagators for the Boson trajectories and the coupling functions are derived in section five.

In section six, we select the leading terms at asymptotic energies which simplifies greatly the problem of evaluating a large number of traces involving γ- matrices, and enables us to isolate the contribution from the nucleon loops.

In the next section, it is shown that the net effect of inserting nucleon loops is to multiply each contribution to the amplitude by a constant, which we show factorising. In section eight, we discuss the effects of not assuming that the nucleon propagators are on mass-shell as was required for the formulae used by us for the coupling functions and propagators. In this respect also, we follow Scadron's (Ref. 26) prescription.

Section 2 - Notation and Kinematics

The $2 \to 2N$ production amplitude with nucleon loops is given by

$$T_{2,2N}(s)$$

$$= \Big\{ G(t_1) G(t_n) \prod_{i=1}^{N-1} \Big\{ \bar{u}_\alpha (c^i) g_{\nu^i}(t_{i+1}, \tau_i, \omega_i)$$

$$\frac{[\not{B}^i + M]_{\alpha\beta}}{B^{i2} - M^2} \cdot g_{\mu^i}(t_i, \tau_i, \omega_i) u_\beta [A_i] \Big\}$$

$$\phi_{\mu^1} [B^0, q^1, B^1] \phi_{\nu^i} [B^{n-1}, q^n, B^n] \prod_{i=1}^{N-2} \phi_{\nu^i \mu^{i+1}} (B^{i-1},$$

$$q^i, B^i) \Big\} \qquad 3.2.1$$

where the momenta are as in Fig. 13

$$\not{B}^i = B^i \cdot \gamma$$

and m is the nucleon-mass $\bar{u}_\alpha$ and u_β are the spinors representing the external nucleons and the $\frac{\not{B}_i + M}{B^{i2} - M^2}$ are the nucleon propagators formed from their momenta and the γ -matrices. We assume that incoming particles are spinless, for convenience. $G(t_1)$ and $G(t_n)$ are the coupling functions linking these external particles to the Reggeons. The $g^i(t_i, \tau_i, \omega_i)$ are the Reggeon-nucleon-nucleon coupling functions occuring at the internal vertices, the ω_i being the Toller angles. We follow the last chapter in assuming that the amplitude is independent of the Toller angles and henceforth omit their inclusion. The subscripts ν^i and μ^i attached to these coupling functions arise from the nucleon spins which have the effect of freeing these labels from the Boson propagators. The $\phi_{\ldots}$ and $\phi_{\ldots}$ are the

Reggeised Boson propagators which contain the input Regge trajectories.

We define the following invariant variables with reference to Fig. 13 (the wavy lines in the figure are Reggeons and the straight lines are particles.)

$$S = [p^0 + p^n]^2 = [B^0 - B^n]^2$$

$$S_i = [B^{i-1} - B^i]^2 = [C^{i-1} - A^i]^2 \qquad i = 1, \ldots n$$

$$t_i = q_i^2 \qquad i = 1, \ldots n$$

$$\sigma_i = (A^i - C^i)^2 = (q^i - q^{i+1})^2 \qquad i = 1, \ldots n-1$$

$$\tau_i = B^{i\,2} \qquad i = 1, \ldots n-1$$

$$S_{ij} = [B^i - B^j]^2 \quad \text{where} \quad i = 0, \ldots n-1 \quad j = 1, \ldots n \quad \text{and} \quad i < j$$

3.2.2

It clearly follows that

$$S_{i-1\,i} = S_i \quad \text{and} \quad S_{0n} = S$$

3.2.3

We make the usual multi-Regge phase-space assumptions analysed in detail by Halliday and Saunders (Ref. 22) and in chapter two of this thesis. These are $S \to \infty$, $S_i \to \infty$

and the t_i are small. We also use the result that the t_i arise from the transverse components that is

$$t_i = -k_i^2 \qquad 3.2.4$$

where the k^i are the transverse components of q^i The sub-energies σ_i across the nucleon loops are assumed to be finite and non-Regge. We postulate M^2 as that energy above which Regge representation is suitable. Thus, we have

$$4m^2 \leq \sigma_i \leq M^2 \qquad 3.2.5$$

where $4m^2$ is the usual two-particle threshold in the s-channel dictated by Kinematic considerations. This result follows from both the A^i and C^i being on the mass-shell. It will be seen that these mass-shell constraints lead to the result that the τ_i also lie between finite limits, which are dependent on the nucleon sub-energies σ_i This is in contrast to the evaluation of Feynman diagrams where all the loop momenta are off mass-shell which leads to divergences requiring the employment of cut-offs to perform the integration. In our diagrams, there are no divergences and we shall be able to carry out the integrations exactly, as will be seen.

The above considerations imply that

$$s \gg s_i \gg \sigma_i, M^2 \gg t_i \qquad 3.2.6$$

These inequalities lead to the following approximate equations which can be derived by considering a particular frame.

$$s \approx [q^i - q^{i+1}]^2 \approx [B^{i-1} - q^{i+1}]^2 \approx [q^{i-1} - B^i]^2 \qquad 3.2.7$$

and

$$S_{ij} \approx [q^i - q^{j+1}]^2 \approx [B^i - q^{j+1}]^2$$

$$\approx [q^i - B^j]^2 \qquad 3.2.8$$

Section 3 - Factorisation of Phase Space and Kinematics

The absorptive part of the $2 \to 2$ amplitude in the forward direction is given by

$$Im\, T_{22}(s) = \sum_{N=2}^{\infty} (\pi d\Omega) T_{2,2N} T^{+}_{2,2N} + A_{22}$$

3.3.1

A_{22} is the two-particles intermediate state consisting of Regge exchanges only and no nucleon exchanges. For convenience, we shall omit this term till we finally sum all the diagrams. (the diagram for A_{22} is given by Fig. 10) when writing down the amplitude. $\pi d\Omega$ represents the phase space integral of the particles intermediate state constibution to the amplitude which is given by Fig. 14. We have

$$\pi d\Omega = \left[\left\{ \prod_{i=1}^{N} d^4 C^{i-1} d^4 A^i \delta(C^{i-1\,2} - M^2) \right.\right.$$

$$\left.\left. \delta(A^{i2} - M^2) \right\} \delta^4 \left[p^0 + p^n - \sum_{i=1}^{n} (C^{i-1} - A^i) \right]\right]$$

3.3.2

Let

$$C^i - A^i = G^i \quad \text{for } i = 1, \ldots n-1$$

$$C^0 = G^0 \quad \text{and} \quad -A^n = G^n$$

Then

$$\pi\, d\Omega = \left[\left\{ \prod_{i=1}^{n} d^4 G^i \delta(G^{i2} - \sigma_i) \delta^4 \left[p^0 + p^n - \sum_{i=0}^{n} G^i \right] \right\} \right.$$

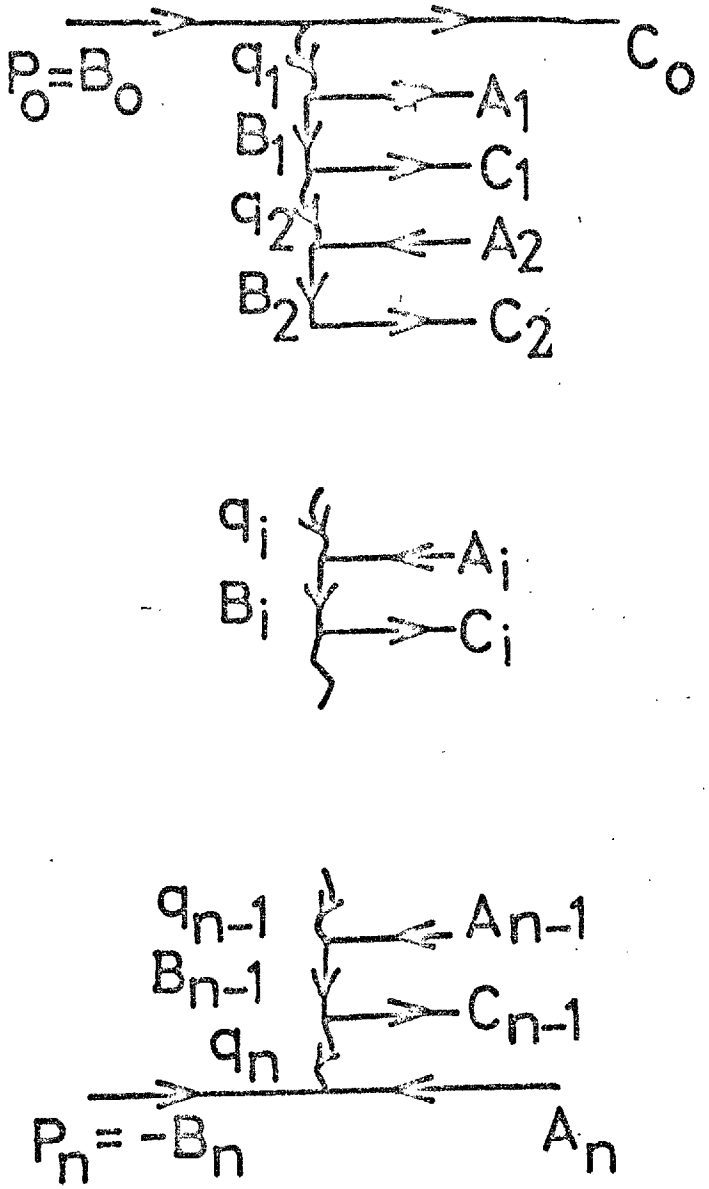
$P_o = B_o$
q_1
A_1
B_1
C_1
q_2
A_2
B_2
C_2
C_o
q_i
A_i
B_i
C_i
q_{n-1}
A_{n-1}
B_{n-1}
C_{n-1}
q_n
$P_n = -B_n$
A_n

Fig. 13

$$\left\{ \prod_{i=1}^{N-1} \int d^4 A^i \, \delta(C^{i2} - M^2) \, \delta(A^{i2} - M^2) \right\}$$

$$\left\{ \prod_{i=1}^{N-1} \int_{4M^2}^{M^2} d\sigma_i \right\} \Bigg] \qquad 3.3.3$$

where

$$\sigma_0 = \sigma_n = M^2$$

The factor in curly brackets is easily identifiable as the multi-Regge phase space for $t=0$ described in the last chapter with σ_i the effective mass of the i^{th} pair of nucleons replacing the pion mass of that chapter. The second factor in curly brackets is the product of the integrations over the loop momenta and the final factor is the integrations over the variations in the nucleon-pair masses which we introduced along with δ-functions in order to effect this factorisation.

Thus symbolically

$$\Pi d\Omega = (\Pi d\Omega)_{M.R.M} \times (\Pi d\Omega)_{N.L} \times \left[\Pi \int d\sigma_i \right] \qquad 3.3.4$$

where $(\Pi d\Omega)_{MRM}$ is the multi-Regge phase-space, $(\Pi d\Omega)_{N.L}$ represents the integrations over the nucleon loops and the last factor is self-explanatory. $(\Pi d\Omega)_{N.L}$ is simplified by transforming to the variables τ_i the Jacobean of the transformation can be expressed as

$$\delta\left[(q^i + A^i)^2 - \tau_i \right]$$

Consider

$$I = \int d^4 A^i \, \delta[A^{i2} - M^2] \, \delta[C^{i2} - M^2] \, \delta[(q^i + A^i)^2 - \tau_i] \qquad 3.3.5$$

Put $$x = A^{i\,2}, \quad y = C^{i\,2}, \quad z = (q^i + A^i)^2$$

Then

$$I = \int dx\,dy\,dz\,\delta(x-M^2)\,\delta(y-M^2)\,\delta(z-\tau_i)\,J \qquad 3\cdot3\cdot6$$

Where

$$J = \left| \frac{\partial(x,y,z)}{\partial(A_0^i, A_1^i, A_2^i)} \right|^{-1}$$

To evaluate 3.3.6, we choose the frame in which

$$\underline{q}^{i+1} = -\underline{q}^i = 0$$

and

$$q_3^i = q_3^{i+1} = 0$$

then

$$A_3^i = B_3^i = C_3^i = \lambda$$

We have

$$\frac{J^{-2}}{64}$$

$$= \left| \begin{pmatrix} A_0^i & A_1^i & A_2^i \\ C_0^i & C_1^i & C_2^i \\ A_0^i + q_0^i & -(A_1^i + q_1^i) & -(A_2^i + q_2^i) \end{pmatrix} \begin{pmatrix} A_0^i & C_0^i & +A_0^i + q_0^i \\ -A_1^i & -C_1^i & -(A_1^i + q_1^i) \\ -A_2^i & -C_2^i & -(A_2^i + q_2^i) \end{pmatrix} \right|$$

$$= \begin{vmatrix} M^2+\lambda^2 & \frac{2M^2-\sigma_i}{2}+\lambda^2 & \frac{\tau_i+M^2}{2}+\lambda^2 \\ \frac{2M^2-\sigma_i}{2}+\lambda^2 & M^2+\lambda^2 & \frac{\tau_i-M^2}{2}+\lambda^2 \\ \frac{\tau_i+M^2}{2}+\lambda^2 & \frac{\tau_i-M^2}{2}+\lambda^2 & \tau_i+\lambda^2 \end{vmatrix}$$

$$= -\sigma_i^2 [\mu^2-\lambda^2]/4 \qquad 3.3.7$$

where

$$\frac{\mu^2}{\sigma_i} = -\sigma_i \tau_i^2 + \bar{\bar{\alpha}}_i \tau_i + \bar{\bar{\beta}}_i \qquad 3.3.8$$

and $\bar{\bar{\alpha}}_i, \bar{\bar{\beta}}_i$ are functions of σ_i and M^2

Hence we have

$$I = \int_{-\infty}^{+\infty} \frac{d\lambda}{2\sigma_i |\mu^2-\lambda^2|^{\frac{1}{2}}} \qquad 3.3.9$$

where there is an extra factor of 2 arising from the $2 \rightarrow 1$ transformation. Obviously, the integration is possible only for positive μ^2 and values of λ^2 less than μ^2

The condition

$$\mu^2 \geq 0$$

$$\Longrightarrow \quad \bar{\bar{\alpha}}_i^2 + \bar{\bar{\beta}}_i \sigma_i \geq 0$$

and

$$\tau_i^+ \geq \tau_i \geq \tau_i^-$$

where

$$\tau_i^{\pm} - M^2 = \frac{-\sigma_i \pm \sigma_i^{\frac{1}{2}} (\sigma_i - M^2)^{\frac{1}{2}}}{2} \qquad 3.3.10$$

3.3.9 then becomes

$$I = \frac{\pi}{2\sigma_i} \qquad 3.3.11$$

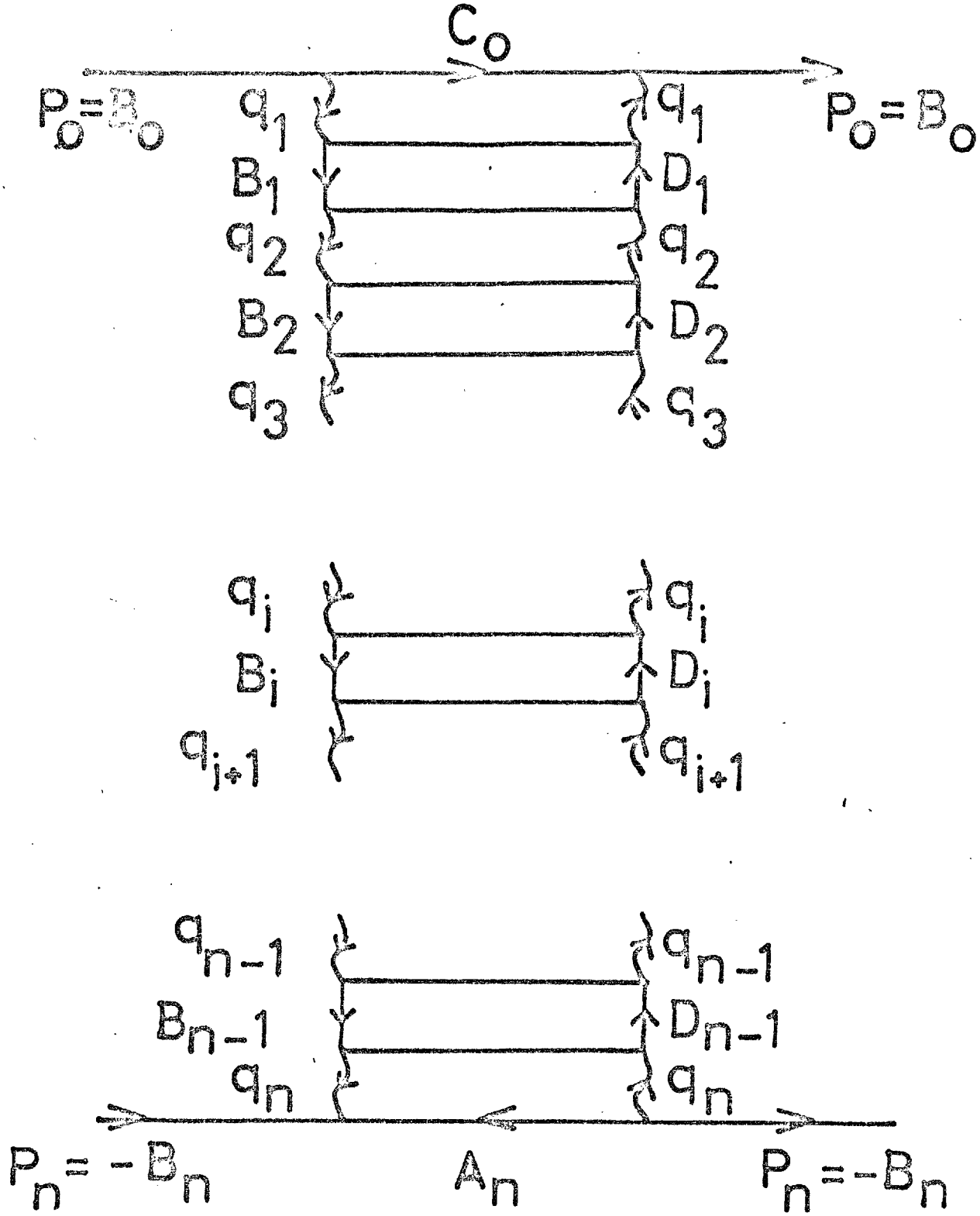
C_o
$P_o = B_o$
q_1
B_1
q_2
B_2
q_3
q_1
D_1
q_2
D_2
q_3
$P_o = B_o$
q_i
B_i
q_{i+1}
q_i
D_i
q_{i+1}
q_{n-1}
B_{n-1}
q_n
q_{n-1}
D_{n-1}
q_n
$P_n = -B_n$
A_n
$P_n = -B_n$

Fig. 14

Then $(\Pi d\Omega)_{N\cdot L}$ becomes

$$(\Pi d\Omega)_{N\cdot L} = \Pi \left[\int_{\tau_i^-}^{\tau_i^+} \frac{\pi d\tau_i}{2\sigma_i} \right] \qquad 3\cdot3\cdot12$$

Thus

$$\Pi d\Omega = (\Pi d\Omega)_{M\cdot R\cdot M} \Pi \left[\int_{4M^2}^{M^2} d\sigma_i \frac{\pi}{2\sigma_i} \int_{\tau_i^-}^{\tau_i^+} d\tau_i \right] \qquad 3\cdot3\cdot13$$

Equation 3.3.12 enables us to extend the inequalities 3.2.6. and write

$$s >> s_i >> \sigma_i, \tau_i, M^2 >> t_i \qquad 3\cdot3\cdot14$$

Hence equation 3.3.4 becomes

$$(\Pi d\Omega) = (\Pi d\Omega)_{M\cdot R\cdot M} \left\{ \Pi \left[\int_{4M^2}^{M^2} d\sigma_i \frac{\pi}{2\sigma_i} \int_{\tau_i^-}^{\tau_i^+} d\tau_i \right] \right\} \qquad 3\cdot3\cdot15$$

The σ_i which play the role of the intermediate particle masses in the M.R.M., act as a link between the s_{ij} and s_i. This corresponding to equation 2.2.31, we have

$$s_{ij} = \frac{\prod_{r=1}^{j-1} s_r}{\prod_{r=1}^{j-2} \mu_{r+1}^2} \qquad 3\cdot3\cdot16$$

where

$$\mu_i^2 = \sigma_i + \chi^{i^2} \qquad 3\cdot3\cdot17$$

and

$$\chi^i = k^{i+1} - k^i \qquad 3\cdot3\cdot18$$

Since the t_i are small, and the expression k^{i2} is a positive definite function of the components, we have from equation 3.2.4 that the quantities k^i are also small, in absolute value. Hence the χ^i are also small quantities which enables us to neglect the second term on the right-hand side of equation 3.3.17. This assumption of the t_i being small which leads to replacing the quantities μ_i^2 by the mass is normally used to solve the multi-Regge integral equation as seen in the last chapter.

Hence we write

$$s_{ij} = s_j \prod_{\lambda=1}^{j-2} \frac{s_{\lambda+1}}{\sigma_{\lambda+1}} \qquad 3.3.19$$

From equation 3.3.19 and the fact that the s_i tend to while the σ_i remain finite and bounded as in 3.2.5, we obtain the inequalities

$$s_{ij} \gg s_{kl}$$

where

$$k \geq i \quad \text{and} \quad l \leq j$$

Section 4 - The $2 \to N$ Contribution

We rewrite equation 3.3.1 as

$$\text{Im } T_{22}(s) = \sum_{N=2}^{\infty} \theta_{2N}(s) \qquad 3.4.1$$

where

$$\theta_{2N} = (\pi d\ell)\, T_{2,2N} T^{\dagger}_{2,2N} \qquad 3.4.2$$

θ_{2N} is the contribution to the amplitude from the $2N$ intermediate particles state. It is represented by Fig. 14, together with all the diagrams that can be obtained from this

by crossing the intermediate particle pairs of one or more nucleon loops (for example, θ_4 is obtained by summing the contributions from the diagrams of Fig. 15). Since each nucleon loop is either crossed or uncrossed, clearly the nucleon loops of Fig. 14 contribute altogether $2(n-1)$ terms to θ_{2N} Clearly, for each of these $2(n-1)$ terms, $T_{2,2N}$ is the same while there is a different $T^{+}_{2,2N}$ contribution. All these contributions can be concisely expressed in one equation which is

$$T^{+}_{2,2N} = G(t_1)\,G(t_n)\prod_{i=1}^{N-1}\Big\{\bar{u}_{\beta}(A^{i})\,g_{\lambda^{i}}(t_i,\tau_i)$$

$$\frac{[\not{B}^{i}+M]}{B^{i2}-M^{2}}\,\beta\delta\; g_{\sigma^{i}}(t_{i+1},\tau_i)\,u_{\delta}[c^{i}]$$

$$\Big[\theta\left(\frac{D^{i}}{B^{i}}\right)+\theta\left(\frac{-D^{i}}{B^{i}}\right)\Big]\,\delta_{\Delta^{i},1}\Big\}\Big[\phi_{\lambda^{1}}[B^{0},q^{1},B^{1}]$$

$$\phi_{\sigma^{n-1}}(B^{n-1},q^{n},B^{n})\Big]\Big\{\prod_{i=1}^{n-2}\phi_{\sigma^{i}\lambda^{i+1}}[B^{i-1},q^{i},B^{i}]\Big\}$$

3·4·3

where

$$\Delta^{i} = \left|\frac{B^{i}}{D^{i}}\right| \qquad 3\cdot4\cdot4$$

Figs. 16(a) and 16(b) correspond to the first and second functions respectively in the above equation and represents the two ways in which a single loop can contribute. The addition of the crossed diagrams are necessary since the loop energies are not in the asymptotic region.

From equations, 3.4.3, 3.4.2 and 3.2.1, we obtain

$$\theta_{2N} = (\Pi\, d\Omega)\, G^2(t_1) G^2(t_n) \Big\{ \phi_{\mu^1}[B^0, q^1, B^1]$$

$$\phi_{\lambda^1}[B^0, q^1, B^1]\, \phi_{\nu^{n-1}}[B^{n-1}, q^n, B^n]\, \phi_{\sigma^{n-1}}[B^{n-1},$$

$$q^n, B^n]\Big\} \Big\{ \prod_{i=1}^{N-2} \phi_{\nu^i \mu^{i+1}}[B^i, q^{i+1}, B^{i+1}]$$

$$\phi_{\sigma^i \lambda^{i+1}}[B^i, q^{i+1}, B^{i+1}]\Big\} \Big\{ \prod_{i=1}^{N-1} [\bar{u}_\gamma(A^i)$$

$$g_{\lambda^i}(t_i, \tau_i)\, (2m\, I)_{\gamma\delta}\, g_{\sigma^i}(t_{i+1}, \tau_i)$$

$$u_\delta(c^i)\, \bar{u}_\alpha(c^i)\, g_{\nu^i}(t_{i+1}, \tau_i) \frac{(B^i + mI]_{\alpha\beta}}{(\tau_i - m^2)^2}$$

$$g_{\mu^i}(t_i, \tau_i)\, u_\beta(A^i)\Big]\Big\}$$

3.4.5

where I is the unit matrix. On summing the right-hand side of the above equation over all the nucleon spins $\alpha, \beta, \gamma, \delta$ we obtain

$$\theta_{2N} = (\Pi d\Omega) M_{2N} \qquad 3.4.6$$

where

$$M_{2N} = G^2(t_1)\, G^2(t_N) \left\{ \prod_{i=1}^{N-1} \left[\frac{2M\, Loop_{\mu^i \nu^i \sigma^i \lambda^i}}{(\tau_i - M^2)^2} \right] \right.$$

$$\prod_{i=1}^{N-2} \left[\phi_{\nu^i \mu^{i+1}} [B^i, q^{i+1}, B^{i+1}] \, \phi_{\sigma^i \lambda^{i+1}} [B^i, q, B^{i+1}] \right]$$

$$\phi_{\mu^1} [B^0, q^1, B^1] \, \phi_{\lambda^1} [B^0, q^1, B^1] \, \phi_{\nu^{n-1}} [B^{N-1}, q, B^N]$$

$$\left. \phi_{\sigma^{n-1}} [B^{N-1}, q^N, B^N] \right\} \qquad 3.4.7$$

and where

$$Loop_{\mu^i \nu^i \sigma^i \lambda^i} = Tr \left[(A^i + M)\, g_{\lambda^i}(t_i, \tau_i)\, g_{\sigma^i}(t_{i+1}, \tau_i) \right.$$

$$(\epsilon^i + M)\, g_{\nu^i}(t_{i+1}, \tau_i)\, (B^i + M)$$

$$\left. g_{\mu^i}(t_i, \tau_i) \right] \qquad 3.4.8$$

Section 5 - The Propagator and Coupling Function

From the preceding sections, it is evident that a knowledge of the propagators ϕ and the nucleon-nucleon-Reggeon coupling functions is required. The covariant formulae for these derived by Scadron are used in our model. Their formulae hold for non-Reggeised propagators of arbitrary spin J. We follow the prescription of Jones and Scadron (Ref. 27) who obtained their method for Reggeising invariant amplitudes based on Scadron's formalism of (Ref. 25).

In the latter, it was shown that high-spin wave functions give rise to covariant on-shell propagators which are related to rest frame rotation group tensors. Thus the propagators which we shall use will be on-shell propagators. In one of the later sections, we shall, following Scadron, show how to incorporate the off-mass-shell effects for the propagators.

The numerator of a propagator for general spin J is given by

$$P_{\mu^1 \ldots \mu^J ; \nu^1 \ldots \nu^J}(k)$$

$$= \sum_{\Lambda} \psi^{(\eta)}_{\mu^1 \ldots \mu^J}(k)\, \overline{\psi}^{(\Lambda)}_{\nu^1 \ldots \nu^J}(k) \qquad 3 \cdot S \cdot 1$$

where $\overline{\psi}_{\mu^1 \ldots \mu^J}$ is either a boson or a Fermion wave function and K is the momentum of the propagated particle of mass M. The expression

$$P_{\mu^1 \ldots \mu^J ; \nu^1 \ldots \nu^J}(k)$$

is contracted with the initial momenta p_ν and the final momenta p'_μ

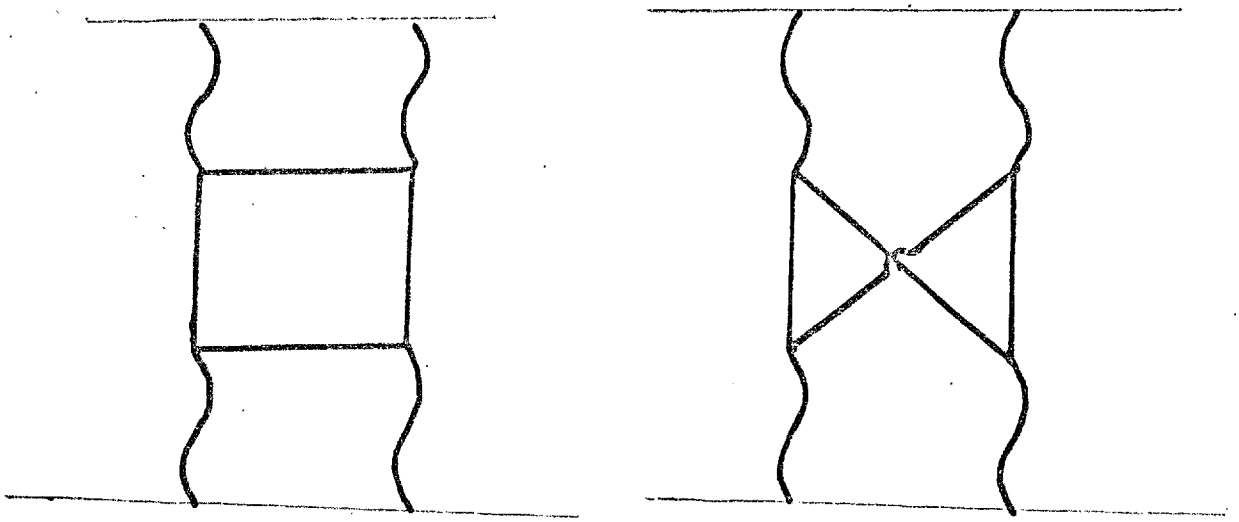

(a) (b)

Fig. 15

which produces the contracted propagator, for a virtual Boson will spin J in its rest frame given by

$$\mathcal{P}^{J}(p', p; k) = \sum_{\lambda', \lambda} \left\{ \rho^{1}_{\lambda'} \cdots \rho^{i}_{\lambda^{J'}} \mathcal{P}_{\lambda_1' \cdots \lambda_J'; \lambda_1 \cdots \lambda_J} \right.$$

$$\left. \rho_{\lambda' \cdots \lambda^{J}} \right\} \qquad 3.5.2$$

which can be expressed as a product of two O(3) tensors of rank J, given by $T_j(\underline{p}')$ and $T_j(\underline{p})$ This leads to

$$\mathcal{P}^{J}(p', p; M) = C_J \, P_J(\underline{p}', p)$$

where $P_J(\underline{p}' \cdot \underline{p})$ is the solid legendre polynomial given by

$$P_J(\underline{p}'; \underline{p}) = |\underline{p}'|^J \, |\underline{p}|^J \, P_J(\hat{\underline{p}}' \cdot \hat{\underline{p}}) \qquad 3.5.4$$

where $\hat{\underline{p}}$ is a unit rector

and C_J is a normalisation factor irrelevant for our purposes. By using the prescriptions

$$\delta_{ij} \rightarrow -(g_{\mu\nu} - k_\mu k_\nu)$$

and

$$p_i \rightarrow -p_\mu(k)$$

where

$$p_\mu(k) \equiv p_\mu - \frac{(p \cdot k)}{M^2} k_\mu \qquad 3.5.5$$

we boost equation 3.5.3 up to momentum K and obtain the covariant on-shell result for the propagator given by

$$\mathcal{P}^{J}(p', p; K) = C_J \, P_J\left[-p'(k) \cdot p(k)\right] \qquad 3.5.6$$

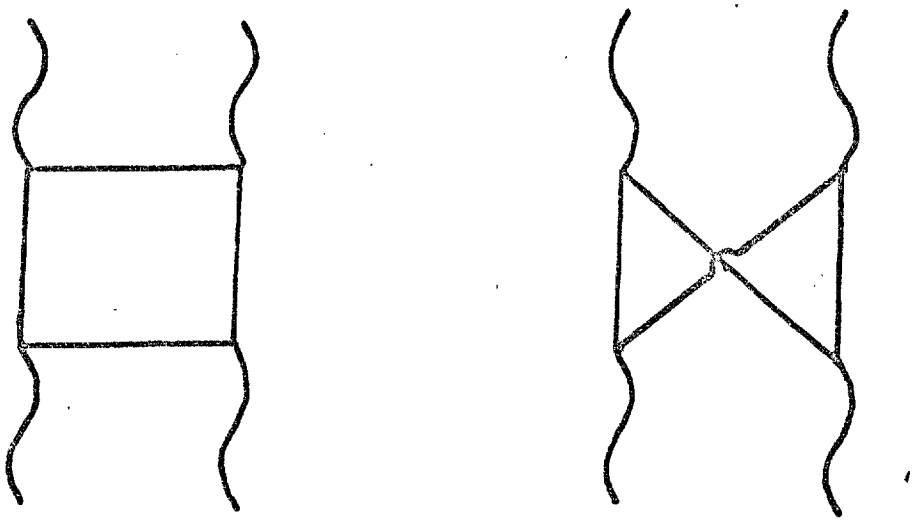

Fig. 16

Equation 3.5.6 gives the Boson propagator with spin J when it is coupled to zero spin particles.

To deal with the case when particles with spin other than zero are coupled to either end of the propagator, covariant labels must be freed from the left-hand side of 3.5.6. The number of labels thus freed is directly related to the spin of the particle concerned.

To derive the resulting propagators, Scadron used a covariant version of Zemach's O(3) differential technique (Ref.45). It involves differentiating the solid harmonic with respect to the momenta of the particles with spin. The following recursion relations satisfied by the spherical Harmonics P_J are used in the derivation

$$J\,P_J = -\nu(k)\,P'_J - p(k^2)\,p'(k)^2\,P'_{J-1} \qquad 3\text{-}5\text{-}7$$

$$(J-1)\,P'_J = -\nu(k)\,P''_J - p(k)^2\,p'(k)^2\,P''_{J-1} \qquad 3\text{-}5\text{-}8$$

$$(J+1)\,P_J = \nu(k)\,P'_J + P'_{J+1} \qquad 3\text{-}5\text{-}9$$

$$(J+2)\,P'_J = \nu(k)\,P''_J + P''_{J+1} \qquad 3\text{-}5\text{-}10$$

$$(2J-1)\,P'_{J-1} = P''_J - P(k)^2\,p'(k)^2\,P''_{J-2} \qquad 3\text{-}5\text{-}11$$

where $\nu(k) = p(k).p'(k)$ and dashes denote differentiation with respect to ν. Using these we obtain the formulae for the Boson propagators which are

$$P^J(p', p, k) = C_J P_J \qquad 3.5.12$$

$$P_{;\alpha}^{J}(p', p; k) = -\frac{C_J}{J}\left\{-p'_\alpha(k) P'_J + p'^2(k) p_\alpha(k) P'_{J-1}\right\} \qquad 3.5.13$$

$$P_{\beta;}^{J}(p', p; k) = -\frac{C_J}{J}\left\{p_\beta(k) P'_J + p^2(k) p'_\beta(k) P'_{J-1}\right\} \qquad 3.5.14$$

$$P_{\beta;\alpha}^{J}(p', p, k) = \frac{C_J}{J^2}\left\{\left[p_{\beta'}(k) p_\alpha(k) + p_\beta(k) p_{\alpha'}(k)\right] P''_J + \left[p^2(k) p'_\beta(k) p'_\alpha(k) + p_1^2(k) p_\beta(k) p_\alpha(k)\right] P''_{J-1} - g_{\beta\alpha}(k) P'_J - 2(J+1) p'_\beta(k) p_\alpha(k) P_{J-1}\right\} \qquad 3.5.15$$

For the interaction of particles with spin s_1 and s_2 at one end and s_1' and s_2' at the other end with spin J Boson propagator, one must consider a Boson propagator with at most $s_1 + s_2$ free α labels and $s_1' + s_2'$ free β labels. Thus for our Boson propagators with a pair of spin half nucleons at either end, we use equation 3.5.15.

The remaining problem is how a spin J propagator couples

to other particles. Scardon dealt with this by considering Lagrangian interactions in the context of the normality of the three-point vertex. The normality n of a particle of spin J is defined as

$$n = (-1)^J \times \text{intrinsic parity}$$

and the normality of the vertex is defined as the product of the normalities of each particle at the vertex. If a spin zero particle couples to particles with spin S and S^1 which is denoted by

$$0 + S \longrightarrow S^1$$

where S and S^1 are fermions, the number of independent on-shell couplings as counted from the rest frame of one of the particles is obviously $2S_M+1$ where

$$S_M = \text{Min}(S, S^1)$$

3·5·16

the fact that S and S^1 are fermions, leads to $\frac{1}{2}(2S_M+1)$ couplings being normal and $\frac{1}{2}(2S_M+1)$ abnormal couplings. This procedure is generalised to the case

$$S_1 + S_2 \longrightarrow S_3$$

Suppose that S_1 and S_2 are the lowest of the 3 spins. Let

$$S = S_1 + S_2$$

Then the problem is reduced to couplings

$$0 + S \rightarrow S_3$$

for

$$|S_1 - S_2| \leq S \leq S_1 + S_2$$

This enables us to show, as before, that if

$$S_1 + S_2 \leq S_3$$

there are $\frac{1}{2}(2S_1+1)(2S_2+1)$ normal couplings and the same number of abnormal couplings for fermion-fermion-Boson interactions where all three particles are on the mass-shell. Thus for two nucleons coupling to a Boson, we have 2 normal couplings C^+ and 2 abnormal couplings C^- We need consider only normal couplings as

$$C^+ \rightarrow C^-$$

where

$$1 \rightarrow \gamma_5$$

in Dirac spin space. Hence the coupling which we use for the nucleon-nucleon-Reggion vertices contain two terms which are given by

$$g_\alpha = g_1 \gamma_\alpha + g_2 P_\alpha \qquad 3.5.17$$

where P_α is the sum of the incoming momenta at the vertex at the other end of the propagator (see Fig. 17)

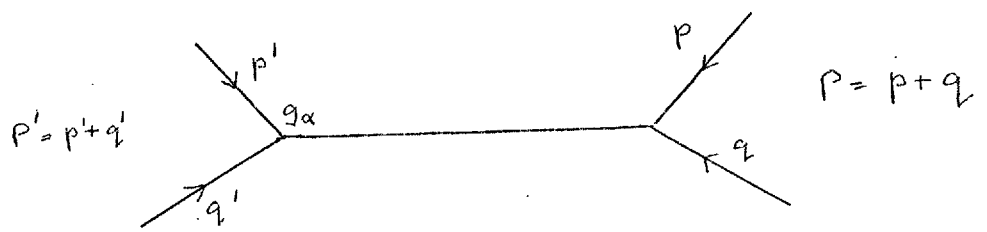

Fig. 17.

It is easy to understand why the coupling at one vertex depends on the momenta at the other vertex when one considers the fact

that the propagators are a function of the Scalar product To allow for particles with spin at a vertex, as mentioned earlier we differentiate with respect to the momenta at the vertex and obviously we are then left with

$$\frac{\partial (P.P')}{\partial P'_\mu} = P_\mu$$

For pion-nucleon scattering, equations 3.5.17, 3.5.13 enables us to recover the two invariant amplitudes A and B (see for example Ref. 46). For nucleon-nucleon scattering which concerns us, equations 3.5.15 and 3.5.17 lead to the 5 independent helicity amplitudes.

We now Reggeise equations 3.5.17 and 3.5.15 for the purposes of our model. The prescription for Reggeisation given by Jones and Scadron (Ref. 27) are the substitutions

(1) The spin J by the Regge trajectory $\alpha(t)$

(2) The coupling constants g_1 and g_2 by the Regge residue functions $g_1(t)$ and $g_2(t)$

(3) The expression $C_J P'_J(v)$ by

$$C_{\alpha(t)} P_{\alpha(t)}(v)\, e^{\frac{1}{2} i\pi\alpha(t)}$$

where t is the momentum transfer flowing along the propagator. For large s we have from the asymptotic properties of Legendre polynomials

$$C_{\alpha(t)} P_{\alpha(t)} \sim s^{\alpha(t)}$$

It must be noted that this procedure is not suitable for an $\alpha(0)=0$ trajectory in view of C_J having a pole at $\alpha(0) = 0$ and the residue g_2 having a zero for this value (Ref. 47).

We can now write down the Reggeisal Boson propagators and coupling functions which we use in equations 3.4.7 and 3.4.8.

The coupling functions are

$$g_{\alpha^i} = g_1(t_i)\,\gamma_{\alpha^i} + g_2(t_i)\,P^{i}_{\alpha^i} \qquad \alpha = \lambda, \mu$$

$$= g_1(t_{i+1})\,\gamma_{\alpha^i} + g_2(t_{i+1})\,Q^{i}_{\alpha^i} \qquad \alpha = \nu, \sigma \qquad 3.5.18$$

where

$$P^i = A^i + B^i \qquad i = 1, \ldots n$$

$$Q^i = B^i + C^i \qquad i = 1, \ldots n$$

The Reggeised Boson propagators are

$$\phi_B = \bar{\tau}_i\, s_1^{\alpha(t_1)-1}\, Q^{0}_{\beta}(q^1) \qquad \beta = \mu^1, \lambda^1 \qquad 3.5.19$$

$$= \bar{\tau}_n\, s_n^{\alpha(t_n)-1}\, P^{n}_{\beta}(q^n) \qquad \beta = \nu^{n-1}_{1}\sigma^{n-1} \qquad 3.5.20$$

$$\phi_{\nu^i \mu^{i+1}}\left[B^i, q^{i+1}, B^{(i+1)}\right]$$

$$= -\bar{\tau}_i\, s_i^{\alpha(t_i)} \Big\{ s_i^{-1}\, Q^{i}_{\mu^{i+1}}(q^{i+1})\, s_i^{-1}\, P^{i+1}_{\nu^i}(q^{i+1})$$

$$+ g_3\, g_{\nu^i}\, g_{\mu^{i+1}}(q^{i+1})\, s_i^{-1}$$

$$+ g_4\, s_i^{-1}\, P^{i+1}_{\mu^{i+1}}(q^{i+1})\, Q^{i}_{\nu^i}(q^{i+1})\, s_i^{-1}$$

$$+ g_5 S_i^{-1} P^{i+1}_{\mu^{i+1}}(q^{i+1}) S_i^{-1} P^{i+1}_{\nu^i}(q^{i+1}) Q^{i\,2}(q^{i+1}) S_i^{-1}$$

$$+ g_6 S_i^{-1} Q^i_{\mu^{i+1}}(q^{i+1}) S_i^{-1} Q^i_{\nu^i}(q^{i+1}) P_i^2(q^{i+1}) S_i^{-1} \Big\}$$

3.5.21

where

$$P_\mu(q) = P_\mu - \frac{(P\cdot q)}{q^2} q_\mu \qquad 3.5.22$$

and

$$g_{\mu\nu}(q) = g_{\mu\nu} - \frac{q_\mu q_\nu}{q^2} \qquad 3.5.23$$

$\bar{\tau}_i$ is the signature factor given by $exp\left[\frac{1}{2} i\pi \alpha(t_i)\right]$ and $\alpha(t_i)$ is the input Regge trajectory. The coefficient of the first term in the right-hand side of equation ?.5.27 is is normalised to unity by absorbing it in the constants g_1 and g_2. Similarly the coefficients of the right-hand sides of equations ?.5.19 and ?.5.20 are normalised to unity by multiplying the Reggeon-particle-particle coupling function by the appropriate factor.

Section 6 - Leader order terms and asymptotic approximation

By examining equations 3.4.8 and 3.5.18 it is clear that Loop $\mu^i \nu^i \sigma^i \lambda^i$ on expansion yields terms which are a product of the following

(i) $X^i_{\alpha^i}$ $(X = A, B, C \;,\; \alpha = \mu, \nu, \sigma, \lambda)$

(ii) $P^i_{\lambda^i}$, $P^{i'}_{\mu^{i'}}$, $Q^i_{\sigma^i}$, $Q^{i'}_{\nu^{i'}}$

(iii) $\delta_{\alpha\beta}$ $(\alpha, \beta = \nu_i, \mu_i, \lambda_i, \sigma_i \quad \alpha \neq \beta)$

(iv) $A^i \cdot B^i$, $A^i \cdot C^i$ and $B^i \cdot C^i$

Each product carries only one each of labels $\mu^i, \nu^i, \sigma^i, \ldots$ and λ^i Because of the $g_{\alpha\beta}$ terms which occur in the Regge propagators (the second term in the right-hand side of equation 3.5.21) each term in each loop couples with each term in every other loop, on contracting all the indices. It is useful to construct tables, listing the values for all couplings. Only a few entries need calculation. The rest follow from straightforward addition. In calculating these tables, inequalities 3.3.14 and 3.3.20 and equations 3.2.7 were used. Therefore, they contain errors to the order of σ_i

Table one for $i-j$ couplings $i<j$

	A^j	B^j	C^j	P^j	Q^j	q^j
A^i	0	$\frac{1}{2}C_i$	0	$\frac{1}{2}C_i$	$\frac{1}{2}C_i$	$\frac{1}{2}C_i$
B^i	$-\frac{1}{2}S_{ij}$	$-\frac{1}{2}S_{ij}$	$\frac{1}{2}C_j$	$-S_{ij}$	$-\frac{1}{2}S_{ij}$	$-\frac{1}{2}S_{i,j-1}$
C^i	$-\frac{1}{2}S_{ij}$	$-\frac{1}{2}S_{ij}$	0	$-S_{ij}$	$-\frac{1}{2}S_{ij}$	$-\frac{1}{2}S_{i,j-1}$
P^i	$-\frac{1}{2}S_{ij}$	$-\frac{1}{2}S_{ij}$	$\frac{1}{2}C_j$	$-S_{ij}$	$-\frac{1}{2}S_{ij}$	$-\frac{1}{2}S_{i,j-1}$
Q^i	$-S_{ij}$	$-S_{ij}$	$\frac{1}{2}C_j$	$-2S_{ij}$	$-2S_{ij}$	$-\frac{1}{2}S_{i,j-1}$
q^i	$-\frac{1}{2}S_{ij}$	$-\frac{1}{2}S_{ij}$	$\frac{1}{2}C_j$	$-S_{ij}$	$-\frac{1}{2}S_{ij}$	$-\frac{1}{2}S_{i,j-1}$

By $i-j$ couplings, we mean Scalar products of momenta with superscripts i and j

Table two for $i-i$ couplings

	A^i	B^i	C^i	P^i	Q^i	q^i
A^i	—	$\frac{1}{2}(\tau_i+m^2)$	$\frac{2m^2-\sigma_i}{2}$	$\frac{3m^2+\tau_i}{2}$	$\frac{3m^2+\tau_i-\sigma_i}{2}$	$\frac{\tau_i-m^2}{2}$
B^i	$\frac{1}{2}(\tau_i+m^2)$	—	$\frac{1}{2}(\tau_i+m^2)$	$\frac{1}{2}(3\tau_i^2+m^2)$	$\frac{3\tau_i+m^2}{2}$	$\frac{\tau_i-m^2}{2}$
C^i	$\frac{2m^2-\sigma_i}{2}$	$\frac{1}{2}(\tau_i+m^2)$	—	$\frac{3m^2+\tau_i-\sigma_i}{2}$	$\frac{3m^2+\tau_i-\sigma_i}{2}$	$\frac{\sigma_i+m^2-\tau_i}{2}$
P^i	$\frac{1}{2}(\tau_i+3m^2)$	$\frac{3\tau_i+m^2}{2}$	$\frac{3m^2+\tau_i-\sigma_i}{2}$	$\frac{4m^2+4\tau_i}{2}$	$\frac{4m^2+4\tau_i-\sigma_i}{2}$	τ_i-m^2
Q^i	$\frac{3m^2+\tau_i-\sigma_i}{2}$	$\frac{3\tau_i+m^2}{2}$	$\frac{3m^2+\tau_i-\sigma_i}{2}$	$\frac{4m^2+4\tau_i-\sigma_i}{2}$	$\frac{4m^2+4\tau_i}{2}$	$\frac{\sigma_i}{2}$
q^i	$\frac{\tau_i-m^2}{2}$	$\frac{\tau_i-m^2}{2}$	$\frac{\sigma_i+m^2-\tau_i}{2}$	τ_i-m^2	$\frac{\sigma_i}{2}$	τ_i

We divide the couplings between the momenta into 3 types.

(I) Internal couplings

(II) Reverse couplings

(III) Forward couplings

The internal couplings are the least complicated. They emerge within each loop when the trace is evaluated by the quantities A^i, B^i and C^i forming scalar-products among themselves, before we contact the loops with the propagator indices. There are only three internal couplings for any loop, namely $A^i.B^i$, $A^i.C^i$ and $B^i.C^i$

Both reverse and forward couplings involve the coupling of loop momenta to momenta occuring in the propagator expressions. Any particular coupling may involve a number of propagators supplying $g_{\mu\nu}$ factors and loops supplying $\delta_{\alpha\beta}$ factors. The actual momenta coupled together after contracting all indices in all the loops and propagators could be from the same or different loops, one or two propagators, either parallel (that is from the same rung of the multiperipheral ladder) or not. All the other propagators and loops involved act as links supplying transitory $g_{\mu\nu}$ and $\delta_{\alpha\beta}$ factors which disappear on contraction.

When at least one pair of parallel propagators participate in a coupling, whether in a transitory or a terminal role it is defined as a reverse coupling. A propagator or loop plays a terminal role when a 4-momenta from it actually figures in a scalar product of tables one or two. All couplings which are neither reverse nor internal are defined forward couplings.

E.g. consider the quantity $B^{c} \cdot q^{c-2}$ Two ways in which this could arise on expansion of equation 3.4.7 are given to illustrate forward couplings and reverse couplings.

(I)

$$B^{c} \cdot \partial_{\mu^{c}} \rightarrow B^{c}_{\mu^{c}}$$

$$B^{c}_{\mu^{c}} \cdot g_{\mu^{c}\nu^{c-1}} \rightarrow B^{c}_{\nu^{c-1}}$$

$$B^{c}_{\nu^{c-1}} \delta_{\nu^{c-1}\lambda^{c-1}} \rightarrow B^{c}_{\lambda^{c-1}}$$

$$B^{c}_{\lambda^{c-1}} \cdot q^{c-2} \rightarrow B^{c} \cdot q^{c-2}$$

This is an example of a forward coupling in which the successive couplings are all along one direction of the multiperipheral ladder.

(II) B^{i} couples as above to form $B^{i}_{\lambda^{i-1}}$ Then it proceeds to a further loop, say the $i-4^{th}$ loop, couples to the δ-function in that loop, then retraces its tracks through the propagators not already used, proceeds back to the $i-1^{th}$ loop and couples to q^{i-2} to form $B^{i}q^{i-2}$ This is an example of a reverse coupling. In table two, all the entries except $A^{i}\cdot B^{i}, A^{i}\cdot C^{i}$ and $B^{i}\cdot C^{i}$ are necessarily reverse couplings.

The second term in the right-hand side of equation 3.5.21 shows that each transition through a propagator effectively provides a multiplying factor of s_{i}^{-1} which is the sub-energy across it (we need not consider the terms $\overline{\tau}_{i}\, s_{i}^{\alpha(t_{i})}$ as it is obvious that the product $\prod \tau_{i}\, s_{i}^{\alpha(t_{i})}$ is a common factor for all the terms of M_{2N}). This means each $i-j$ value of table one and the reverse $i-i$ values of table two have to be multiplied by the corresponding s_{i}^{-1} factor for each transitional propagator link involved in the coupling. Since the reverse couplings have more transitional links than the forward couplings for the same $i-j$ and $i-i$ values, clearly they are negligible asymptotically in view of the s_{i} tending to infinity. Hence we omit all reverse couplings in selecting the leading terms. On restricting ourselves to forward couplings, it is evident from table one for $i-j$ couplings, the corresponding table for $i+1-j$ couplings (i.e., we substitute $i+1$ for i in table one), and equations 3.3.19 and 3.3.20 that equations 3.5.18 up to 3.5.23 become

$$\phi_{B} = \overline{\tau}_{1}\, s_{1}^{\alpha(t_{1})-1}\, Q^{0}_{\beta} \qquad B=\mu^{1},\lambda^{1} \qquad 3.6.1$$

$$= \overline{\tau}_{n}\, s_{n}^{\alpha(t_{n})-1}\, p^{n}_{\beta} \qquad \beta=\nu^{n-1},\sigma^{n-1} \qquad 3.6.2$$

$$\phi_{\nu^c \mu^{c+1}}[B^c, q^{c+1}, B^{c+1}] = -\bar{\tau}_c S_{c+1}^{\alpha(t_c)} [\psi_{\nu^c \mu^{c+1}} + \zeta_{\nu^c \mu^{c+1}}] \quad 3.63$$

where

$$\psi_{\nu^c \mu^{c+1}} = g_3 g_{\nu^c \mu^{c+1}} S_{c+1}^{-1} \quad 3.6.4$$

and

$$\zeta_{\nu^c \mu^{c+1}} = S_{c+1}^{-1} P^{c+1}_{\nu^c} S_{c+1}^{-1} Q^c_{\mu^{c+1}} \quad 3.65$$

It is easy to see how most of the terms of equations 3.5.21 drop out when we derive equation 3.6.3. For instance $q^c.X$ and $P^c.X$ are negligible compared to $Q^{c-1}.X$ where X is any momentum in Fig. 14, such that all these three quantities are forward couplings. It may be noted that the q_c terms in 3.5.21 arising from 3.5.22 all disappear on selecting the leading order terms. This is a crucial factor which helps us to analyse the effects of treating the propagators and couplings as off-mass shell, which they actually are, in Section 8.

Though the internal couplings of table two do not have any S_c dependence, it is obvious from equation 3.4.8 that they appear on the same footing as the m^2 terms which act as coefficients of the leading order terms. Considering forward couplings, altogether they belong to three categories; $X^c.Y^j$ $X^c.U^j$ and $U^c.V^j$ where X and Y belong to the set (A,B,C,P,Q) as can be seen from equations 3.4.8 and 3.5.18 and U and V belong to the set (P,Q) as seen from equations 3.6.1 up to 3.6.5. From table one and equations 3.3.19 and 3.6.1 - 3.6.5 it can be easily deduced that S_c^{-1} factors of these couplings, which are picked up each time a propagator figures in them, (are exactly cancelled by the S_c factors which arise from the values of table one of these

couplings.

Thus we can write

$$M_{2N} = \left\{ \left[\prod_{i=1}^{n} \tau_i s_i^{\alpha(t_i)} \right]^2 \left[\Pi g(t_i) g^*(t_i) \right] G^2(t_1) \right.$$

$$\left. G^2(t_n) \right] \Big\} \sum L_{2N} \qquad 3.6.6$$

$$g_1(t_i) = g_1 g(t_i) \qquad 3.6.7$$

and

$$g_2(t_i) = g_2 g(t_i)$$

where g_1 and g_2 are constants and $g(t_i)$ is the same as the expression $\sqrt{g}\, f(t_i)$ which we used in the last chapter as one of the factors in the Reggeon-Reggeon-particle coupling functions. We define the two nucleon-Reggeon coupling functions thus in order that the model of this chapter may be compared with the single-pole model described in the last chapter. L_{2N} is independent of the s_i, each L_{2N} being a product of terms, one from each loop $\mu^i \nu^i \sigma^i \lambda^i$ and one from each Boson propagator. The summation is over all such possible L_{2N}

It can be seen from tables one and two, that the leading order non-reverse couplings, in the asymptotic approximation, are independent of the t_i This implies that the same holds for L_{2N} However, it is not possible to draw the conclusion that it is true for $\sum L_{2N}$ also. The leading terms of all the L_{2N} could cancel, forcing us to examine the next leading terms in each L_{2N} to extract the asymptotic behaviour of M_{2N} These non-leading order terms of L_{2N}

will have complicated s_i and t_i dependence in two ways.

(I) They contain the terms dropped because of the asymptotic arguments in the earlier part of this section.

(II) It will be necessary to rewrite the approximate equations 3.2.7 in exact form to take into account lower order terms.

The L_{2N} can be grouped according to different orders of the coupling constants and summed, enabling us to write

$$\bar{M}_{2N} = \sum \bar{L}_{2N}$$

$$= \sum_{K=0}^{4n-4} \sum_{\lambda=1}^{N} g_2^{4n-4-k} g_1^{k} g_3^{2\lambda-k,\lambda} \bar{L}_{2N} \qquad 3.6.9$$

We proceed to show that at least one $\bar{L}_{2N}^{k,\lambda}$ on integration over all the τ_i and σ_i gives a non-zero result.

Consider $\bar{L}_{2N}^{4n-4,0}$ From equations 3.6.3.- 3.6.5, it is obvious that the $\bar{L}_{2N}^{k,0}$ factorises for all K owing to the absence of transitory propagator links($(g_{\mu\nu})$ terms) which correlate different loops. Each factor is dependent only on g_1^2, g_2^2, σ_i and τ_i the corresponding loop energies. Since the loop energies have integration limits $4m^2$ and M^2 independent of the position of the loop in the multiperipheral ladder, we can write without altering the value of θ_{2N}

$$\prod_{i=1}^{n-1} \left[\frac{\pi}{2} \int_{4m^2}^{M^2} \frac{d\sigma_i}{\sigma_i} \int_{\tau_i^-}^{\tau_i^+} d\tau_i\right] \bar{L}_{2N}^{4n-4,0}$$

$$= \left\{\left[\frac{\pi}{2} \int_{4m^2}^{M^2} \frac{d\sigma}{\sigma_i} \int_{\tau_i^-}^{\tau_i^+} d\tau_i\right] \bar{L} \cdot \frac{M}{(\tau_i - M^2)^2}\right\}^{N-1} \qquad 3.6.10$$

where $\bar{\bar{L}} = S_i^{-2} Q^{i-1}_{\mu^i} Q^{i-1}_{\lambda^i} L^4_{\mu^i\nu^i\sigma^i\lambda^i} P^{i+1}_{\nu^i} P^{i+1}_{\sigma^i} S_{i+1}^{-2}$

3·6·11

and $L^K_{\mu^i\nu^i\sigma^i\lambda^i}$ is the coefficient of the g_1^K term in $Loop_{\mu^i\nu^i\sigma^i\lambda^i}$

Since the number of terms in the expansion of expression of the type

$$Tr[\not{A}_1 \not{A}_2 \not{A}_3 \ldots \not{A}_n]$$

where

$$\not{A} = A \cdot \gamma$$

is given by zero when n is odd (because the trace of an odd number of γ-matrices is zero, and by $(n-1)!!$ when n is even (Ref. 47) the number of terms $\bar{n}$ in the expansion of $Loop_{\mu^i\nu^i\sigma^i\lambda^i}$ is given by

$$\bar{n} = {}^7C_6 * 5!! + {}^7C_4 \cdot 3!! + {}^7C_2 \cdot 1!! = 232$$

We group the 232 terms according to different orders of the coupling constants and express $Loop_{\mu^i\nu^i\sigma^i\lambda^i}$ according to the equation

$$Loop_{\mu^i\nu^i\sigma^i\lambda^i} = 4\left[g_2^4 F_4 + g_2^3 g_1 F_3 + g_2^2 g_1^2 F_2 + g_2 g_1^3 F_1 + g_1^4 F_0\right]$$

where, (in the following four equations, we drop the subscript for convenience, since it is common to all momenta) 3·6·12

$$F_4 = M P_\mu Q_\nu Q_\sigma P_\lambda \left[M^2 + A\cdot B + B\cdot C + A\cdot C\right]$$

3·6·13

$$F_3 = M^2 \left\{ Q_\nu Q_\sigma P_\lambda \partial^\mu \cdot [\not{A} + \not{B} + \not{C}] + P_\mu Q_\sigma P_\lambda \partial^\nu [\not{A} + \not{B} + \not{C}] + P_\mu Q_\nu P_\lambda \partial^\sigma [\not{A} + \not{B} + \not{C}] + P_\mu Q_\nu Q_\sigma \partial^\lambda [\right.$$

$$[\not{A}\not{B}\not{\epsilon}] + Q_\nu Q_\sigma P_\lambda \not{A} \partial^\mu \not{B} \not{\epsilon} + P_\mu Q_\sigma P_\lambda \not{A} \not{B} \partial^\nu \not{\epsilon}$$
$$+ P_\mu Q_\nu P_\lambda \not{A} \not{B} \not{\epsilon} \partial^\sigma + P_\mu Q_\nu Q_\sigma \not{A} \not{B} \not{\epsilon} \partial^\lambda \} \qquad 3.6.14$$

$$F_2 = M\{P_\mu Q_\nu [M^2 \partial^\sigma \partial^\lambda + \not{A}\not{B} \partial^\sigma \partial^\lambda + \not{A}\not{\epsilon} \partial^\sigma \partial^\lambda + \not{B}\not{\epsilon} \partial^\sigma \partial^\lambda]$$
$$+ P_\mu Q_\sigma [M^2 \partial^\nu \partial^\lambda + \not{A}\not{B} \partial^\nu \partial^\lambda + \not{A} \partial^\nu \not{\epsilon} \partial^\lambda + \not{B} \partial^\nu \not{\epsilon} \partial^\lambda]$$
$$+ P_\mu P_\lambda [M^2 \partial_\nu \partial_\sigma + \not{A}\not{B} \partial^\nu \partial^\sigma + \not{A} \partial^\nu \not{\epsilon} \partial^\sigma + \not{B} \partial^\nu \not{\epsilon} \partial^\sigma]$$
$$+ Q_\nu Q_\sigma [M^2 \partial^\mu \partial^\lambda + \not{A} \partial^\mu \not{B} \partial^\lambda + \not{A} \partial^\mu \not{\epsilon} \partial^\lambda + \partial^\mu \not{B} \not{\epsilon} \partial^\lambda]$$
$$+ Q_\nu P_\lambda [M^2 \partial^\mu \partial^\sigma + \not{A} \partial^\mu \not{B} \partial^\sigma + \not{A} \partial^\mu \not{\epsilon} \partial^\sigma + \partial^\mu \not{B} \not{\epsilon} \partial^\sigma]$$
$$+ Q_\sigma P_\lambda [M^2 \partial^\mu \partial^\sigma + \not{A} \partial^\mu \not{B} \partial^\nu + \not{A} \partial^\mu \partial^\nu \not{\epsilon} + \partial^\mu \not{B} \partial^\nu \not{\epsilon}]$$

$$F_1 = P_\mu \{M^2 [\not{A} \partial^\nu \partial^\sigma \partial^\lambda + \not{B} \partial^\nu \partial^\sigma \partial^\lambda + \partial^\nu \not{\epsilon} \partial^\sigma \partial^\lambda] + \not{A}\not{B} \partial^\nu \not{\epsilon} \partial^\sigma \partial^\lambda \}$$
$$+ Q_\nu \{M^2 [\not{A} \partial^\mu \partial^\sigma \partial^\lambda + \partial^\mu \not{B} \partial^\sigma \partial^\lambda + \partial^\mu \not{\epsilon} \partial^\sigma \partial^\lambda] + \not{A} \partial^\mu \not{B} \not{\epsilon} \partial^\sigma \partial^\lambda \}$$
$$+ Q_\sigma \{M^2 [\not{A} \partial^\mu \partial^\nu \partial^\lambda + \partial^\mu \not{B} x^\nu \partial^\lambda + \partial^\mu \partial^\nu \not{\epsilon} \partial^\lambda] + \not{A} \partial^\mu \not{B} \partial^\nu \not{\epsilon} \partial^\lambda \}$$
$$+ P_\lambda \{M^2 [\not{A} \partial^\mu \partial^\nu \partial^\sigma + \partial^\mu \not{B} \partial^\nu \partial^\sigma + \partial^\mu \partial^\nu \not{\epsilon} \partial^\sigma]$$
$$+ \not{A} \partial^\mu \not{B} \partial^\nu \not{\epsilon} \partial^\sigma \} \qquad 3.6.16$$

and

$$F_0 = M \{M^2 \partial^\mu \partial^\nu \partial^\sigma \partial^\lambda + \not{A} \partial^\mu \not{B} \partial^\nu \partial^\sigma \partial^\lambda$$
$$+ \not{A} \partial^\mu \partial^\nu \not{\epsilon} \partial^\sigma \partial^\lambda + \partial^\mu \not{B} \partial^\nu \not{\epsilon} \partial^\sigma \partial^\lambda \} \qquad 3.6.17$$

To simplify equations 3.6.13 - 3.6.17, we use the following relations satisfied by expressions containing γ- matrices (Ref. 47)

$$Tr[A\,B] = 4A\cdot B \qquad 3.6.18$$

$$Tr[A_1 A_2 \ldots A_N] = Tr[A_N A_{N-1} \ldots A_2 A_1] \qquad 3.6.19$$

$$Tr[A_1 A_2 \ldots A_N] = Tr[A_N A_{N-1} \ldots A_2 A_1] \qquad 3.6.20$$

$$Tr[A_1 A_2 \ldots A_C A_{C+1} \ldots A_N] + Tr[A_1 A_2 \ldots A_{C+1} A_C \ldots A_N]$$

$$= 2(A_C \cdot A_{C+1})\, Tr[A_1 A_2 \ldots A_{C-1} A_{C+2} \ldots A_N] \qquad 3.6.21$$

$$Tr[A_1 A_2 \ldots A_C A_{C+1} \ldots A_N]$$

$$= A_C^2\, Tr[A_1 A_2 \ldots A_{C-1} A_{C+2} \ldots A_N] \qquad 3.6.22$$

for $A_C = A_{C+1}$

We also use the following rules, based on the asymptotic reasonings earlier in this section, to select the leading order terms. This enables us to reduce the number of terms to less than 100.

(I) All $\delta_{\lambda\mu}$ and $\delta_{\sigma\nu}$ terms are omitted as they give rise to reverse couplings.

(II) All terms containing $A_{\mu i}$, $A_{\sigma i}$, $C_{\mu i}$ and $C_{\lambda i}$ are excluded, since from table one (the first row and the third column) it is clear that they can give rise to forward couplings of non-leading order only.

These two rules, together with equations 3.6.18 up to 3.6.22 enable us to rewrite equations 3.6.13 up to 3.6.17 as

$$F_4 = P_\mu Q_\nu Q_\sigma P_\lambda \{M^3 + M(A\cdot B + B\cdot C + A\cdot C)\} \qquad 3\text{-}6\text{-}23$$

$$F_3 = 4M^2 P_\mu Q_\nu Q_\sigma P_\lambda + Q_\nu Q_\sigma P_\lambda [(B\cdot C)A_\mu + (A\cdot C)B_\mu] + P_\mu Q_\sigma P_\lambda [(A\cdot B)C_\nu + (A\cdot C)B_\nu] + P_\mu Q_\nu P_\lambda [(A\cdot B)C_\sigma - (A\cdot C)B_\sigma] + P_\mu Q_\nu Q_\sigma [(B\cdot C)A_\lambda - (A\cdot C)B_\lambda] \qquad 3\text{-}6\text{-}24$$

$$\begin{aligned} F_2 = M\{ & P_\mu Q_\nu \delta_{\lambda\sigma}[A\cdot B + A\cdot C + B\cdot C + M^2] \\ & + P_\mu Q_\nu \delta_{\lambda\nu}[A\cdot B - A\cdot C - B\cdot C + M^2] \\ & + P_\lambda Q_\nu \delta_{\mu\sigma}[-A\cdot B - A\cdot C + B\cdot C + M^2] \\ & + P_\lambda Q_\sigma \delta_{\mu\nu}[-A\cdot B + A\cdot C - B\cdot C + M^2] \\ & + P_\mu Q_\nu [A_\lambda B_\sigma + A_\lambda C_\sigma + B_\lambda C_\sigma] \\ & + P_\mu Q_\sigma [A_\lambda B_\nu + A_\lambda C_\nu + B_\lambda C_\nu] \\ & + P_\lambda Q_\nu [A_\mu B_\sigma + A_\mu C_\sigma + B_\mu C_\sigma] \\ & + P_\lambda Q_\sigma [A_\mu B_\nu + A_\mu C_\nu + B_\mu C_\nu]\} \end{aligned} \qquad 3\text{-}6\text{-}25$$

$$F_1 = [P_\mu A_\lambda + A_\mu P_\lambda][B_\nu C_\sigma + B_\sigma C_\nu]$$

$$+ [Q_\nu C_\sigma + Q_\sigma C_\nu][B_\mu A_\lambda + B_\lambda A_\nu]$$

$$+ \delta_{\lambda\sigma}[P_\mu C_\sigma (AB+M^2) + P_\mu B_\nu (AC+M^2)$$

$$+ Q_\nu A_\mu (BC+M^2) + Q_\nu B_\mu (AC+M^2)]$$

$$+ \delta_{\lambda\nu}[P_\mu C_\sigma (AB+M^2) - P_\mu B_\sigma (AC+M^2)$$

$$- Q_\sigma A_\mu (BC-M^2) - Q_\sigma B_\mu (A\cdot C-M^2)]$$

$$+ [Q_\sigma A_\lambda (M^2-B\cdot C) + Q_\sigma B_\lambda (A\cdot C-M^2)$$

$$+ P_\lambda C_\sigma (M^2-A\cdot B) + P_\lambda B_\sigma (A\cdot C-M^2)]\delta_{\mu\nu}$$

$$+ [Q_\nu A_\lambda (M^2+BC) - Q_\nu B_\lambda (M^2+AC)$$

$$+ P_\lambda C_\sigma (M^2-AB) + P_\lambda B_\nu (M^2-AC)]\delta_{\mu\sigma} \qquad 3.6.26$$

and

$$F_0 = L^4 \mu' \nu' \sigma' \lambda'$$

$$= M\{(M^2 + A\cdot C - A\cdot B - B\cdot C)(\delta_{\mu\nu}\delta_{\sigma\lambda} - \delta_{\mu\sigma}\delta_{\lambda\nu})$$

$$+ \delta_{\lambda\sigma}(A_\mu B_\nu + A_\mu C_\nu + C_\nu B_\mu) + \delta_{\lambda\nu}[-A_\mu B_\sigma$$

$$+ A_\mu C_\sigma + C_\sigma B_\mu] + \delta_{\mu\sigma}[A_\lambda B_\nu + A_\lambda C_\nu - C_\nu B_\lambda]$$

$$+ \delta_{\lambda\nu}[-A_\lambda B_\sigma + A_\lambda C_\sigma - C_\sigma B_\lambda]\} \qquad 3.6.27$$

On the insertion of 3.6.27 in 3.6.11, all the terms antisymmetric in either $\mu \leftrightarrow \lambda$ or $\nu \leftrightarrow \sigma$ disappear. Thus equation 3.6.27 effectively becomes, for the purposes of

3.6.11

$$F_0 = \mu \left[A_\lambda \zeta_\nu \delta_{\mu\sigma} + A_\lambda \zeta_\sigma \delta_{\mu\nu} + A_\mu \zeta_\nu \delta_{\lambda\sigma} + A_\mu \zeta_\sigma \delta_{\lambda\nu} \right]$$

3.6.28

Then using table one and equation 3.3.19, we have

$$\bar{\bar{L}} = \frac{32}{\sigma_i}$$

3.6.29

We can easily perform the integrations of equation 3.6.10 and write

$$I = \int_{4m^2}^{M^2} \frac{d\sigma_i}{\sigma_i} \int_{\tau_i^-}^{\tau_i^+} \frac{\bar{\bar{L}}}{(\tau_i - m^2)^2}$$

3.6.30

$$\propto \left[1 - \frac{4m^2}{M^2} \right]^{3/2}$$

3.6.31

Obviously I is non-zero as otherwise we would have

$$M^2 = 4m^2$$

which implies zero phase-space in view of the limits of the integration.

Therefore, it is clear that the leading order terms of $\bar{H}_{2N}$ after integration over the loop energies and momenta and substitution in θ_{2N} can cancel only if terms to different order in g_1, g_2 and g_3 cancel. It will be seen in the next section that such cancellations cannot occur whatever the value of g_3 and will occur at most only for 4 specific values of g_1/g_2. In the absence of any reason to the contrary, we assume that g_1 and g_2 do not take such values. Otherwise, we shall have to analyse those four cases separately. In fact, if

the trajectory is the Pomeron, then helicity conservation in the s-channel suggest that g_2 is zero or close to it, ruling out cancellations since then the values of $\text{Loop}_{\mu^i \nu^i \sigma^i \lambda^i}$ is given by 3.6.29.

Section 7 - The impact of nucleon loops on the M.R.M.

From equations 3.3.1, 3.3.15, 3.4.1, 3.4.6, 3.6.6 and 3.6.9, we have

$$\text{Im } T_{22}(s) = A_{22} + \sum_{N=1}^{\infty} \left\{ [\Pi d\Omega]_{M\cdot R\cdot M} \right.$$

$$\prod_{i=1}^{N-1} \left[\int_{4M^2}^{M^2} d\sigma_i \frac{\pi}{2\sigma_i} \int_{\tau_i^-}^{\tau_i^+} d\tau_i \right]$$

$$\left[\prod_{i=1}^{N} \bar{\tau}_i s_i^{\alpha(t_i)} \right]^2 \left[\prod_{i=1}^{N-1} g(t_i) \right.$$

$$g^*(t_i') \Big]^2 \left[G^2(t_1) G^2(t_n) \right]$$

$$\left. \left[\bar{M}_{2N} \right] \right\} \qquad 3.7.1$$

Let

$$f_N = \prod_{i=1}^{N-1} \left[\int_{4M^2}^{M^2} d\sigma_i \frac{\pi}{2\sigma_i} \int_{\tau_i^-}^{\tau_i^+} d\tau_i \right] \bar{M}_{2N} \qquad 3.7.2$$

Examination of equation 3.7.1 then shows that were it not for the factors f_N equation 3.7.1 would be identical to the multi-Regge integral equation, in the factorisable approximation with a single pole input derived in the last chapter. The arguments of section six make it obvious that $\bar{M}_{2N}$ is the residual factor after all

the s_i dependence in M_{2N} has been extracted and absorbed into the multi-Regge part of equation 3.7.1.

f_N therefore depends only on the constants M^2, m^2, g_1, g_2 and g_3 and therefore is itself a constant expressible in terms of these by means of equation 3.7.2. Equation 3.7.1 is obtained by multiplying each intermediate state contribution to the amplitude in the multi-Regge integral equation by the factor f_N. In the factorisable approximation, the multi-Regge version of the unitarity equation in the j-plane at $t=0$ can be expressed as

$$\mathrm{Im}\, T_{22}(j) = A_{22} + \sum_{N=1}^{\infty} \left(g^2 \frac{A_{22}}{G_4} \right)^{N-1} A_{22} \qquad 3.7.3$$

where g and G are the Reggeon-Reggeon-particle and the Reggeon-particle-particle coupling constants respectively. This equation, except for the 1^{st} term which is included later there, can be obtained from equation 2.3.17 of the last chapter by putting

$$j = 2\alpha(0) - 1 - \frac{i\gamma}{\log s} \qquad 3.7.4$$

and taking the Mellin transform. On going through the arguments leading from equation 2.3.3. to 2.3.17 in the last chapter, it is obvious that multiplying each term, representing an intermediate state, in the unitarity sum by a different constant does not affect it.

Thus remembering that g^4 of equation 3.7.1 is equivalent to g^2 of equation 3.7.3, 3.7.1 leads to

$$\mathrm{Im}\ T_{22}(j) = A_{22} + \sum_{N=1}^{\infty} f_N \left(\frac{g^4 A_{22}}{G^4} \right)^{N-1} A_{22}$$

3.7.5

It is convenient to extract the factors

$$\prod_{i=1}^{N-1} \frac{1}{(\tau_i - M^2)^2}$$

from $\bar{M}_{2N}$ and write

$$f_N = \prod_{1}^{N} \left[\int_{4m^2}^{M^2} d\sigma_i \frac{\pi}{2\sigma_i} \int_{\tau_i^-}^{\tau_i^+} \frac{d\tau_i}{(\tau_i - m^2)^2} \right] Q_{2N}$$

3.7.6

Then we have from section 6,

$$Q_{2N} = \left\{ Q^0_{\mu}, Q^0_{\lambda}, P^n_{\sigma^{n-1}} P_{\sigma^{n-1}} \prod_{i=1}^{N-1} [\mathrm{Loop}\ \mu^i \nu^i \sigma^i \lambda^i] \right.$$
$$\left. \prod_{i=1}^{N-2} \left[\left(P^{i+1}_{\nu^i} Q^i_{\mu^{i+1}} + g_3 g_{\nu^i \mu^{i+1}} \right) \left(P^{i+1}_{\sigma^i} Q^i_{\lambda^{i+1}} + g_3 g_{\sigma^i \lambda^{i+1}} \right) \right] \right\}$$

3.7.7

Section 6 makes it clear that only the entries $B^i.A^j$, $B^i.B^j$, $B^i.P^j$, $C^i.A^j$, $C^i.B^j$, $C^i.P^j$, $Q^i.A^j$, $Q^i.B^j$ and $Q^i.P^j$ of table one and $A^i.B^i$, $A^i.C^i$ and $B^i.C^i$ of table two figure in the expansion of the right-hand side of equation 3.7.7. Of these, the entries of table two, being internal couplings are not the result of contraction of the propagator subscripts with the loop subscripts. Only the first nine, which are from table one result from such contraction. The negative signs of these entries are irrelevant as in each term of loop $\mu^i \nu^i \sigma^i \lambda^i$

the momenta occur in pairs, thus cancelling out the sign. It must be noted that the values given, in table one are not what we use in evaluating equation 3.7.7. Because $\bar{M}_{2N}$ and hence Q_{2N} is the residual factor after all the s_i factors are extracted from M_{2N} we must multiply each entry in table one by the factor Δ given by

$$\Delta = \prod_{\lambda=i}^{j-1} \frac{1}{s_{\lambda+1}} \qquad 3.7.8$$

On examination of the relevant entries of table one, it can be observed that when only A^i, B^i or C^i occur in the Scalar product, its value is given by $\frac{1}{2} s_{ij}$ irrespective of whether the correlating momenta are A, B or C. If one of P or Q replaces these, the Scalar product doubles and if both P and Q replace the quantities A, B or C in the pair of correlating momenta, giving P.Q, the value of the product quadruples to $2 s_{ij}$

This means that in equation 3.7.7, we can replace P^{i+1} and Q^i by quantities $2X^{i+1}$ and $2X^i$ where these are defined by the equation

$$X^i . X^j = \frac{\frac{1}{2} s_{ij}}{\prod_{\lambda=1}^{j-1} s_{\lambda+1}} \qquad \text{for all } i,j. \quad i \neq j \qquad 3.7.9$$

Similarly, in equations 3.6.23 up to 3.6.27, we can replace all the P's and Q's by 2X's and all the A's and B's by X's, taking care that these replacements are not carried out for the internal couplings of these equations, viz. $A^i.B^i$, $A^i.C^i$ and $A^i.B^i$ whose values are given in table two.

Equations 3.7.9 and 3.3.19 lead to

$$X^i . X^j = \frac{1}{2} \frac{1}{\prod_{\lambda=i}^{j-2} \sigma_{\lambda+1}} \qquad 3.7.10$$

Now X^i correlates with X^j through the $g_{\mu\nu}$ terms in the propagators and δ terms in the loops between the i^{th} and the j^{th}. One and only one term participates from each loop in this correlation. Equation 3.7.10 demonstates that each loop between the i^{th} and the j^{th} there is a corresponding σ factor in the denominator in the right-hand side. Hence if we make the transformation

$$\delta_{\alpha^i \beta^i} \longrightarrow \frac{\delta_{\alpha^i \beta^i}}{\sigma_i}$$

in equations 3.6.23 - 3.6.27, where

$$\alpha = \mu, \lambda$$
$$\beta = \sigma, \nu$$

we can then replace equation 3.7.10 with

$$X^i . X^j = \frac{1}{2} \qquad 3.7.11$$

If we make the further transformations

$$X^i \longrightarrow \frac{1}{\sqrt{2}} X^i$$

in equations 3.6.23 - 3.6.27 and 3.7.7, we can write

$$X^i . X^j = 1 \quad \text{for all} \quad i,j$$

3.7.12

This result allows us to make the final replacement of all the subscripted quantities in equations 3.6.23 - 3.6.27 and 3.7.7, with the Scalar unity.

That is

$$X^i \rightarrow 1 \quad \text{for all } i$$

and

$$\left.\begin{aligned} &\delta_{\alpha^i \beta^i} \rightarrow 1 \\ &g_{\alpha^i \beta^{i+1}} \rightarrow 1 \end{aligned}\right\} \quad \begin{aligned} &\text{for all } i \\ &\text{and } \alpha = \mu, \lambda \\ &\beta = \nu, \sigma \end{aligned}$$

Then these equations become

$$Q_{2N} = 2^4 \left\{ \prod_{i=1}^{N-1} \text{Loop}_i \right\} \left[4 + g_3 \right]^{2(N-2)}$$

3.7.13

where

$$\begin{aligned} 4\,[\text{Loop}_i] = {} & g_1^4\, 16 \left\{ m^4 + m^2 \left(\tau_i + 2m^2 - \frac{\sigma_i}{2} \right) \right\} \\ & + g_2^3 g_1 \left\{ 64\, m^3 + 16m \left(\tau_i + m^2 \right) \right\} \\ & + g_2^2 g_1^2 \left\{ \frac{32 m^4}{\sigma_i} + 48\, m^2 \right\} \\ & + g_2 g_1^3 \left\{ 16m + \frac{32 m^3}{\sigma_i} \right\} + g_1^4 \frac{8 m^2}{\sigma_i} \end{aligned}$$

3.7.14

Then 3.7.6 leads to

$$f_N = 16\left[\frac{\pi}{2}\int_{4m^2}^{M^2}\frac{d\sigma_i}{\sigma_i}\int_{\tau_i^-}^{\tau_i^+}\frac{d\tau_i}{(\tau_i-m^2)^2}\,Loop_i\right]^{N-1}\left[4+g_3\right]^{2N-4} \qquad 3.7.15$$

The double integration is easily performed by splitting $Loop_i$ into 3 parts, each part being separable in the variables σ_i and τ_i. After doing the integration, we finally obtain

$$f_N = 16\left(\frac{\pi}{2}\right)^{N-1}\left\{\beta_1 g_2^4+\beta_2 g_2^3 g_1+\beta_3 g_2^2 g_1^2 + \beta_4 g_2 g_1^3+\beta_5 g_1^4\right\}^{N-2}\left[4+g_3\right]^{2N-4} \qquad 3.7.16$$

where

$$\beta_1 = 4m^2(\delta_1+4m^2\delta_2-\tfrac{1}{2}\delta_3) \qquad 3.7.17(a)$$

$$\beta_2 = 4m(\delta_1+6m^2\delta_2) \qquad 3.7.17(b)$$

$$\beta_3 = 4m(2m^2\delta_4+3\delta_2) \qquad 3.7.17(c)$$

$$\beta_4 = 4m(\delta_2+2m^2\delta_4) \qquad 3.7.17(d)$$

$$\beta_5 = 2m^2\delta_4 \qquad 3.7.17(e)$$

and

$$\delta_1 = \int_{4m^2}^{M^2}\frac{d\sigma}{\sigma}\log\left[\frac{\sigma-\sigma^{1/2}(\sigma-4m^2)^{1/2}}{\sigma+\sigma^{1/2}(\sigma-4m^2)^{1/2}}\right]$$

$$= 2\left[\log\frac{M}{2m}\right]^2-\left[\log\left\{1-\frac{4m^2}{M^2}\right\}^{\frac{1}{2}}\right]^2 + \log\left\{1-\left(1-\frac{4m^2}{M^2}\right)^{1/2}\right\}\left[2\log 2-2\log\left\{1+\left(1-\frac{4m^2}{M^2}\right)^{1/2}\right]+\sum_{k=1}^{\infty}\frac{1}{k^2}\left\{1-\left(1-\frac{4m^2}{M^2}\right)^k\right\}\right. \qquad 3.7.18(a)$$

$$\delta_2 = \frac{1}{m^2} \int_{4m^2}^{M^2} \frac{d\sigma}{\sigma} \left[1 - \frac{4m^2}{\sigma}\right]^{1/2}$$

$$= \frac{2}{M^2} \left\{ \log \left[\frac{M + \left(1 - \frac{4m^2}{M^2}\right)^{1/2}}{2m} \right] - \left[1 - \frac{4m^2}{M^2}\right]^{1/2} \right\}$$

3.7.18(b)

$$\delta_3 = \frac{1}{M^2} \int_{4m^2}^{M^2} d\sigma \left[1 - \frac{4m^2}{\sigma}\right]^{1/2}$$

$$= 4 \left\{ \frac{M}{2m} \left[1 - \frac{4m^2}{M^2}\right]^{1/2} - \log \left[\frac{M + \left(1 - \frac{4m^2}{M^2}\right)^{1/2}}{2M} \right] \right\}$$

3.7.18(c)

$$\delta_4 = \frac{1}{m^2} \int_{4m^2}^{M^2} \frac{d\sigma}{\sigma^2} \left[1 - \frac{4m^2}{\sigma}\right]^{1/2}$$

$$= \frac{1}{6m^4} \left[1 - \frac{4m^2}{M^2}\right]^{3/2}$$

3.7.18(d)

For purposes of numerical calculation, it can be noted that the first series in the right-hand side of 3.7.18(a) is the Zeta

function of Reimann. Also, the second series converges very rapidly since M^2 is not much larger that $4m^2$ and hence taking the first few terms would be a reasonable approximation.

From equation 3.7.16, it is obvious that the cancellation referred to at the end of the last section can occur only if g_1/g_2 satisfies the equation.

$$\sum_{i=1}^{s} \beta_i \, g_2^{s-i} \, g_1^{i-1} = 0 \qquad 3.7.19$$

We assume that it does not. In fact, as mentioned in the last section, if the input trajectory is the Pomeron, it cannot satisfy 3.7.19 since g_2 is then small or zero. However, if g_1 and g_2 take values satisfying 3.7.19, then, we will have to consider this case separately as all the asymptotic arguments of this chapter would no longer be valid.

In view of the foregoing, f_N can be put in the form

$$f_N = \gamma \eta^{n-1} \qquad 3.7.20$$

and equation 3.7.5 becomes

$$\mathrm{Im}\, T_{22}(j) = A_{22} + \sum_{N=1}^{\infty} (\gamma A_{22}) \left(\frac{\eta g^4}{G^4} A_{22} \right)^{n-1}$$

$$= A_{22}(1-\gamma) + \frac{\gamma T_{22}}{1 - \frac{\eta g^4 A_{22}}{G^4}} \qquad 3.7.21$$

At high energy, the second term on the right-hand side of 3.7.21 dominates over the first as the latter is the contribution

from the elastic (two-particle unitarity) amplitude, while the latter is the total contribution from the production amplitudes. By putting

$$\bar{g}^2 = \frac{\eta g^4}{G^4} \qquad 3.7.22$$

and comparing with the result for the standard multi-Regge model, derived in the last chapter

$$\mathrm{Im}\, T_{22}(j) = \frac{A_{22}}{1 - \bar{g}^2 A_{22}} \qquad 3.7.23$$

where $\bar{g}$ is the Reggeon-Reggeon-particle coupling constant, it follows that the net effect of inserting the low energy nucleon loops in the M.R.M. is to multiply this coupling constant by another constant depending on M^2, m^2, g_1, g_2 and g_3 This has the apparent effect of pushing up the trajectory as it is well known that the position of the trajectory depend on the kernel and enhancing the coupling constant means effectively enhancing the kernel. However, this is not true in the multi-Regge bootstrap, the mechanism of which acts so as to keep $\alpha(o)$ at the same value, as can be seen on deriving the bootstrap equations as in chapter 2 from equation 3.7.21.

Section 8 - Incorporation of off-mass-shell terms.

As explained in section five, the formulae for the Boson propagators and the coupling functions were based on Scadron's results which were derived assuming that the propagators and spinors were on the mass-shell. The same paper gives the prescription for incorporating extra terms for off mass-shell

propagators and spinors. The method used there was to keep the propagator numerators on mass-shell and alter the coupling functions in order to allow for the off-mass shell effects. This involves adding terms proportional to q^{α} the momentum flowing through the propagator. Also, if the off-shell particle is a fermion, couplings proportional to $\gamma \cdot p$ need to be added.

Since, at each Reggeon-nucleon-nucleon vertex of our model, the Reggeon and one of the nucleons are off mass-shell, we need to add these extra terms. On inclusion of these terms to the coupling function, equation 3.5.18 becomes

$$g_{\alpha^i} = \left\{ \left[g_1(t_i) \gamma_{\alpha^i} + g_2(t_i) p^i_{\alpha^i} + \bar{g}_3(t_i) q^i_{\alpha^i} \right] \left[1 + \bar{\beta} \not{\beta} \right] \right\} \qquad 3.8.1$$

where $\bar{\beta}$ is a constant and

$$\bar{g}_3(t_i) = \bar{g}_3 \cdot g(t_i) \qquad 3.8.2$$

We write $\bar{g}_3(t_i)$ according to 3.8.2, in order to separate the multi-Regge component as we did for g_1 and g_2 These alterations lead to corresponding alterations in equation 3.4.8 It will be recalled that our asymptotic arguments of section 6 enabled us to neglect the terms containing q^i The same reasoning applies to equation 3.8.1, allowing us to omit the term containing q^i The factor $[1 + \bar{\beta} \not{\beta}]$ in 3.8.1 then leads to the replacement of 3.4.8 with the equation

$$Loop_{\mu^i \nu^i \sigma^i \lambda^i} = Tr \left\{ (\not{p}^i + m) g_{\lambda^i} g_{\sigma^i} (1 + \beta \not{\beta}^i) \right.$$

$$\left. (1 + \beta \not{\beta}^i)(\not{q}^i + M) g_{\nu^i} (1 + \beta \not{\beta}^i) \right.$$

$$(m + \not{B}^c)(1+\beta \not{B}^c)\, g_{\mu^c} \qquad 3.8.3$$

where the $g_{\alpha^c}\ (\alpha = \mu, \nu, \lambda, \sigma)$ are the expressions defined in section 5 and not as in 3.8.1. With the use of the relations satisfied by the γ-matrices, given in section 6, it is clear that the factor

$$[1+\beta \not{B}^c][m + \not{B}^c][1+\beta \not{B}^c]$$

can be replaced by

$$[m' + m'' \not{B}^c]$$

where m' and m'' depend on β, m and M^2. Similarly the factor

$$(1+\beta \not{B}^c)(1+\beta \not{B}^c)$$

can be replaced by quantities depending on β, m and M^2. Therefore, the insertion of these off-mass shell terms does not change qualitatively any of the arguments of the preceding sections. They only serve to "renormalise" the values of the coupling constants g_1 and g_2

Conclusion

The insertion of low energy nucleon loops in the multi-Regge model has failed to produce the enhanced asymptotic s-behaviour shown by similar Feynman diagrams calculated in high-energy quantum electrodynamics. The inclusion of crossed rungs, we found, did not make our calculations more complicated, but actually simplified them considerably by leading to the cancellation of several terms in the expansion of the loop.

The inclusion of the nucleon loops did not involve complicated phase space integrals. The phase space factorised very neatly, allowing us to isolate the contribution from the loops. For each intermediate particle state, the loops acted as a multiplying factor. This multiplier itself was found to factorise in the same way as the multi-Regge amplitude, which meant that the sole impact of the loops was to act as a multiplier for the kernel, which dependson the constants g_1, g_2 which are the Reggeon-nucleon-nucleon coupling constants and the quantities M^2 and m^2 which are the Regge threshold energies and nucleon mass respectively. Owing to the workings of the multi-Regge bootstrap mechanism, the intercept of the trajectory is unaltered in spite of a changed kernel. All our results were derived using the approximation that our propagators were on the mass-shell. We also analysed the effects of considering them off-mass-shell and found that it only served to renormalise the Reggeon-nucleon-nucleon coupling constants.

Chapter 4 - Non adjacent correlations

Section 1 - Introduction

As stated in chapter two, it has been established that the position of the output trajectory in the single-pole input version of the multi-Regge model in the factorisable approximation falls short of unity. The model derived by us in chapter two, failed to improve on this. In this chapter, it will be shown how the addition of certain correction terms to the multi-Regge amplitude helps to push up the trajectory close to one. These correction terms represent long range correlations. It is one of the fundamental features of multiperipheral models that the influence of particles adjacent in the multiperipheral chain dominate over that of those further away. That is, the multiperipheral correlations are of short range order. The factorisable approximation of the multi-Regge model, described in chapter two, embodies this to the utmost. Each link of the chain is calculated independent of the other links and the amplitude with n links is just kx^n where k is a constant and x is proportional to the elastic (single link) amplitude. The correction terms which we add are amplitudes incorporating correlations between links. These, by virtue of multiperipheralism are small compared to the factorised multi-Regge model.

Section 2 - The corrected multi-Regge model.

In the multi-Regge model, let $T_N(j)$ be the n intermediate particles state contribution to the absorptive part of the $2 \longrightarrow 2$ amplitude in the forward direction.

$T_N(j)$ is given by

$$\mathrm{Im}\ T_{22}(j) = \sum_{N=2}^{\infty} T_N(j) \qquad 4.2.1$$

Then

$$T_4(j) = G^4 (gg^*)^2 A^3 \qquad 4.2.2$$

and

$$T_N(j) = G^4 [gg^*]^{N-2} A^{N-1} \qquad 4.2.3$$

where

$$T_2(j) = G^4 A \qquad 4.2.4$$

G and g are the Reggeon-particle-particle and Reggeon-Reggeon-particle coupling constants respectively. T_4 is given by Fig. 18 and contains only correlations between neighbouring links on the chain. These correlations are reflected in the Reggeon-Reggeon-particle coupling functions at the vertices which are given by $\bar{g}(t_i, t_{i+1})$ where the t_i and t_{i+1} are momentum transfers flowing through successive links. In the factorisable approximation, these functions are seperable in t_i and t_{i+1} and can be put in the form

$$\bar{g}(t_i, t_{i+1}) = g f(t_i) f(t_{i+1}) \qquad 4.2.5$$

enabling us to calculate each link separately, which leads to equations 4.2.2 - 4.2.4.

Let $T_4'(j)$ which is given by Fig. 19, represent a 4-particles intermediate state amplitude in which all 4 particles correlate. In multi-Regge terms, it incorporates correlation between non-adjacent particles in the chain separated by a single link.

$T'_4(j)$ is the Mellin transform of the s-plane amplitude $T'_4(s)$ which is given by

$$T'_4(s) = \Big\{ \int d^4q_1\, d^4q_4\, \delta(q_1^2 - m^2)\, \delta(q_4^2 - m^2)$$
$$s_1^{2\alpha(t_1)}\, s_3^{2\alpha(t_3)}\, G^2(t_1)\, G^2(t_3)$$
$$\delta[p_1 + p_2 - q_1 - q_4 - k_1 + k_3]\, A(s_2, t_2, t_1, t_3) \Big\}$$

4.2.6

where the momenta are as in Fig. 18,

$$s_i = (k_{i-1} - k_{i+1})^2 \qquad i = 1,2,3$$

4.2.7(a)

and

$$t_i = k_i^2 \qquad i = 1,2,3$$

4.2.7(b)

$A(s_2, t_2, t_1, t_3)$ is a high-energy off-mass shell amplitude which is represented by Fig. 20. Corresponding to 4.2.6, the uncorrected amplitude $T_4(s)$ is given by

$$T_4(s) = \Big\{ \int d^4q_1\, d^4q_4\, \delta(q_1^2 - m^2)\, \delta(q_4^2 - m^2)\, s_1^{2\alpha(t_1)}$$
$$s_3^{2\alpha(t_3)}\, G^2(t_1)\, G^2(t_3)\, \delta(p_1 + p_2 - q_1 - q_4 - k_1 + k_3)$$
$$[B(s_2, t_2, t_1, t_3)] \Big\}$$

4.2.8

where

$$B(s_2, t_2, t_1, t_3) = \int d^4q_2\, d^4q_3 \Big[\bar{g}^2(t_1, t_2)$$
$$\bar{g}^2(t_2, t_3)\, s_2^{2\alpha(t_2)} \Big]$$

4.2.9

We now assume that

$$A(s_2,t_2,t_1,t_3) = \frac{1}{X} B(s_2,t_2,t_1,t_3) \qquad 4.2.10$$

where X is a constant and $|X|$ is large as stated at the end of the last section. This assumption is equivalent to replacing the constant factor g^4 in T_4 (see equations 4.2.5 and 4.2.8) with the factor g^4/X An example of this is given in the last chapter where we studied a multi-Regge model with nucleon loops. These resulted in the introduction of non-adjacent correlations through the spinor and propagator indices, whose total effect was to multiply the kernel of the integral equation by a constant. However, as will be shown later, including a correction with nucleon loops will not serve to enhance the value of the trajectory intercept as we shall require the correction term to be negative which cannot be satisfied by the nucleon loops amplitude.

$$\text{Let } \bar{T}_4 = T_4 + T_4' \qquad 4.2.11$$

$\bar{T}_4$ is our corrected version of the four intermediate particles state contribution to $Im\, T_{22}$. We now proceed to insert this correction in each T_N in the unitarity sum. It means that the expression

$$(gg^*)^2 A^2$$

where the two (gg^*) factors come from two adjacent rungs of the multiperipheral ladder has to be factored out upto the maximum possible number of lines in all possible ways and replaced with

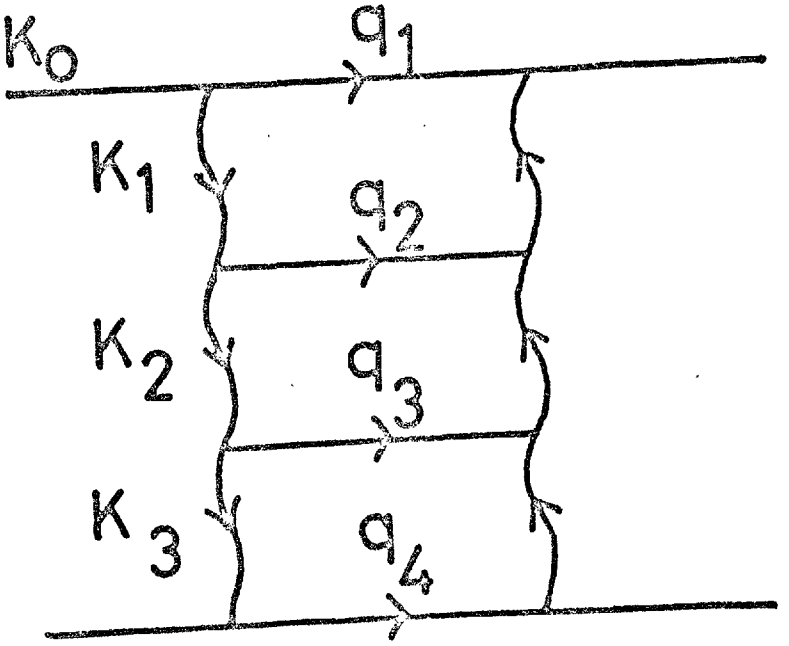

Fig. 18

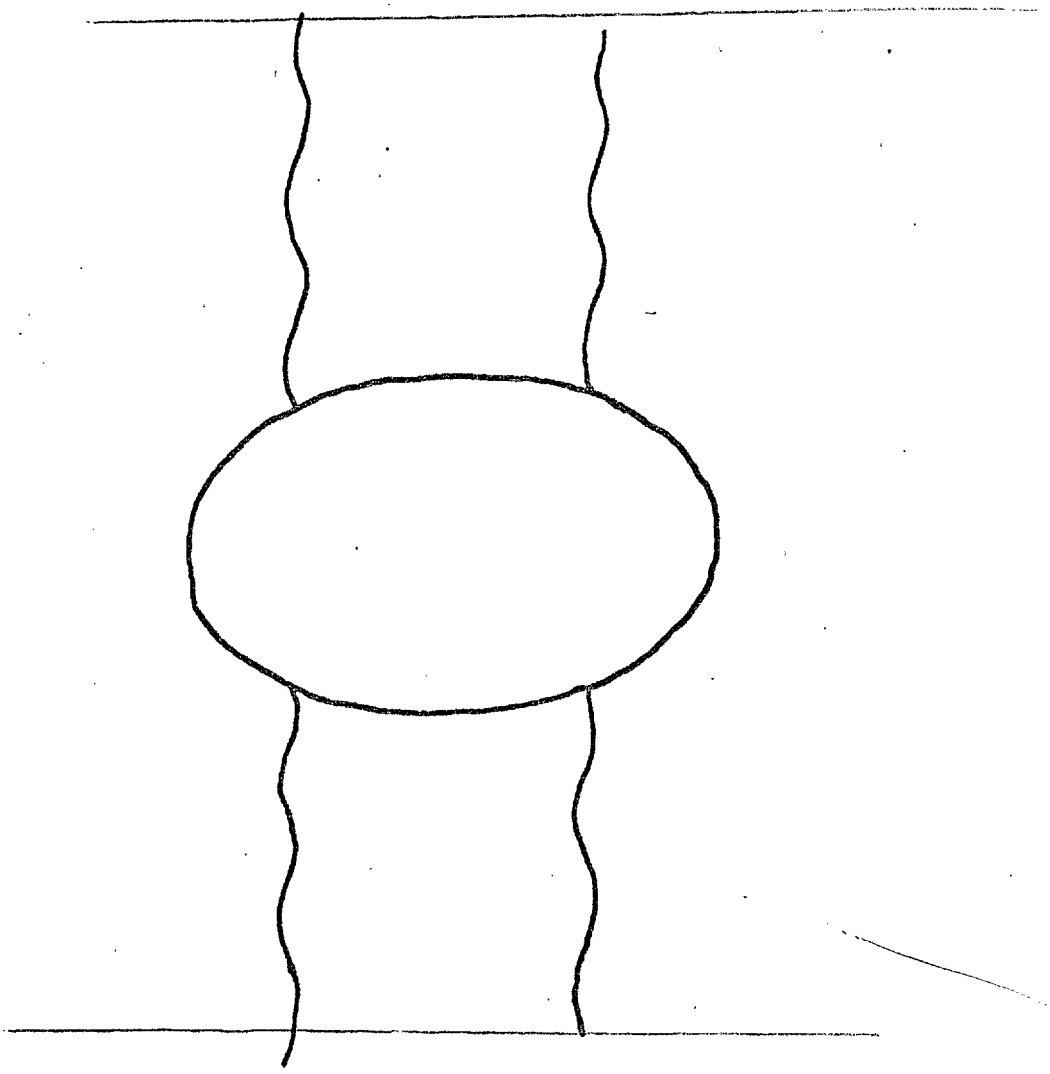

Fig. 19

the expression,

$$(gg^*)^2 A^2 \left(1 + \frac{1}{X}\right)$$

In diagrammatic terms, it amounts to removing two adjacent rungs of $\overline{T}_N$ and replacing with the blob of Fig. 19 in all possible ways.

This is represented by cutting the diagram for $\overline{T}_N$ in all possible ways across the Regge propagators such that between cuts, these appear at most two rungs and at least one. Wherever there are exactly two rungs between a pair of adjacent cuts, we extract a factor

$$(gg^*)^2 A^2$$

and replace it with

$$(gg^*)^2 \frac{A^2}{X}$$

All possible diagrams are then added. The external horizontal lines at the top and bottom of the diagram are treated as cutting the first and last pairs of propagators. Fig. 21, illustrates the foregoing for $\overline{T}_5$ which is equal to the sum of the three diagrams there (the cuts are represented by dotted lines).

Thus

$$T_5 = G^4 A \left[gg^* A\right]^3$$

is replaced by

$$T_5 = G^4 A \left\{ \left[gg^* A\right]^3 + \frac{(gg^* A)^2}{X} (gg^* A) + (gg^* A) \frac{(gg^* A)^2}{X} \right.$$

4.2.12

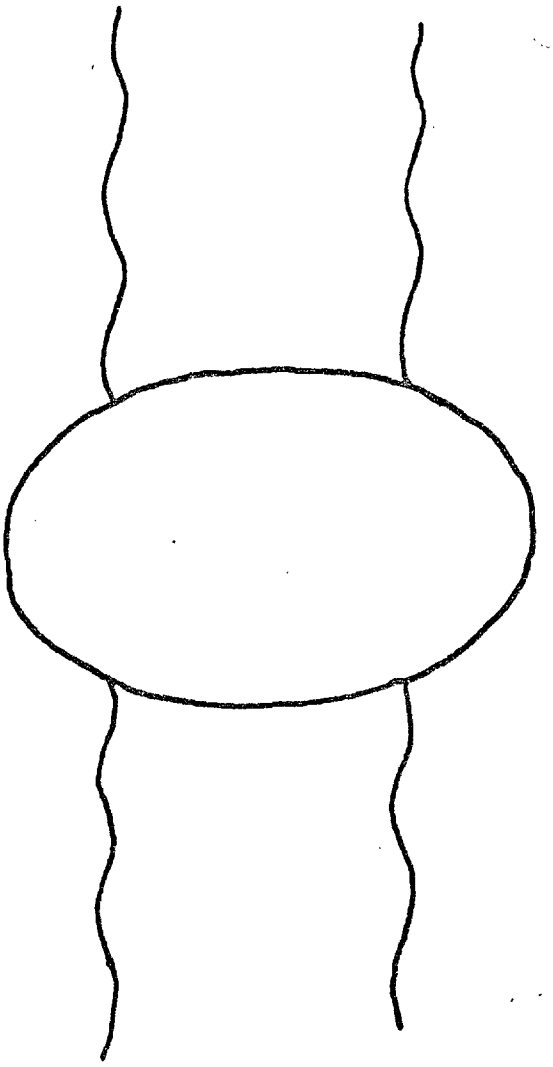

Fig. 20

each term on the right-hand side corresponding to a diagram of Fig. 21.

Let $\bar{T}_N$ be the sum of all diagrams with N intermediate particles i.e. $\bar{T}_N$ is the corrected form of T_N. Clearly, an amplitude T_1^N, represented by any particular diagram cut in a specific way, that contributes to $\bar{T}_N$ is given by

$$T_1^N = G^4 A \left[(gg^*)A\right]^{a_1} \left[\frac{(gg^*A)^2}{X}\right]^{a_2} \qquad 4.2.13$$

where

$$a_1 + 2a_2 = N - 2 \qquad 4.2.14$$

This amplitude will have a_2 blobs and a_1 rungs, not counting the top and bottom rungs. Obviously, there are several amplitudes, all contributing to $\bar{T}_N$ and equal to the right-hand side of 4.2.13. Their number is equal to the number of different ways of choosing a_2 pairs of rungs from $(N-2)$ ordered rungs and replacing each pair with a blob. Clearly, $\bar{T}_N$ is obtained by summing the right-hand side of 4.2.13 over all a_1 and a_2, subject to the restriction 4.2.14. Hence, after including these corrections, the modified unitarity equation becomes

$$\begin{aligned}
&\mathrm{Im}\, T_{22} \\
&= G^4 A + G^4 A \sum_{M=1}^{\infty} \delta_{M, a_1+2a_2} \sum_{a_1=0}^{\infty} \sum_{a_2=0}^{\infty} \frac{(a_1+a_2)!}{a_1!\,a_2!} \\
&\qquad \left\{(gg^*A)^{a_1} \left[\frac{(gg^*A)^2}{X}\right]^{a_2}\right\} \\
&= G^4 A + G^4 A \sum_{M=1}^{\infty} \delta_{M, a_1+2a_2} \frac{\left[gg^*A\right]^M}{M!} \sum_{a_1=0}^{\infty} \sum_{a_2=0}^{\infty} \left\{ \right. \\
&\qquad \left. \frac{(a_1+a_2)!}{a_1!\,a_2!} X^{-a_2} \right\}
\end{aligned}$$

$$= G^4 A + G^4 A \sum_{M=1}^{\infty} \frac{(gg^* A)^M}{M!} \left(\frac{\partial}{\partial y}\right)^M_{y=0} \left[\sum_{a_1=0}^{\infty} \sum_{a_2=0}^{\infty} \frac{(a_1+a_2)!}{a_1!\, a_2!}\, y^{a_1} \left(\frac{y^2}{X}\right)^{a_2} \right]$$

$$= G^4 A + G^4 A \sum_{M=1}^{\infty} \frac{(gg^* A)^M}{M!} \left(\frac{\partial}{\partial y}\right)^M_{y=0} \sum_{k=1}^{\infty} \left[y + \frac{y^2}{X}\right]^k$$

We now use Taylor's theorem to obtain

$$\mathrm{Im}\, T_{22} = G^4 A + G^4 A \sum_{k=1}^{\infty} \left[gg^* A + \frac{(gg^* A)^2}{X} \right]^k$$

$$= \frac{G^4 A}{1 - \left[gg^* A + \frac{(gg^* A)^2}{X} \right]}$$

4.2.15

By letting $X \longrightarrow \infty$ i.e. the correction $\longrightarrow 0$, we recover

$$\mathrm{Im}\, T_{22} = \frac{G^4 A}{1 - gg^* A}$$

4.2.16

which is directly obtainable from 4.2.1 and 4.2.3.

At this stage, we shall use the crude result in the multi-Regge bootstrap of Ref. 15, which we obtained in chapter 2, given by

$$gg^* A = \frac{|g|^2}{k(1-\alpha(0))} = \lambda$$

4.2.17

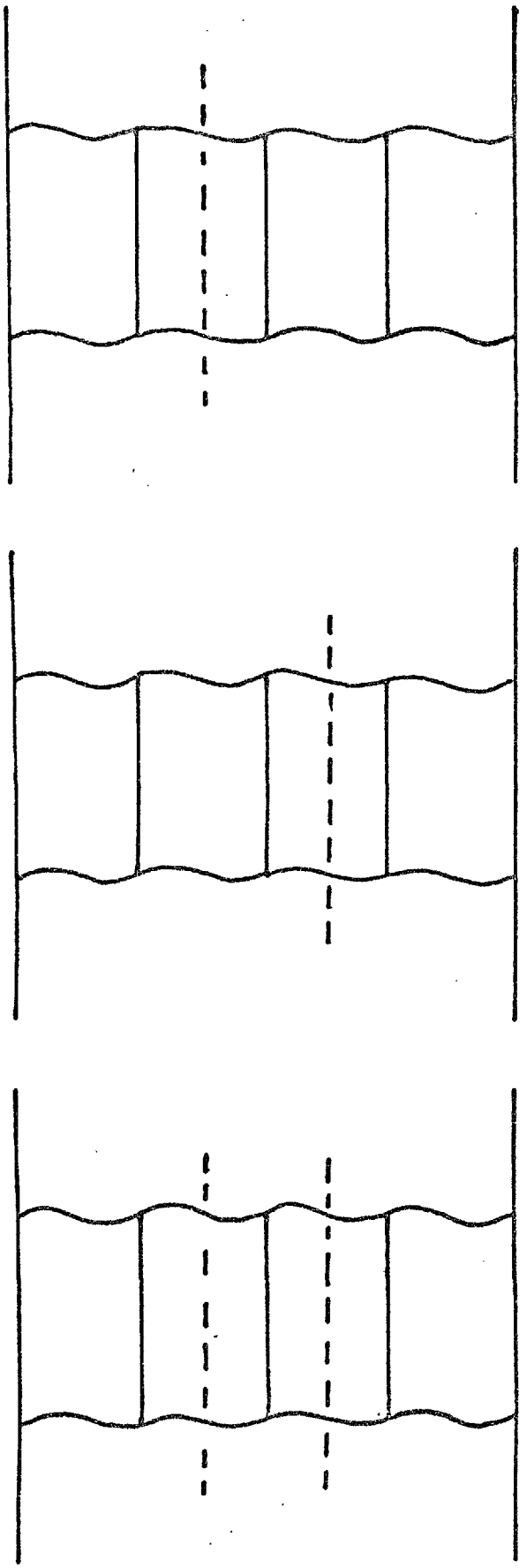

Fig. 21

where k is the exponent in the Regge residue function and $\alpha(t)$ is the Regge trajectory. In the given reference, the factor k^{-1} does not appear as it should, because of normalisation. This leads to, after equating the denominator of equation 4.2.16 to zero to obtain the output pole

$$\alpha(0) = 1 - \frac{|g|^2}{k} \qquad 4.2.18$$

In our corrected version, the position of the output pole is given by 4.2.15, which together with 4.2.17 lead to

$$\frac{\lambda^2}{X} + \lambda - 1 = 0$$

Thus we get

$$\alpha(0) = 1 + \frac{2g^2}{kX\left\{1 \pm \sqrt{1+\frac{4}{X}}\right\}} \qquad 4.2.19$$

For large X, if we take the minus sign, we get

$$\alpha(0) \approx 1 - \frac{|g|^2}{k}$$

which is the same as in the uncorrected multi-Regge model. If we take the plus sign

$$\alpha(0) \approx 1 + \frac{|g|^2}{kX} \qquad 4.2.20$$

If $X > 0$ this means equation 4.2.15 violates the Froissart bound.

If $X < 0$ we have $\alpha(0)$ of 4.2.20 closer to one than the $\alpha(0)$ of 4.2.18 for the same values of $|g|^2$ and k. This implies that the addition of a correction term representing the

correlation of non-adjacent particles has been instrumental in pushing the output trajectory closer to one.

For example, if we take the crude result of Ref. 15,

$$\alpha(0) \approx 0.68, \quad |g|^2 k^{-1} \approx 0.32$$

by putting $X = -10$ we get

$$\alpha(0) \approx 0.97$$

Section 3 - The Mechanism of a negative correction

We shall illustrate in this section, a specific way in which X can become negative.

Let Γ_4 be represented by Fig. 22 and Γ_4' by Fig.23. The latter is the correction term representing non-adjacent correlations, to be added to the $2 \longrightarrow 4$ amplitude.

Put

$$\left| \frac{\Gamma_4'}{\Gamma_4} \right| = \frac{1}{|X|^{\frac{1}{2}}} \qquad 4.3.1$$

Γ_4 can be written

$$\Gamma_4 = |c||g|^2 e^{i\phi} \qquad 4.3.2$$

The phase ϕ comes from both the signature factor and g which is complex, as stated in chapter 2 as (Ref. 36 and 41)

Let $\Gamma_4' = |f| e^{i\psi}$ 4.3.3

Then

$$\Gamma_4' = \frac{|c||g|^2 e^{i\psi}}{|X|^{\frac{1}{2}}}$$

where

$$|X|^{1/2} = |c||g|^2|f|^{-1}$$

Thus we can write symbolically

$$T_4 = \Gamma_4 \Gamma'_4$$
$$= |c|^2 |g|^4 .$$

4.3.4

and to the first order in $|X|^{-1/2}$

$$\overline{T}_4 = [\Gamma_4 + \Gamma'_4][\Gamma_4 + \Gamma'_4]^*$$

$$= c^2|g|^4 + c^2\frac{|g|^4}{|X|^{1/2}} 2\cos(\phi - \psi)$$

4.3.5

It must be noted that a correction term by itself cannot constitute an amplitude which is always positive. The sole function of the correction term is to reduce the numerical value of the amplitude, though for convenience, we have been referring to it as an amplitude in its own right. Considering equation 4.3.5, if

$$\pi/4 < \phi - \psi < \pi/2$$

the correction $\overline{T}_4 - T_4$ becomes negative as required by the preceding section to push up the trajectory.

Section 4 - The correlating amplitude.

In section two, we postulated an off-mass-shell amplitude $A(s_2, t_2, t_1, t_3)$ representing non-adjacent correlations. In this section, we describe how such an amplitude can arise that will be consistent with the mechanism of section 3.

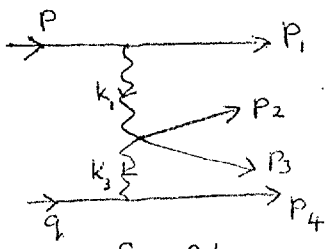

fig 24

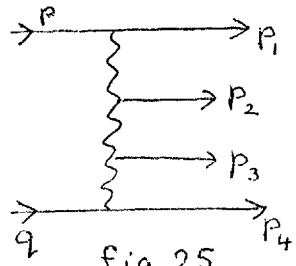

fig 25

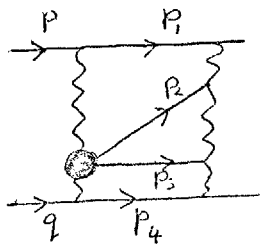

fig 26

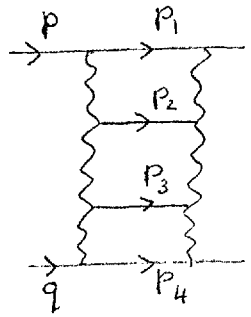

fig 27

We define the following invariants with respect to Figs. 24 - 27.

$$s_i = (p_i + p_{i+1})^2 \qquad i = 1,2,3$$

$$t_i = k_i^2 \qquad i = 1,2,3$$

$$t_2 = (k_1 - p_2)^2$$

If $s_1, s_3 \longrightarrow \infty$ but s_2 remained finite, we can represent the reaction

$$p + q \longrightarrow p_1 + p_2 + p_3 + p_4$$

by means of Fig. 24 where the off mass-shell amplitude represented by

$$k_1 + (-k_3) \longrightarrow p_2 + p_3$$

is at low energy. If s_2 becomes sufficiently large, then we can express this amplitude also in peripheral terms with Regge pole exchange and Fig. 24 becomes Fig. 25 which is the M.R.M.

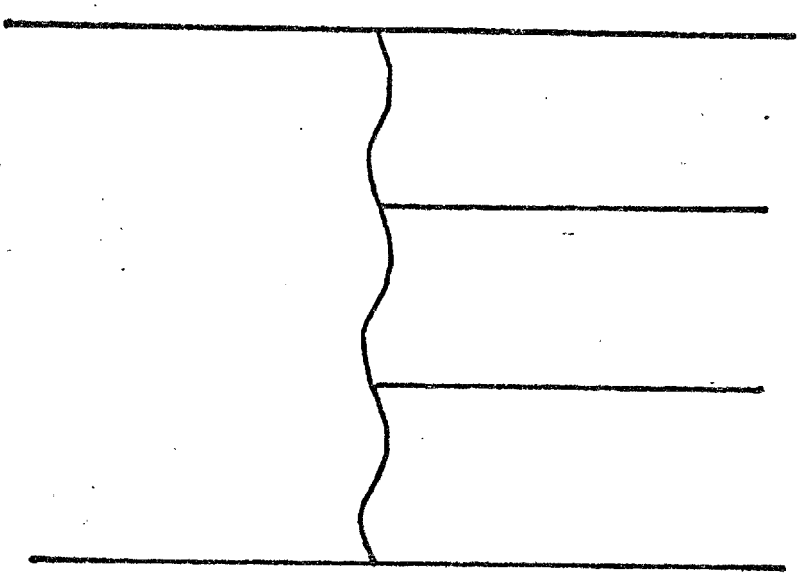

Fig. 22

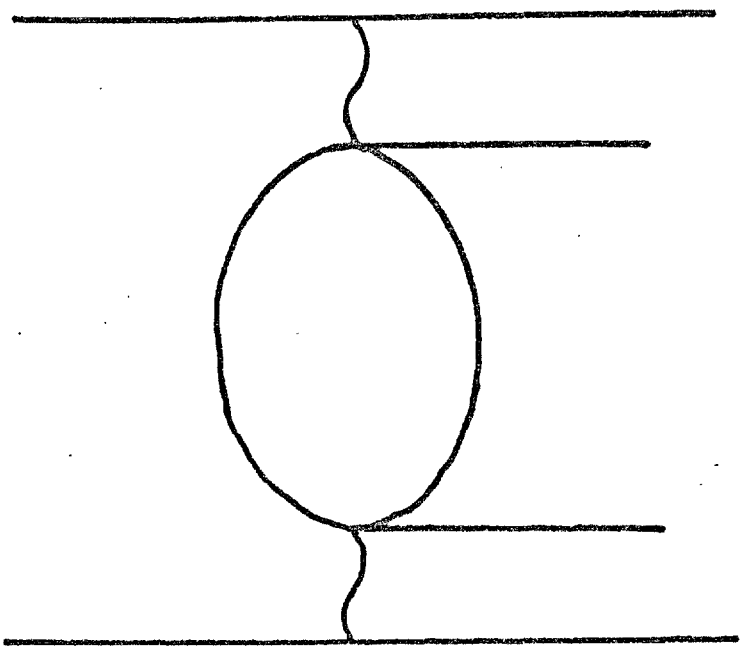

Fig. 23

Let $F(s_2, t_2, t_1, t_3)$ be the low-energy off mass-shell amplitude discussed above. In the multi-Regge model, when $s_2 \longrightarrow \infty$

$$F(s_2, t_2, t_1, t_3) \longrightarrow \tau\, g(t_1, t_2)\, g(t_2, t_3)\, s_2^{\alpha(t_2)}$$

4.4.1

Where τ is the signature factor and the g's are coupling functions at the two internal vertices of Fig. 25 the factor $g(t_1, t_2)\, g(t_2, t_3)$ is a feature of multiperipheralism which imposes short range order. The power dependence $s_2^{\alpha(t_2)}$ is independent of multiperipheralism, being a more widely accepted feature of high-energy scattering. It was argued by Amati, Fubini and Stanghellani (Ref. 1, Appendix 1) that by adding the most peripheral contributions alone, one cannot expect to achieve constant cross-sections. Hence we include less peripheral contributions which are small compared to the multiperipheral contribution. Our assumption is that these less peripheral contributions also have the same power dependence, their smallness arising from the vertex functions. In addition to the power dependence and the signature factor, these less peripheral amplitudes will also be dependent on the masses and the two usual Mandelstam invariants. Thus Fig. 24 can represent a non-peripheral correction at high-energy which makes the cross-sections more accurate. We assume that the amplitude represented by Fig. 24 at high-energy is given by

$$\bar{F} = \tau\, \tilde{g}(t_1, t_3, t_2)\, s_2^{\alpha(t_2)}$$

4.4.2

It must be remembered that t_1, t_2 and t_3 are all small quantities. We have to consider under what circumstances $\left|\frac{\bar{F}}{F}\right|$ can be a constant as required by section 3. If this is possible, then $\bar{F}$ and F will play the roles of Γ_4' and Γ_4 of section 3. With Frazer and Mehta's (Ref. 15) parametrisation, we have

$$g(t_1,t_2)\,g(t_2,t_3) = g^2 e^{k\left(\frac{t_1}{2}+\frac{t_3}{2}+t_2\right)} \qquad 4.4.3$$

Consider the possibility that

$$\bar{g}(t_1,t_3,t_2) = \bar{g}^2 J_0\left[\sqrt{-4k\left(\frac{t_1}{2}+\frac{t_3}{2}+t_2\right)}\right] \qquad 4.4.4$$

Bessel functions with their argument as the square-root of the momentum transfer have occured in the multi-Regge bootstrap (see chapter 2).

We have to the second order in x

$$\frac{\exp\left[-x/4\right]}{J_0\left[x^{1/2}\right]} = \frac{2x^2}{(8-x)^2} \qquad 4.4.5$$

For $x<1$, the right-hand side of 4.4.5 represents a percentage difference of less than 4%. Hence for sufficiently small values of t_1, t_3 and t_2 we can write 4.4.4 as

$$\bar{g}(t_1,t_3,t_2) = \frac{g^2}{|X|^{1/2}} e^{k\left(\frac{t_1}{2}+\frac{t_3}{2}+t_2\right)} e^{iX}$$

where 4.4.6

$$|X|^{1/2} = \frac{|\bar{g}|^2}{g^2}$$

Similarly, any function that is meromorphic around the origin and converges sufficiently fast when expressed in series form can be put in the form 4.4.6 for sufficiently small value of the argument, which itself would have to be a suitable function of t_1, t_2 and t_3. Thus our amplitude Γ_4' of section 3 can be represented by Fig. 24 and the correction amplitude of section 2 incorporating $A(s_2, t_2, t_1, t_3)$ can be represented by Fig. 26, the corresponding non-corrected terms being Fig. 25 and 27 respectively.

Conclusion

We have shown how an amplitude incorporating non-adjacent correlations can help to push up the trajectory nearer to one and hence produce cross-sections that vanish to zero more slowly with increasing s.

References

1. Amati, Fubini and Stanghellani - Nuovo Cimento 26,896 (1962). This paper is referred to in the text as the AFS paper.
2. Bertocchi, Fubini and Tonin - Nuovo Cimento 25,626 (1962).
3. Berestetski and Pomeranchuk - Nucl. Phys., 22,629 (1961).
4. S. Fubini - Comments on Nuclear and Particle Physics - 4,102 (1970).
5. S. Mandelstam - Nuovo Cimento 30,1127 (1963).
6. T.W.B. Kibble - Phys. Rev., 131,2282 (1963).
7. K.A. Ter Martriosyan - Sov. Phys. JETP, 17,341 (1963).
8. Chan, Loskievsky and Allison - Nuovo Cimento, 57A,93 (1968).
9. Dolen, Horn and Schmid - Phys. Rev., 166,1768 (1968).
10. Chew, Rogers and Snider - Phys.Rev., D2,765 (1970).
11. Chew and Pignotti - Phys. Rev., 176,2112 (1968).
12. Caneschi and Pignotti - Phys. Rev., 180,1525 (1969).
13. Chew, Goldberger and Low - Phys. Rev. letters, 22,208 (1969).
14. I.G. Halliday - Nuovo Cimento 60,177 (1969).
15. Frazer and Mehta - Phys. Rev. letters, 23,258 (1969).
16. Frazer and Mehta - Phys. Rev., D1,696 (1970).
17. Bali, Chew and Pignotti - Phys. Rev., 163,1572 (1967).
18. Chew and de Tar - Phys. Rev., 180,1577 (1969).
19. Chew and Frazer - Phys. Rev., 181,1914 (1969).
20. Ciafaloni, de Tar and Mishelloff - Phys. Rev., 188,2522 (1969).
21. V.V. Sudakov - Zurn. Eksp. Teor. Fiz., 30,87 (1956).
22. Halliday and Saunders - Nuovo Cimento 60,115 (1969).

23. I.G. Halliday - Nucl. Phys., B21,445 (1970).

24. Jacob and Fiukelstein - Nuovo Cimento 56A,681 (1968).

25. Cheng and Wu - Phys. Rev., D1,2775 (1970).

26. M.D. Scadron - Phys. Rev., 165,1640 (1968).

27. Jones and Scadron - Nucl. Phys., B4,267 (1968).

28. Finkelstein and Kajantie - Phys. letters, 26B,305 (1968).

29. R.J. Eden - High Energy collisions of Elementary particles - Cambridge University Press - 1967 - page 148.

30. Chew and Snider - Phys. Rev., D1,3453 (1970).

31. The Analytic S-Matrix by Eden, Landshoff, Olive and Polkinghorne - Cambridge University Press - 1966.

32. R.C. Hwa - Phys. Rev., D1,1790 (1971).

33. D. Branson - Nuovo Cimento 3A,271 (1971).

34. J.B. Bronzan - Phys. Rev., D4,1097 (1971).

35. J.D. Jackson - Models for High Energy processes - UCRL preprint 19205 - May 1969.

36. Drummond, Landshoff and Zakrewski - Nucl. Phys., B11,383 (1969).

37. Chan Ho Mo, Kajantie and Ranft - Nuovo Cimento 49A,157 (1967).

38. R.A. Morrow - Phys. Rev., 176,2147 (1968).

39. Lipes, Zweig and Robertson - Phys. Rev. letters 22,433 (1969).

40. Tan and Wang - Phys. Rev., 185,1899 (1969).

41. Halliday and Saunders - Nuovo Cimento, 60,494 (1969).

42. T.W.B. Kibble - Phys. Rev., 117,1160 (1960).

43. Bronzan and Jones - Phys. Rev., 160,1494 (1967).

44. I.G. Halliday - Nucl. Phys., B18,125 (1970).

45. C. Zemach - Phys. Rev., 140,1397 (1965).

46. Jones and Scadron - Phys. Rev., 171,1809 (1968).

47. Janch and Rohlrich - Theory of Photons and Electrons - Addison - Wesley (1957).